

Stars in the Galactic Centre:  
Sources and Probes of the Accretion Flow

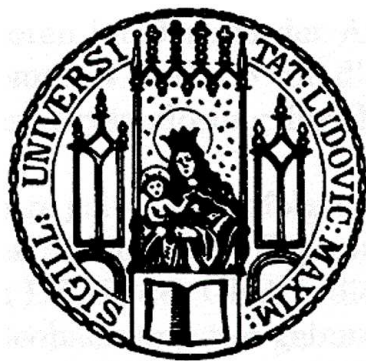
DISSERTATION

der Fakultät für Physik  
der Ludwigs-Maximilians-Universität München

zur Erlangung des Grades  
Doktor der Naturwissenschaften  
Dr. rer. nat.

vorgelegt von

Jorge R. CUADRA STIPETICH  
aus San Bernardo, Chile



München, den 26. Oktober 2006

1. Gutachter: Prof. R. A. Sunyaev
  2. Gutachter: Prof. R. Bender
- Tag der mündlichen Prüfung: 24. Oktober 2006

“Now there’s a look in your eyes  
Like black holes in the sky”  
(Roger Waters)



# Abstract

In the centre of our Galaxy lies Sgr A\*, a  $3.5 \times 10^6$  solar mass black hole, immersed in a star cluster with dozens of massive stars. The very low luminosity of Sgr A\*, and the presence of young stars in the close proximity of a super-massive black hole, make the Galactic centre a very interesting region on its own. Moreover, its proximity allows the study of the physics of galactic nuclei with a level of detail unattainable in any other system.

In this thesis, we first show that the interaction of massive stars with an accretion disc would appear as strongly variable emission in the near infra-red. Since observations have not shown this variability, we strongly constrain the current existence of such a disc in the Galactic centre. We argue however that a massive gaseous disc existed around Sgr A\* only a few million years ago. The evidence for this idea comes from the presence of young massive stars in two stellar discs. We estimate the properties of the gaseous disc that gave rise to the massive stars, and we analyse the stellar orbits to constrain this scenario. A related but separate topic presented here is the role of the stellar winds expelled by the same stars in feeding Sgr A\* and shaping its immediate gaseous environment. We find that a fraction of these stellar winds form cold clumps that coexist with the X-ray emitting gas, forming a two-phase medium. Only a small fraction of the gas is captured by Sgr A\*, with an accretion rate strongly variable on time-scales of hundreds of years. This variability suggests that the time-averaged energy output of Sgr A\* may be much larger than what is currently observed.



# Zusammenfassung

Im Zentrum der Milchstraße befindet sich, eingebettet in einen Sternhaufen mit Dutzenden massereicher Sterne, das Schwarze Loch Sgr A\* mit einer Masse von  $3.5 \times 10^6$  Sonnenmassen. Die geringe Leuchtkraft von Sgr A\* sowie die Anwesenheit junger Sterne in der unmittelbaren Umgebung dieses supermassiven Schwarzen Lochs machen das Galaktische Zentrum zu einer sehr interessanten Region. Darüberhinaus erlaubt seine geringe Entfernung die Untersuchung der Physik galaktischer Kerne mit einer in keinem anderen System erreichbaren Detailliertheit.

In dieser Arbeit zeigen wir zuerst, dass die Wechselwirkung von massereichen Sternen mit einer Akkretionsscheibe sich als stark variable Emission im nahen Infraroten äußert. Da eine derartige Variabilität nicht beobachtet wird, können wir strenge Schranken für eine derartige Scheibe im Galaktischen Zentrum der Gegenwart angeben. Wir argumentieren allerdings, dass eine massereiche Gasscheibe vor wenigen Millionen Jahren um Sgr A\* existiert hat. Gestützt wird diese Annahme durch die Anwesenheit junger massereicher Sterne, die in zwei Ebenen angeordnet sind. Wir schätzen die Eigenschaften der Gasscheibe, aus der die massereichen Sterne entstanden, ab und analysieren die stellaren Orbits, um dieses Szenario zu quantifizieren. Ein verwandtes, aber separates Thema, welches hier diskutiert wird, befasst sich mit der Rolle der Sternwinde, die von eben jenen Sternen emittiert werden, für Sgr A\* und seine unmittelbare gashaltige Umgebung. Wir kommen zu dem Schluss, dass ein Teil dieser Sternwinde kalte Klumpen bildet, die mit dem im Röntgenbereich emittierenden Gas koexistieren und somit ein zwei-Phasen-Medium bilden. Nur ein kleiner Bruchteil des Gases wird von Sgr A\* akkretiert, wobei die Akkretionsrate auf Zeitskalen von einigen hundert Jahren stark schwankt. Diese Variabilität lässt die Vermutung zu, dass die zeitlich gemittelte Energieabgabe durch Sgr A\* weitaus stärker sein könnte als die gegenwärtig beobachtete.





# Resumen

En el centro de la Vía Láctea se encuentra Sgr A\*, un agujero negro de  $3.5 \times 10^6$  masas solares rodeado por docenas de estrellas masivas. La baja luminosidad de Sgr A\* y la presencia de estrellas jóvenes muy cerca de un agujero negro supermasivo hacen que el centro galáctico sea una región de por sí muy interesante. Pero lo más importante es que su proximidad nos permite estudiar la física de núcleos galácticos con un nivel de detalle inalcanzable en ningún otro sistema.

En esta tesis, primero mostramos que la interacción entre estrellas masivas y un disco de acreción sería detectada como emisión variable en el infrarrojo cercano. Como esta variabilidad no ha sido observada, encontramos que es muy difícil que un disco exista actualmente en el centro de la Vía Láctea. Sin embargo, argumentamos que hubo un disco masivo alrededor de Sgr A\* hace sólo unos millones de años. La presencia de estrellas jóvenes masivas en dos discos estelares da evidencia en favor de esta idea. Estimamos las propiedades del disco de gas que originó las estrellas, usando también las órbitas de las estrellas que se observan hoy en día. Otro tema relacionado que presentamos aquí es el rol de los vientos de estas mismas estrellas en el crecimiento de Sgr A\* y la morfología del ambiente gaseoso. Encontramos que parte de los vientos estelares forman grumos fríos que quedan inmersos en el gas caliente que emite en rayos X. Sólo una pequeña fracción del gas es capturado por Sgr A\*, con una tasa de acreción que varía fuertemente en escalas de tiempo de cientos de años. Esta variabilidad sugiere que la energía promedio liberada por Sgr A\* puede ser mucho más grande que lo que se observa actualmente.



# Contents

<b>1</b>	<b>Introduction</b>	<b>1</b>
1.1	Super-massive black holes . . . . .	1
1.1.1	Accreting SMBHs in AGN . . . . .	1
1.1.2	SMBHs in nearby galaxies . . . . .	2
1.1.3	Sgr A*, the closest SMBH . . . . .	3
1.2	Stars around Sgr A* . . . . .	4
1.2.1	Stellar populations at the Galactic Centre . . . . .	4
1.2.2	Sgr A*'s confirmation as a massive black hole . . . . .	5
1.3	The puzzles of Sgr A* . . . . .	6
1.3.1	The young stars . . . . .	6
1.3.2	Sgr A* is a very underluminous black hole . . . . .	7
1.3.3	Inactive disc and X-ray flares . . . . .	8
1.4	This thesis . . . . .	9
1.4.1	Star-disc interactions: no disc now . . . . .	9
1.4.2	Self-gravitating disc and star formation . . . . .	9
1.4.3	Feeding Sgr A* with stellar winds . . . . .	10
<b>2</b>	<b>Bright stars and an optically thick inactive disc in Sgr A* and other dormant galaxy centres.</b>	<b>13</b>
2.1	Introduction . . . . .	14
2.2	Eclipses (and flares) . . . . .	15
2.2.1	The method . . . . .	15
2.2.2	Sample results . . . . .	17
2.2.3	Constraints on Disc Size and Orientation . . . . .	20
2.2.4	Eclipses and flares for S2: Summary . . . . .	20
2.3	Disc reprocessed emission . . . . .	23
2.3.1	Setup . . . . .	23
2.3.2	Reprocessed emission of an infinite disc . . . . .	27
2.3.3	The reprocessed disc emission for S2's orbit . . . . .	29
2.3.4	The case of S2 and discs with empty inner regions . . . . .	32
2.3.5	Summary: constraints due to disc reprocessed emission . . . . .	33
2.4	Star cluster asymmetry due to stellar eclipses . . . . .	34
2.5	Discussion . . . . .	37
2.5.1	A cold disc in Sgr A*? . . . . .	37

2.5.2	Constraints on the disc in Sgr A*	38
2.5.3	Star cluster asymmetry due to disc presence	40
2.6	Conclusions	40
<b>3</b>	<b>A self-gravitating accretion disc in Sgr A* a few million years ago: is Sgr A* a failed quasar?</b>	<b>41</b>
3.1	Introduction	42
3.2	The minimum mass of a self-gravitating disc in Sgr A* is $10^4 M_\odot$	44
3.3	Capturing low mass stars and growing them by accretion: too slow	46
3.4	Velocity dispersion of an isolated stellar disc	47
3.5	Destruction of stellar rings by orbital precession: the maximum disc mass	50
3.6	Rotating the accretion disc midplane: do stars remain embedded?	51
3.6.1	Forces keeping the stars embedded	51
3.6.2	Critical rotation time	52
3.6.3	The case of Sgr A*	52
3.7	Accretion onto embedded stars	54
3.8	Growth of ‘mini star clusters’ and intermediate mass black holes in accretion discs	55
3.9	Discussion	56
3.10	Conclusions	58
<b>4</b>	<b>Accretion of cool stellar winds on Sgr A*: another puzzle of the Galactic Centre?</b>	<b>59</b>
4.1	Introduction	60
4.2	Analytical estimates	61
4.3	Method and initial conditions	62
4.4	Results	63
4.4.1	Gas morphology	63
4.4.2	Accretion on to Sgr A*	65
4.4.3	Existence of cold disc in sub-arcsecond region of Sgr A*	65
4.4.4	Note on the importance of initial conditions	67
4.5	Discussion and Conclusions	68
<b>5</b>	<b>Galactic Centre stellar winds and Sgr A* accretion</b>	<b>71</b>
5.1	Introduction	72
5.2	The Numerical Method	73
5.3	Models with fast winds	74
5.3.1	Fixed stars	74
5.3.2	Stars in orbits around Sgr A*	80
5.4	Fast and slow (two-phase) winds	84
5.4.1	Stellar wind sources placed in two discs	84
5.4.2	Simulation with isotropic orbits	91
5.4.3	Comparison of both simulations	94
5.4.4	Comparison of the two-phase and one phase simulations	94
5.5	What would Chandra see?	97

5.6	Discussion . . . . .	102
5.6.1	Reduction of accretion due to anisotropy and net angular momentum . . . . .	102
5.6.2	Cool phase of stellar winds . . . . .	103
5.6.3	Long term evolution of the disc . . . . .	104
5.6.4	Variability . . . . .	105
5.6.5	Circularisation of the flow . . . . .	105
5.7	Conclusions . . . . .	106
<b>6</b>	<b>Summary and prospects</b>	<b>109</b>
6.1	Observing star–disc interactions . . . . .	109
6.2	Self-gravitating discs and star formation . . . . .	110
6.3	Feeding Sgr A* with stellar winds . . . . .	111



# Chapter 1

## Introduction

Like many galaxies, the Milky Way hosts a super-massive black hole (SMBH) in its centre. Unlike any other, our Galactic centre (GC) is close enough for us to observe many details of the physical processes associated with a SMBH. Sgr A\* was first discovered as a radio source. Later its emission has also been detected in the near-infrared and X-ray bands. The motion of stars orbiting around Sgr A\* has confirmed its identification as a black hole.

In this thesis we focus on the interplay between the stars in the vicinity of Sgr A\* and the gas that the SMBH feeds upon. We will study the stars not only as the sources of most of the material that is currently accreted by Sgr A\*, but also as the fossil of a massive accretion disc, and as beacons revealing the current properties of the accretion flow.

### 1.1 Super-massive black holes

Black holes are concentrations of mass so compact, that not even light can escape from their gravity. In the standard astrophysics scenario, black holes of a few solar masses are formed when massive stars run out of fuel and collapse.

The formation of SMBHs, weighting millions to billions of solar masses, is not yet understood. Nevertheless, they are now believed to be present at the nuclei of most if not all galaxies. The central black holes in some galaxies manifest themselves as the brightest sources, radiating more than the whole galaxies hosting them. This is the case for the bright quasi-stellar objects (QSOs) and for active galactic nuclei (AGN) in general. In most nearby galaxies, however, the presence of a SMBH is only determined because of its gravitational influence on the galactic nucleus.

#### 1.1.1 Accreting SMBHs in AGN

AGN are bright sources found at the centre of some galaxies. AGN spectra are clearly different from stellar emission, so they need to be explained by more

exotic mechanisms. The source appears point-like when measured with the current instrumental resolution, therefore indirect arguments have to be used to constrain its size. A common feature in AGN emission is strong variability on timescales as short as hours. Since the variability has to come from a region causally connected, the emitting region can be at most as large as the distance travelled by light during those timescales, i.e., of the order of a few astronomical units (few times  $10^{13}$  cm).

The brightest AGN have luminosities  $\sim 10^{48}$  erg s $^{-1}$ . Such a radiative power carries a strong pressure, which could actually destroy the source if it exceeds the gravitational force that keeps it bound (see the Eddington limit, eq. 1.1 below). To fulfil the Eddington limit, a very massive central object is required. In some galaxies it reaches up to  $10^{10} M_{\odot}$ .

Besides the requirements on mass and size, an important constraint on the nature of the emitting object is the source of energy. Accretion onto a compact object seems to be the most efficient mechanism for transforming mass into energy: when matter falls deep in the potential well of a black hole, the energy liberated is an important fraction of its rest mass.

When gas is infalling in a galactic nucleus, it usually has some angular momentum. The gas, instead of going directly into the black hole, will form a disc orbiting the black hole. The gas could in principle stay in such an orbit indefinitely – it is due to viscosity that the angular momentum is transferred to the outskirts of the disc, allowing the mass to flow inwards. Viscosity heats the disc through dissipation of gravitational energy, which is then radiated away to yield the observed bright point-like sources, i.e., AGN and quasars. The nature of the viscosity is still not well understood, however, Shakura & Sunyaev (1973) introduced a useful parametrisation that explains quite well the general behaviour of accretion discs.

### 1.1.2 SMBHs in nearby galaxies

Most nearby galaxies show little or no sign of accreting SMBHs. However, the gravitational effect of a SMBH is felt by both stars and gas in galactic nuclei. In some galaxies, gas can be observed orbiting the galactic nucleus, and from this motion the mass of the central object is inferred. The interpretation, however, is not trivial, because gas also responds to non-gravitational forces.

Unlike gas, stars only feel gravitational forces. For this reason, studying stellar dynamics has been the preferred method to probe gravitational potentials. For external galactic nuclei, the integrated light of many stars is analysed, extracting the velocity distribution from the broadening and shape of spectral lines. A strong peak in the velocity dispersion is interpreted as a large mass concentration. With this approach, a dark central object has been found in most nearby galaxies, with masses in the range  $10^6$ – $10^{9.5} M_{\odot}$  (e.g., Ferrarese & Ford, 2005).

Moreover, a tight correlation has been found between the mass of the SMBHs and the velocity dispersion  $\sigma$  of stars in the host galaxies, well outside the direct black hole influence. The so-called  $M_{\text{BH}}-\sigma$  relation, with  $M_{\text{BH}} \propto \sigma^{\beta}$  and  $\beta \approx 4$ ,



suggests that a profound relation exists between the growth of SMBHs and the formation of their host galaxies.

In addition, there is a broad correspondence in SMBH numbers and masses between ‘normal’ galaxies in the local universe and high redshift QSOs. This suggests that all galaxies at some point in their history were actually AGN, and had episodes of radiatively efficient accretion (e.g., Yu & Tremaine, 2002). Nowadays, however, practically none of them are radiating much.

The dimness of nearby galactic nuclei is not that surprising considering that most of the black holes growth happened far in the past (e.g., Kauffmann & Haehnelt, 2000). However, the low luminosity is quite unexpected given the large amount of gas available for accretion in their immediate environment. Considering the observed hot gas and mass-losing stars in galactic nuclei, Ho (2003) estimates that nearby SMBHs can be accreting at rates  $\dot{M}_{\text{BH}} \gtrsim 10^{-5} - 10^{-3} M_{\odot} \text{ yr}^{-1}$ . If accretion proceeded efficiently (see § 1.3.2), these galactic nuclei would be a few orders of magnitude brighter than the measured  $\sim 10^{42} \text{ erg s}^{-1}$ . New models of accretion have been developed to account for this discrepancy. Such models need as input the amount and physical properties of the material that is captured by the black hole. Observationally, this information can be obtained only roughly for nearby galaxies. Our GC will prove very useful, as only there it is possible to get this input in detail (§ 1.4.3).

### 1.1.3 Sgr A\*, the closest SMBH

Sgr A\* is the super-massive black hole at the centre of our Galaxy. It was discovered in the mid-1970s as a compact radio source (Balick & Brown, 1974). Later, more precise observations located it at the dynamical centre of the gas streamers in the Galactic nucleus (Brown et al., 1981), and discovered that it is a variable source (Brown & Lo, 1982). More recently, Sgr A\*’s proper motion has been determined to be essentially zero (Backer & Sramek, 1999; Reid et al., 1999), as expected from a massive object.

During the last few years Sgr A\* has been detected in the X-rays and near-infrared (NIR) bands. Baganoff et al. (2001) reported the first clear detection of Sgr A\* emission in X-rays. The source is extremely faint for AGN standards, but has strong flares lasting for about one hour (see also Baganoff et al., 2003; Goldwurm et al., 2003; Porquet et al., 2003). Genzel et al. (2003a) discovered Sgr A\* emission in the NIR, which also shows variability, although at a much lower level (see also Ghez et al., 2004; Eisenhauer et al., 2005).

All these data, in particular Sgr A\*’s variability and its location at the very centre of the Galaxy, suggest that Sgr A\* is associated with a SMBH. Nevertheless, the confirmation for its identification as a black hole comes from the observed stellar dynamics (§ 1.2.2).

Sgr A\*’s extremely low luminosity has motivated the development of radiative inefficient accretion flow models (§ 1.3.2). It is also in Sgr A\* where these ideas can be tested, as it is the only galactic nucleus where it is possible to resolve the region where the gas becomes bound to the SMBH. Moreover, individual mass-losing stars can be observed, which are the source of the gas that

Sgr A\* is accreting nowadays (§ 1.4.3).

More recently, it became apparent that young massive stars were most likely formed around Sgr A\* (§ 1.3.1). This seems to be the first evidence for a process long predicted by AGN theorists: accretion discs on parsec scales are massive enough to become gravitationally unstable and form stars. This is quite interesting because it implies that a few million years ago Sgr A\* was a normal AGN. Again, this can only be observed in our GC. In other galaxies (notably Andromeda, see Bender et al. 2005) nuclear stellar clusters are observed, but individual stars cannot be resolved.

Summarising, studying Sgr A\* and its vicinity is crucial for understanding galactic nuclei. It is the only place where we can observe in detail what the black hole is accreting now, and resolve the stars that are signatures of AGN activity in the past. Extrapolating from Sgr A\* it will be possible to learn about the growth and duty cycle of SMBHs, and the relation between star formation and AGN activity. This is likely to be relevant to understand the origin of the correlation between black hole masses and the stellar velocity dispersion in their host galaxies, one of the open issues in the standard cosmological scenario.

## 1.2 Stars around Sgr A\*

Determining stellar dynamics has been a key ingredient to study Sgr A\* and confirm its identification as a black hole. Observing stars in the GC can also shed light on a range of astrophysical areas: from tests of general relativity to the physics of star formation, and from galaxy formation to accretion theories (e.g., Alexander, 2005).

The radius of influence of Sgr A\*, i.e., the distance up to where the stellar dynamics are dominated by the SMBH gravitational potential, is of the order of one parsec ( $1 \text{ pc} = 3.086 \times 10^{18} \text{ cm}$ ). We shall refer to this region as the central or the inner parsec. Another length unit used in the GC literature and through this thesis is the arcsecond ( $1''$ ), which corresponds to  $1.2 \times 10^{17} \text{ cm}$ , or 0.039 pc, at the distance to the GC.

### 1.2.1 Stellar populations at the Galactic Centre

The stellar population in the inner parsec of the Galaxy has several components on top of the old, dynamically relaxed, population extending from outside this region. It is important to review the stellar properties, in particular their dynamics, because they are used to constrain the stellar origin (§ 1.3.1), and also the nature of Sgr A\* (§ 1.2.2) and its accretion flow (§ 1.4.1 and 1.4.3).

The inner  $10''$  are dominated by the ‘He-stars’, stars showing strong helium emission lines (e.g., Najarro et al., 1997). Many are catalogued as Wolf–Rayet (WR) stars or luminous blue variable (LBV) candidates. Such stars lose mass very rapidly and are believed to be the main source of material that is currently accreted by Sgr A\*. In addition, these stars have lifetimes of only a few million years, which constrains their epoch of formation. Most of them are confined

into two overlapping discs that rotate around Sgr A\* (Levin & Beloborodov, 2003; Genzel et al., 2003b).

The He-stars discs are moderately thick, with aspect ratio  $H/R \approx 0.15$ . The stellar discs are almost perpendicular to each other and, depending on the projection of their motion in the sky, are referred to as the clockwise (CWS) and counter-clockwise systems (CCWS). The inner radii of the discs are  $\sim 1''$  and  $3''$ , respectively, and, while the stars in the CWS seem to describe circular orbits, the CCWS orbits are better fitted by ellipses (Paumard et al., 2006).

In the inner  $1''$  the stellar properties change abruptly. Most of the observed stars in this region are massive B main sequence stars. Contrary to the ordered motion in the  $1''$ – $10''$  region, the orbits of the so-called ‘S-stars’ are randomly oriented, with no signs of alignment with any of the discs. Moreover, most of them are in highly eccentric orbits, with  $e > 0.9$  (Eisenhauer et al., 2005).

### 1.2.2 Sgr A\*'s confirmation as a massive black hole

During the 1990s, two independent groups (see e.g., Ghez et al., 1998; Genzel et al., 2000) used near-infrared observations to measure proper motions and line-of-sight velocities for about a hundred stars in the inner few arcseconds of the Galaxy. The high velocity dispersion observed implied a very large mass of  $2.8 \pm 0.5 \times 10^6 M_\odot$  confined to the inner  $\sim 0.01$  pc. This high density of more than  $10^{12} M_\odot \text{pc}^{-3}$  could still correspond to a cluster of dark stellar remnants (stellar mass black holes or neutron stars). However, such a system would be dynamically unstable and disperse in less than  $10^7$  yr (Maoz, 1998), which is much shorter than the age of most stars in the Galactic centre, making this scenario highly improbable (Genzel et al., 2000).

With better data and longer time coverage, the next step was the detection of stellar accelerations. Ghez et al. (2000) and Eckart et al. (2002) noticed that 2 or 3 of the innermost stars were *not* describing straight lines in the sky. The curvature was interpreted as acceleration caused by the gravitational potential of a central point mass. This measurement increased the minimum density of the central object to almost  $10^{13} M_\odot \text{pc}^{-3}$ , making it even harder for the dark mass to be composed of stellar objects.

One of these stars, known as S2, was observed by Schödel et al. (2002) at its pericentre in April 2002. The distance to the black hole at that time was only  $6 \times 10^{-4}$  pc. Similar individual orbits have been measured, including also line-of-sight velocities (Ghez et al., 2003b), for half a dozen stars (Schödel et al., 2003; Ghez et al., 2005; Eisenhauer et al., 2005), confirming what was learned from S2. The central object is now constrained to be smaller than the measured pericentres and therefore at least a few times  $10^{17} M_\odot \text{pc}^{-3}$  in density, ruling out any cluster of dark stellar objects.

More exotic alternatives are also severely constrained. A degenerate ball of fermions would need to be extremely compact, therefore composed of particles with masses in excess of 75 keV, larger than the  $\sim 15$  keV fermion ball that could explain dark masses in other galactic nuclei (e.g., Munyaneza & Viollier, 2002). The only option left is a ball of bosons, such an object could be compact

enough, but it would likely collapse to a black hole after accreting some of the gas abundant in the inner region of the Galactic centre (Torres et al., 2000). Therefore, it has been concluded that Sgr A\* must be a SMBH.

### 1.3 The puzzles of Sgr A\*

The proximity of our GC allows astronomers to observe galactic nuclei phenomena with exquisite detail. The same observations also pose serious questions to the standard star formation and accretion theories. How is it possible that young stars exist so close to a SMBH? Why is Sgr A\* so dim, if it has plenty of material to accrete from?

#### 1.3.1 The young stars

The presence of young stars in the vicinity of Sgr A\* requires explanations that go beyond the standard star formation scenario. Particle densities as high as  $10^8 \text{ cm}^{-3}$  are needed to overcome the huge tidal field of the SMBH to allow star formation. Such densities are orders of magnitude higher than those in observed molecular clouds. Some of the proposed solutions involve migration from larger distances, rejuvenation of older stars, and *in situ* formation in a massive accretion disc. While the discussion below focuses on the disc He-stars, it should be noticed that the complications are accentuated for the ‘S-stars’ in the inner arcsecond.

Outside the central parsec, the tidal force of the super-massive black hole is weak and cannot prevent star formation. Early calculations (Gerhard, 2001) showed that if the stars were in a cluster, then the dynamical friction force would be efficient enough to bring the stars to the inner parsec. The model has been studied further, showing that the cluster has to be unrealistically massive and compact for the scenario to work in the Galactic centre (McMillan & Portegies Zwart, 2003; Kim & Morris, 2003). The presence of a  $\sim 10^3 M_\odot$  black hole in the stellar cluster would help (Hansen & Milosavljević, 2003; Portegies Zwart et al., 2006), but that mass is much larger than the one expected from stellar clusters core collapse (Kim et al., 2004). An even more stringent constraint on this model comes from the fact that the infalling cluster is expected to lose a large fraction of its stars as it migrates inward. Nayakshin & Sunyaev (2005) showed that the lack of the expected X-ray emission from low mass stars *outside* the inner parsec practically rules out the inspiral cluster scenario.

A second alternative is that the stars were indeed formed *in situ*. To overcome the density problem, Morris (1993) suggested that star formation was the result of the collision of clouds. Perhaps a more natural explanation is that star formation occurred inside a massive accretion disc. Standard accretion discs (Shakura & Sunyaev, 1973) are expected to be massive enough to become self-gravitating and clumpy in their outer parts (e.g., Paczyński, 1978; Kolykhalov & Sunyaev, 1980; Shlosman & Begelman, 1989; Collin & Zahn, 1999; Goodman, 2003). If the cooling processes are fast enough, stars or planets should form in

these clumps (Gammie, 2001). The fact that most of the He-stars are located in two discs lends support to this scenario for the Galactic centre (Levin & Beloborodov, 2003, see also § 1.4.2).

### 1.3.2 Sgr A\* is a very underluminous black hole

The mass of Sgr A\*,  $3.5 \times 10^6 M_\odot$  (see § 1.2.2), makes it a ‘normal’ SMBH, even if in the low-mass end of the family. Its luminosity however,  $\sim 10^{36} \text{ erg s}^{-1}$ , is not only much smaller than that of bright AGN, it is also far lower than what has been measured for any nearby galactic nucleus. Because of its low luminosity and its proximity, Sgr A\* might be the key for understanding inefficient accretion onto SMBHs.

To understand the dimness of Sgr A\*, it is interesting to compare it with the maximum luminosity expected from a black hole. In general, the luminosity produced by accretion will exert radiation pressure on the infalling material. When this pressure is equal to the gravitational attraction from the central object the accretion cannot grow anymore. The maximum value is called the *Eddington limit*, and the luminosity at this regime can be expressed as (e.g., Frank et al., 2002)

$$L_{\text{Edd}} = \frac{4\pi G M_{\text{BH}} m_{\text{p}} c}{\sigma_{\text{T}}} \approx 1.3 \times 10^{38} \text{ erg s}^{-1} \frac{M_{\text{BH}}}{M_\odot}. \quad (1.1)$$

The Eddington limit for Sgr A\* is  $\sim 5 \times 10^{44} \text{ erg s}^{-1}$ , almost nine orders of magnitude higher than its observed luminosity.

The actual luminosity of an accreting object can be better estimated observing the available material. Knowing the physical properties of the gas far from the black hole, one can assume that accretion proceeds in a steady and spherically symmetric way, a process known as Bondi accretion. In this case, the gas will be accreted at a rate given by (Bondi, 1952)

$$\dot{M}_{\text{BH}} \approx \pi G^2 M_{\text{BH}}^2 \left( \frac{\rho}{c_s^3} \right), \quad (1.2)$$

where the density  $\rho$  and the sound speed  $c_s$  are measured at the Bondi radius,  $R_{\text{B}} = 2GM_{\text{BH}}/c_s^2$ , roughly the distance where the material becomes bound to the black hole.

Further, a conversion between accretion rate and emitted luminosity is needed. A simple way to estimate this efficiency is by assuming that the gas emits all the gravitational energy it gains before reaching the last stable orbit. The Newtonian approximation yields  $E_{\text{iso}} = -mc^2/12$ , i.e., almost 10 percent of the rest mass energy can be radiated during accretion. The proper relativistic calculation also gives values of the order of one tenth.

Baganoff et al. (2003) used the *Chandra* X-ray observatory to measure the density and temperature of the gas at a distance of  $\sim 1''$  from Sgr A\*, which is approximately the Bondi radius for the black hole. The resulting accretion rate is  $\dot{M}_{\text{BH}} \approx 3 \times 10^{-6} M_\odot \text{ yr}^{-1}$ . Using the standard efficiency  $\eta = 0.1$ , the expected luminosity is  $\sim 10^{40} \text{ erg s}^{-1}$ , again much more than the measured luminosity.

Since the infalling gas has angular momentum, the Bondi model is hardly realistic. However, it is still useful to estimate how much mass is captured by the black hole. In more realistic models, the gas settles in a disc, where the energy is dissipated and radiated away. On the other hand, in the so-called advection-dominated accretion flows (ADAF), most of the energy is not emitted, instead, it is carried along with the gas and lost into the black hole (Narayan & Yi, 1994). This is possible if the ions and electrons in the plasma have different temperatures. When the density is low enough, Coulomb interactions cannot transfer energy from the ions to the much lighter electrons. Since ions are heavy, they do not radiate much and just get hotter.

The ADAF model and its generalisations are able to fit Sgr A\*’s spectrum (e.g., Narayan et al., 1995; Narayan, 2002). However, to test the models further, it is necessary to establish exactly how the gas is captured by the black hole. Sgr A\* is the only SMBH for which this study is becoming possible. X-ray observations now detail the distribution of hot gas in the inner parsec (Baganoff et al., 2003), while in the NIR it is possible to detect streamers of ionised gas in the same region (Paumard et al., 2004). In addition, most of the material that is currently accreted by Sgr A\* originates in the evolved stars orbiting around them. Spectral analyses of these stars is now revealing the properties of their outflows (Paumard et al., 2001, Martins et al, in prep), allowing for the first time to model the feeding of a black hole from the origin of the gas until its accretion. As the stars are distributed non-isotropically, the expected gas distribution is quite complex and a numerical treatment is needed (§ 1.4.3).

### 1.3.3 Inactive disc and X-ray flares

One of the extensions of the ADAF models is the additional presence of an inactive accretion disc. Sgr A\* seems to be an extreme example of low luminosity AGN (Ho, 1999), and a cold accretion disc seems to exist in these objects (Ho, 2003). Nayakshin (2003) proposed that such a disc could also be present around Sgr A\*. An inactive disc could be the remnant of a past episode of stronger accretion, and nowadays would act as an efficient cooling surface for an ADAF-like flow. The hot material would condensate on top of the disc, at radii typically much larger than the Schwarzschild radius, without radiating much of its gravitational energy.

A nice feature of the Nayakshin (2003) disc is that it provided a natural explanation for the X-ray flares, that could arise from collisions between stars and the disc (Nayakshin & Sunyaev, 2003). There are thousands of stars in the inner parsec of the Galaxy. These stars would cross the disc twice per orbit. Nayakshin, Cuadra, & Sunyaev (2004) made a simple model for the emission expected from such star-disc interactions. We found the observed characteristic of the flares (duration, rate, spectra, position) as known at that time to be roughly the same as what is expected from the collisions. The star-disc interaction can in principle also leave observational signatures on the NIR, so this should be studied further to check the validity of the model (§ 1.4.1).

## 1.4 This thesis

In this thesis we study some of the most important puzzles of Sgr A\*. First is how does accretion work there. We have seen that there is plenty of material available to make Sgr A\* radiate as an AGN. But, how much gas is actually captured by the black hole, and which properties does it have? In addition, is a disc really producing the X-ray flares? Is there any disc at all around Sgr A\*?

The second issue is the origin of the young stars. Is it really possible that they were formed in an accretion disc? What can we learn about the accretion history of Sgr A\* observing the stars today?

### 1.4.1 Star–disc interactions: no disc now

If an inactive disc were present in the GC, it could eclipse the stars that happen to be behind it (Nayakshin & Sunyaev, 2003). In Chapter 2 (published by Cuadra, Nayakshin, & Sunyaev 2003) we study how the observations of bright stars constrain the properties of a disc in the Galactic centre. In particular we focus on the star S2, that has been measured more thoroughly. Since no variability has been detected in its luminosity we exclude the occurrence of eclipses and therefore constrain the geometry of the disc. It has to either be small enough ( $R_{\text{out}} \lesssim 0.1''$ ), or have a relatively large inner hole ( $R_{\text{in}} \gtrsim 0.03''$ ), in addition to having the ‘right’ orientation (§ 2.2).

However, we find that the stronger constraints come not from the absence of eclipses, but rather from the lack of large increases in the stars’ luminosity (§ 2.3). A massive young star like S2 emits most of its energy as ultraviolet radiation. When such a star approaches the disc, the ultra-violet (UV) photons heat up the disc material up to  $10^3$ – $10^4$  K, making it radiate as a black body. In the observed near-infrared bands, such reprocessed emission can exceed the intrinsic stellar luminosity by more than a factor of a hundred. This strong effect has not been observed, so any disc existing in the Galactic centre would have to have a large inner hole ( $R_{\text{in}} \gtrsim 0.1''$ ), or, alternatively, be optically thin in the near-infrared, with  $\tau \lesssim 0.01$ .

The constraints we find on the disc properties complicate the feasibility of the Nayakshin et al. (2004) model for the production of X-ray flares. The surface density required to produce the X-ray flares is  $\Sigma \sim 0.2 \text{ g cm}^{-2}$ , which could be reconciled with the above constraint on optical depth if the disc is dominated by grains with sizes larger than about  $30 \mu\text{m}$ .

In addition, we study how a disc embedded at the centre of a stellar cluster would influence the cluster’s observational appearance (§ 2.4). This method does not need individual orbits, nor resolved stars, so it can in principle be used for galactic nuclei other than our GC.

### 1.4.2 Self-gravitating disc and star formation

In Chapter 3 (published by Nayakshin & Cuadra, 2005), we study analytically the idea of a self-gravitating accretion disc as the formation place for the He-

stars in the Galactic centre. We show that the disc had to be more massive than  $\sim 10^4 M_\odot$  in order to become unstable to its own gravity (§ 3.2). Once star formation proceeds, we calculate that the stars remain embedded in the disc (§ 3.6), where they accrete the gas very rapidly (§ 3.7).

Additionally, we use the current observed stellar dynamics to constrain the maximum mass of the disc at that time. We find that if any of the discs was more massive than  $\sim 3 \times 10^5 M_\odot$ , the  $N$ -body scattering would distort the stellar dynamics beyond the observed velocity dispersion (§ 3.4). A more stringent limit can be obtained considering the effect of one disc on the other. The non-spherical potential of a disc will make orbits precess. As the rate of precession depends on the radial distance, the interacting discs will warp each other (Nayakshin, 2005b). In § 3.5 we show analytical estimates suggesting an upper limit on the disc mass of  $\sim 10^5 M_\odot$ .

Another possibility for explaining the disc orbits is that some stars from the nuclear cluster were captured by a gaseous disc, and later grown by accretion from that gas. We find that this mechanism is much less efficient than the *in situ* formation. The necessary accretion disc mass of a few times  $10^5 M_\odot$  practically rules out this possibility (§ 3.3).

### 1.4.3 Feeding Sgr A\* with stellar winds

In Chapters 4 and 5 (originally published by Cuadra et al., 2005, 2006) we study the dynamics of the gas in the inner half parsec of the GC, following it since its emission from the stars, until either it is accreted by Sgr A\* or it escapes from this inner region. In Chapter 4 we present analytical estimates and a preliminary simulation, while in Chapter 5 we explain the numerical model and analyse in detail many different runs.

We first perform several simulations with different configurations for the stellar orbits. We find that the angular momentum of the gas has a strong dependence on the orbital motions. Moreover, only the fraction of the gas with the ‘right’ low angular momentum goes to the inner region and can be accreted. Therefore, when the stars are rotating in a disc, the gas has more angular momentum and the accretion rate is lower than in the case where stars orbit the central black hole isotropically (§ 5.3).

We also compare these results with the case where the stars are kept fixed in space, as done previously in the literature. Obviously with fixed stars the angular momentum is not properly taken into account, and the accretion rate is over-estimated. Another interesting conclusion is that the stellar motion produces variability in the accretion rate. This is just the result of the geometry of the stellar system changing with time.

Different wind sources also affect the accretion onto Sgr A\*. The LBV candidates appear to be particularly important. These stars have wind velocities  $v_w \approx 300 \text{ km s}^{-1}$ , low enough to be susceptible to radiative cooling (§ 4.2). We find that once the winds emitted from these stars are shocked by the neighbouring winds, they cool and form clumps and filaments, creating a complex two-phase medium together with the hotter gas coming from WR stars (§ 5.4).



In addition, the existence of clumps adds variability to the accretion rate. Every time a clump is captured by the black hole, a sharp peak is produced. While we cannot resolve the inner accretion flow to predict the actual accretion rate onto Sgr A\*, we estimate that variability by a factor of a few should still reach the black hole. In the extremely sub-Eddington regime of Sgr A\*, a small change in the accretion rate produces a non-linear response on the luminosity. Perhaps the very low luminosity we observe nowadays is not representative of the average power output of Sgr A\*, and this quiescent black hole is actually important for the energetics of the Galactic centre (§ 5.6.4).



## Chapter 2

# Bright stars and an optically thick inactive disc in Sgr A\* and other dormant galaxy centres.

Originally published by Cuadra, Nayakshin & Sunyaev in *Astronomy & Astrophysics* **411**, 405

*Cold inactive discs are believed to exist in Low Luminosity AGN (LLAGN). They may also exist in the nuclei of inactive galaxies and in the centre of our own Galaxy. These discs would then be embedded in the observed dense nuclear stellar clusters. Making the simplest assumption of an optically thick disc, we explore several ways to detect the disc presence through its interaction with the cluster. The first of these is the eclipse of close bright stars by the disc. The second is the increase in the infrared flux of the disc due to illumination of its surface by such stars during close passages. Finally the surface brightness of the star cluster should show an anisotropy that depends on the inclination angle of the disc. We apply the first two of the methods to Sgr A\*, the super-massive black hole in our Galactic Centre. Using the orbital parameters of the close star S2, we strongly rule out a disc optically thick in the near infrared unless it has a relatively large inner hole. For discs with no inner holes, we estimate that the data permit a disc with infrared optical depth no larger than about 0.01. Such a disc could also be responsible for the detected 3.8  $\mu\text{m}$  excess in the spectrum of S2. The constraints on the disc that we obtain here can be reconciled with the disc parameters needed to explain the observed X-ray flares if dust particles in the disc have sizes greater than  $\sim 30\mu\text{m}$ . The destruction of small dust particles by strong UV heating and shocks from star passages through the disc, and grain growth during ‘quiescent’ times, are mentioned as possible*

*mechanisms of creating the unusual grain size distribution. We estimate the emissivity of the thin layer photo-ionised by the star in Hydrogen Br $\gamma$  line and in the continuum recombination in the 2.2  $\mu\text{m}$  band, and find that it may be detectable in the future if the disc exists.*

## 2.1 Introduction

In the last decade or so, dramatic improvements in the capabilities of the infrared instruments (e.g., Ott et al., 2003) produced unprecedentedly high quality data on the distribution of stars in Sgr A\* (e.g., Genzel et al., 2003b; Ghez et al., 2003a) and in the centres of other inactive galaxies. These high quality data prove that a super massive black hole (SMBH) exists in the centre of our Galaxy (e.g., Schödel et al., 2002; Ghez et al., 2003b) and that the majority of the bright stars in Sgr A\* cluster are early-type stars (Gezari et al., 2002; Genzel et al., 2003b), raising interesting questions about the star formation history in the vicinity of Sgr A\*.

In analogy to the discs present in LLAGN (e.g., Miyoshi et al., 1995; Quataert et al., 1999; Ho, 2003), a thin inactive (i.e. formerly accreting; Kolykhalov & Sunyaev, 1980) disc may exist in Sgr A\*. In addition, the disc presence may help to explain (Nayakshin, 2003; Nayakshin & Sunyaev, 2003; Nayakshin et al., 2004) two major mysteries of Sgr A\*: its amazingly low luminosity (e.g., see Baganoff et al., 2003, and reviews by Melia & Falcke, 2001 and Narayan, 2002) and the recently discovered large amplitude X-ray flares (Baganoff et al., 2001). Direct observational detection of the disc could be possible if the disc were massive and thus bright enough (e.g., Falcke & Melia, 1997 and Narayan, 2002) but a very dim inactive disc could have eluded such detection (Nayakshin et al., 2004).

Nayakshin & Sunyaev (2003) pointed out that the *three dimensional* orbits of stars such as S2 could be used to test the putative disc hypothesis. Here we extend the work of these authors by doing a much more thorough analysis of the parameter space as well as including new physics. In particular, under the simplest assumption of an optically thick disc, we discuss three methods to do so: (i) stellar eclipses; (ii) re-processing of the stellar UV and visible radiation into infrared; (iii) asymmetry of the integrated star cluster light. We apply the first two of the methods to the star S2, whose orbit is currently known the best out of all the close sources in the Sgr A\* cluster. We find (§2.2) that absence of eclipses for S2 could be explained by a disc with a ‘large’ inner hole,  $R_{\text{in}} \gtrsim 0.03''$ , for a rather broad range of disc orientations. Note that for a distance of 8 kpc to the Galactic Centre,  $1''$  corresponds to  $\simeq 1.2 \times 10^{17}$  cm or  $\simeq 1.3 \times 10^5 R_{\text{g}}$ , where  $R_{\text{g}} = 2GM_{\text{BH}}/c^2 \simeq 9 \times 10^{11}$  cm is the gravitational radius for the  $M_{\text{BH}} = 3 \times 10^6 M_{\odot}$  black hole. The re-processing of the optical-UV luminosity of the star in the infrared, however, creates (§2.3) a variable and very bright emission in the standard near infrared spectral bands. This emission would add to the total ‘stellar’ flux observed from the source (see Figure 2.7 below). Considering discs with no inner hole and all possible orientations we

find that this additional emission would have been detected by the Genzel et al. and Ghez et al. teams. Therefore an optically thick (in  $\lambda \simeq \text{few } \mu\text{m}$ ) disc is ruled out for the Sgr A\* star cluster. We estimate that the maximum near infrared optical depth of the disc that would not violate observational constraints is about 0.01. Finally, the cluster asymmetry measurement is suggested (§2.4) as a mean to constrain disc size and orientation in nearby galaxies whose nuclear regions are visible in the optical and UV light. In the discussion section (§2.5) we summarise our main results.

## 2.2 Eclipses (and flares)

### 2.2.1 The method

In this paper we consider an inactive disc optically thick in all relevant frequencies. In our study of the effects of the disc on individual stars, we pick the star S2 (Schödel et al., 2002; Ghez et al., 2003b)<sup>1</sup> as the best example. This is a very bright ( $L_{\text{bol}} \sim 10^5 L_{\odot}$ ) star whose orbit is constrained with better precision than that for any other star near Sgr A\*. The existing data on the star positions in the last  $\sim 10$  years cover (Schödel et al., 2002; Schödel et al., 2003; Ghez et al., 2003b, see also Figure 2.2 below) as much as  $\sim 70\%$  of its orbit. The coverage will clearly further increase with time. In addition, the star passed a mere  $\sim 0.02''$  or about 2000 gravitational radii,  $R_g$ , from the black hole in the pericentre (Schödel et al., 2002).

The geometrical thickness of a cold disc is very small (see Nayakshin et al., 2004) so we treat the disc as a flat surface. The disc is assumed to be in Keplerian circular rotation and is described by its inner and outer radii:  $R_{\text{in}}$  and  $R_{\text{out}}$ . An example of the projection of such a disc is shown in Fig. 2.1. We need *two* angles to describe the observational appearance of the disc: inclination  $0 \leq i \leq \pi/2$ , between the direction normal to the disc and the line of sight, and rotation  $0 \leq \beta \leq 2\pi$ , between the West direction and the semi-minor axis of the disc as seen in projection. (Out of the two possible semi-minor axes, we pick the one that lies on the side of the disc closest to the observer.)

Note that the angle  $\beta$  is of no importance for discs that have azimuthal symmetry, and is thus rarely defined. For our problem, however, this angle is important since it determines the orientation of the disc relative to stellar orbits. This angle definition is somewhat different from those commonly used to define stellar orbits (see e.g., Roy, 1982, §14.8), nevertheless we feel that ours is simpler to use:  $\beta$  immediately shows which side of the disc is in front of the plane of the sky centred on Sgr A\*.

We use the S2 orbital parameters given by Schödel et al. (2003) and the sign of the inclination angle measured by Ghez et al. (2003b) to calculate the 3-dimensional positions of the star as a function of time. For each given set of the disc parameters, we determine the parts of the star's orbit that are eclipsed by the disc (i.e. physically behind the disc) and those that are not. A physically

---

<sup>1</sup>Ghez et al. (2003b) refer to this star as S0-2.

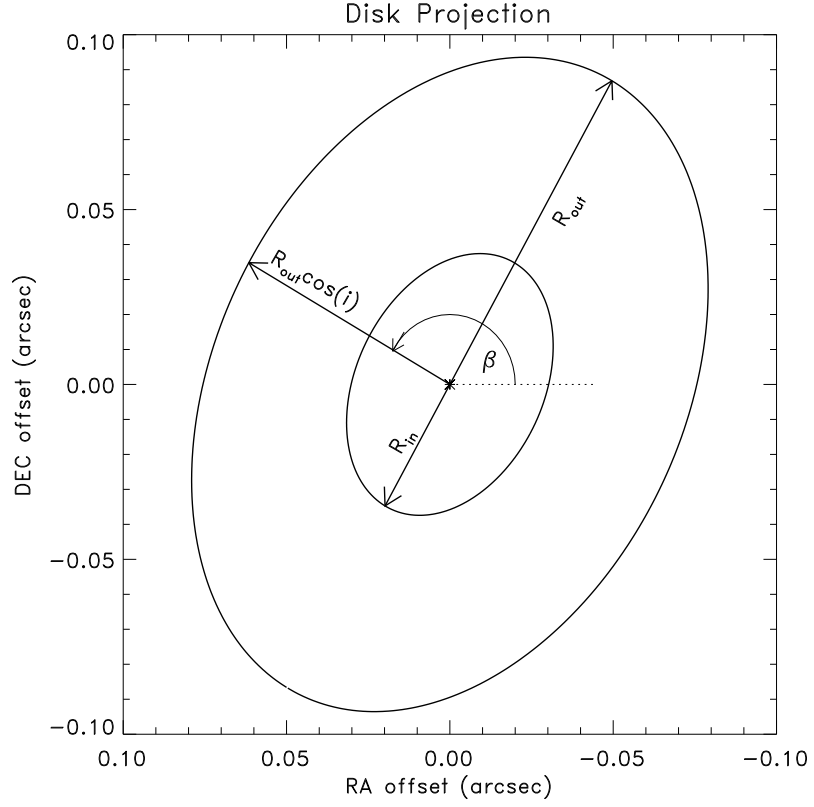


Figure 2.1: Projection of the disc in the plane of the sky. The disc is described by two radii,  $R_{in}$  and  $R_{out}$ , and two angles: disc inclination angle,  $i$ , and rotation angle,  $\beta$ . The latter is defined as the angle between the West projection and the semi-minor axis of the disc projection *directed to the part of the disc closest to the observer*.

plausible disc should not eclipse any of the star positions measured by Schödel et al. (2002); Schödel et al. (2003)<sup>2</sup>. Note that since the Sun prevents observations of the GC region for about half of a year, there are large portions of the star's orbit when it simply could not be observed.

The method described in this section can be easily extended to other stars in Sgr A\*, once their orbital parameters are precisely determined. S12 and S14 passed relatively close to Sgr A\* so they could also be useful in constraining the disc properties. The orbit of S12 is indeed known quite well, except for the sign of its inclination angle (Schödel et al., 2003; Ghez et al., 2003a), so a degeneracy in the 3-dimensional positions remains.

### 2.2.2 Sample results

To demonstrate typical results, we present two examples of discs that are *not* in conflict with the observations of S2. First, we consider a disc with no (or a very small,  $R_{\text{in}} \simeq 0$ ) inner hole, outer radius of  $0.1''$ , inclination  $i = 71^\circ$ , and  $\beta = 46^\circ$ . In this calculation S2 was eclipsed between 2001.7 and 2002.2 (see Fig. 2.2), and between 2002.75 and 2003.3. The end of the eclipse in 2002.2 coincides with a flare in X-rays and NIR that results from the shock heating of the disc by the star (Nayakshin et al., 2004). The NIR flare may in fact be quite strong due to the disc re-processing of S2 radiation incident on the disc surface, last for months, and be asymmetric (see §2.3). The same may be said about the second flare in around 2002.75, except that for this one the eclipse begins (rather than ends) with the flare. While fitting the observed data, this set of disc parameters is a rather fine tuned one. Thus such a disc (with  $R_{\text{in}} = 0$ ) is likely to be ruled out by future NIR observations of Sgr A\*.

Nayakshin et al. (2004) found that the too frequent crossings of the disc by the close stars in the innermost region of the stellar cluster will actually destroy the disc there. They estimated that the inner radius of the disc may be as large as  $R_{\text{in}} \sim 10^3 R_g$ , roughly  $0.01''$ . In addition, the ‘accretion’ discs in LLAGN do appear to have empty inner regions (Quataert et al., 1999; Ho, 2003) with similar values for  $R_{\text{in}}/R_g$ . Similarly, there are arguments for the existence of an inner hole in the standard disc surrounding the black hole in Cyg X-1 (Churazov et al., 2001). Thus it is sensible to study a disc with an inner radius  $R_{\text{in}} \neq 0$ . As an example, we take a much larger disc with  $R_{\text{out}} = 0.2''$ ,  $R_{\text{in}} = 0.04''$ , and  $i = 39^\circ$  and  $\beta = 347^\circ$  (Fig. 2.3). In this example the star is eclipsed by the disc only once per orbit, not twice as in Figure 2.2. The star crossed the disc in 2001.8 (producing a flare) and appeared in the projection of the inner disc hole in 2002.2.

An important point to take from Fig. 2.3 is that the outer disc radius is unconstrained in this case, i.e. it can be arbitrarily large. This is partially due to the ‘fortunate’ orientation of S2 orbit: Ghez et al. (2003b) showed that out of  $\sim 15$  years, the S2 orbital period, the star spent only 0.5 year behind the black

---

<sup>2</sup>Ghez et al. (2003b) observed this star in similar epochs, so using their data should yield similar constraints.

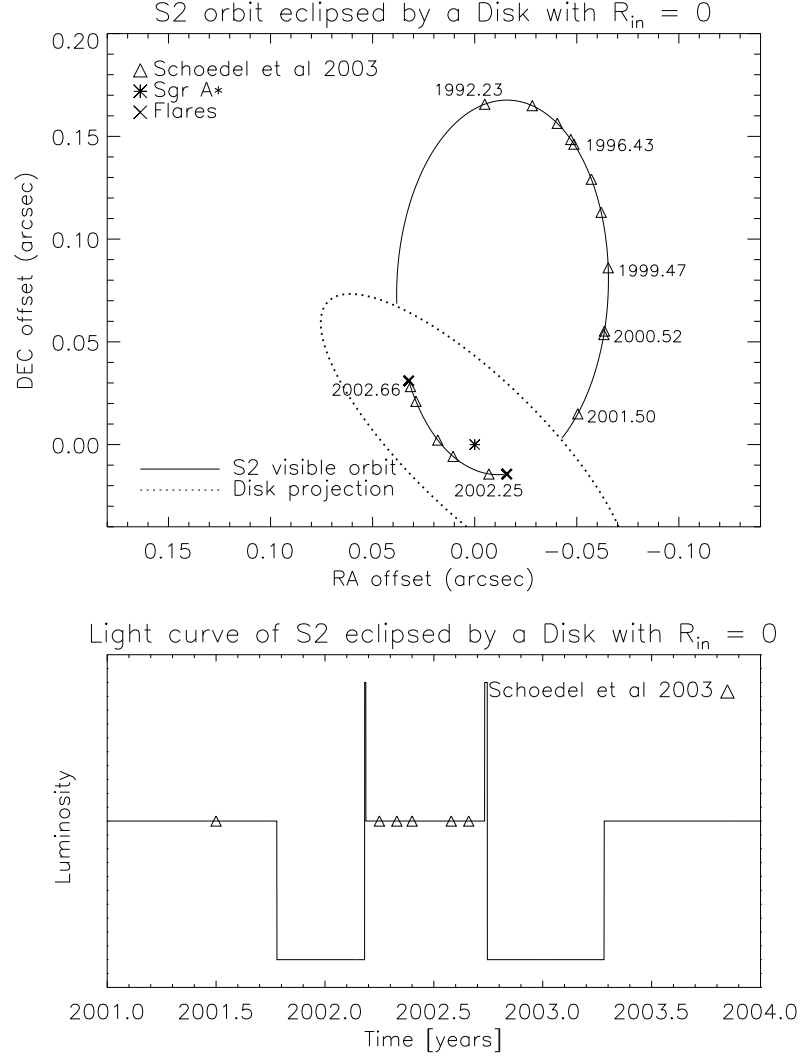


Figure 2.2: The orbit (top panel) and the light curve (bottom) produced by S2 passing through a disc with inner radius  $R_{\text{in}} = 0$  and outer one  $R_{\text{out}} = 0.1''$ ,  $i = 71^\circ$  and  $\beta = 46^\circ$ . Triangles show the positions of the star as given by Schödel et al. (2003). Respective times of the observations are shown on the Figure for some of the measurements. The two small crosses mark the points where the star would actually pass through the disc and when X-ray and NIR flares are emitted. The S2 luminosity in the bottom panel is shown schematically, in arbitrary units.



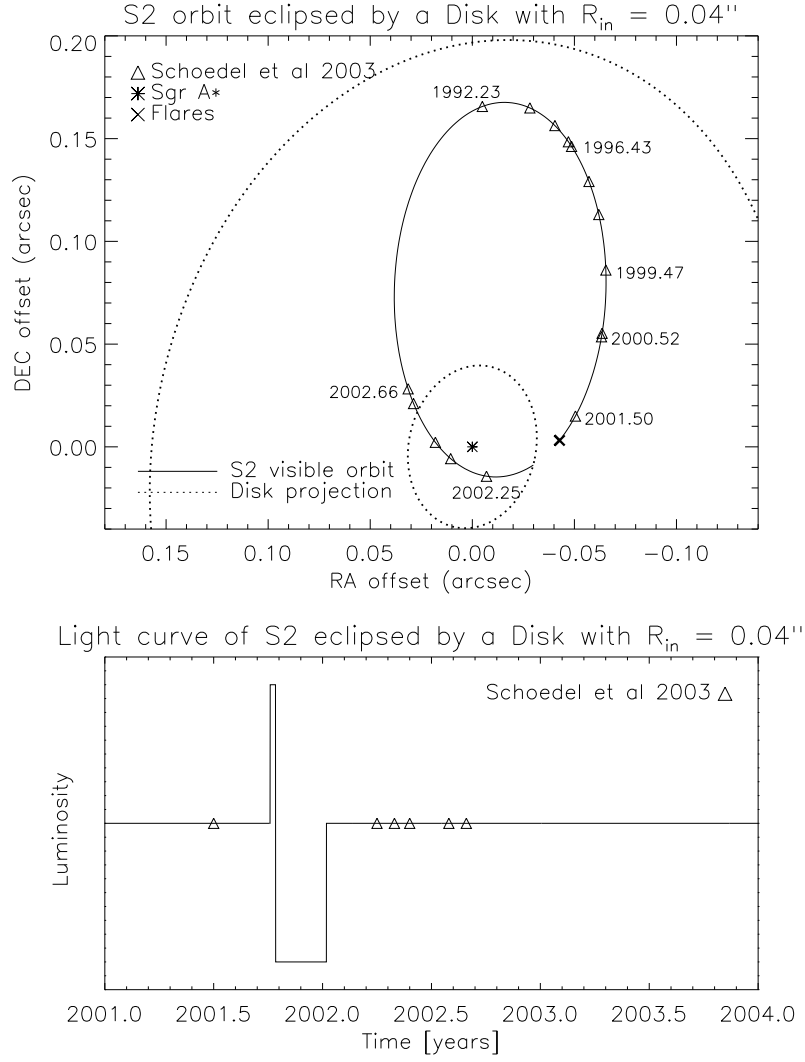


Figure 2.3: Same as Fig. 2.2, but for a disc with inner radius of  $0.04''$ ,  $R_{\text{out}} = 0.2''$ ,  $i = 39^\circ$  and  $\beta = 347^\circ$ . Note that S2 is seen through the hole in early 2002 and that there are no constraints on the disc outer radius in this case.

hole in the year 2002. If we take the simplest case of  $i = 0$ , i.e. a disc coinciding with the plane of the sky, then only the innermost 2002 points will be eclipsed if  $R_{\text{in}} = 0$ . If  $R_{\text{in}}$  is greater than about  $0.03''$ , then the three measured positions of S2 that were behind the plane of the sky in 2002 are observed through the hole and the rest of the star's orbit is in front of the disc. Therefore in this case there are no eclipses even if the disc is infinitely large.

### 2.2.3 Constrains on Disc Size and Orientation

We now search the parameter space to determine the likelihood, in a rough statistical sense, of a disc with some fixed parameters producing no eclipses that would disagree with observations. We make a fine grid in the parameter space ( $R_{\text{in}}$ ,  $R_{\text{out}}$ ,  $\cos i$  and  $\beta$ ) for this purpose, and for each combination of these parameters we check whether the disc eclipses any of the measured (Schödel et al., 2002; Schödel et al., 2003) star positions. If it does, then this combination of parameters is rejected.

We concentrate first on a disc with  $R_{\text{in}} = 0.035''$ . In Fig. 2.4 we show the maximum disc size,  $R_{\text{out}}$ , as a function of the rotation angle,  $\beta$ , for three different disc inclination angles  $i$ . Any value of  $R_{\text{out}}$  greater than the respective curve shown in Fig. 2.4 would produce one or more observable eclipses contradicting the data. It is seen from the Figure that smaller values of the inclination angle generally allow larger discs. This simply reflects the fact that the projected area of the inner missing disc increases as  $i$  decreases.

If there is no physically preferred orientation of the disc, then all the points in the  $\beta$ - $\cos i$  parameter space are equally probable. Therefore, to give a rough statistical assessment of the results, we may define the probability  $P(R_{\text{out}})$  as the fraction,  $F$ , of the area in this parameter space that allows the outer radius to be larger than  $R_{\text{out}}$ . Fig. 2.5 shows this fraction for different cases (for a disc with and without an inner hole). If there is no inner hole in the disc, then only 10% of the disc orientations allow outer radius  $R_{\text{out}}$  greater than  $0.1''$ . When  $R_{\text{in}} = 0.02''$ , this fraction grows to about 1/4. If the inner hole is even larger ( $0.05''$ ), only a small fraction of the orientations exclude the optically thick disc. This result is at least partially due to the already noted fact that S2 spends only  $\sim 0.5$  year behind the plane of the sky (Ghez et al., 2003b).

For the sake of the forthcoming data from the new observing season (i.e. in 2003), we added an extra point corresponding to the predicted S2 position on 2003.22. However the effect on the results was rather minor – the fraction  $F$  changed by only  $\sim 3\%$ . Finally, since the putative disc is very geometrically thin ( $H/R \sim 10^{-3}$ , Nayakshin et al., 2004), a nearly edge-on ( $\cos i = 0$ ) disc could be rather easily ‘hidden’.

### 2.2.4 Eclipses and flares for S2: Summary

Using the fact that the observations of the S2 star (Schödel et al., 2002; Schödel et al., 2003; Ghez et al., 2003b) showed no eclipses in the last 10 years or so we found that an optically thick disc with no inner hole (i.e.  $R_{\text{in}} = 0$ ) is allowed

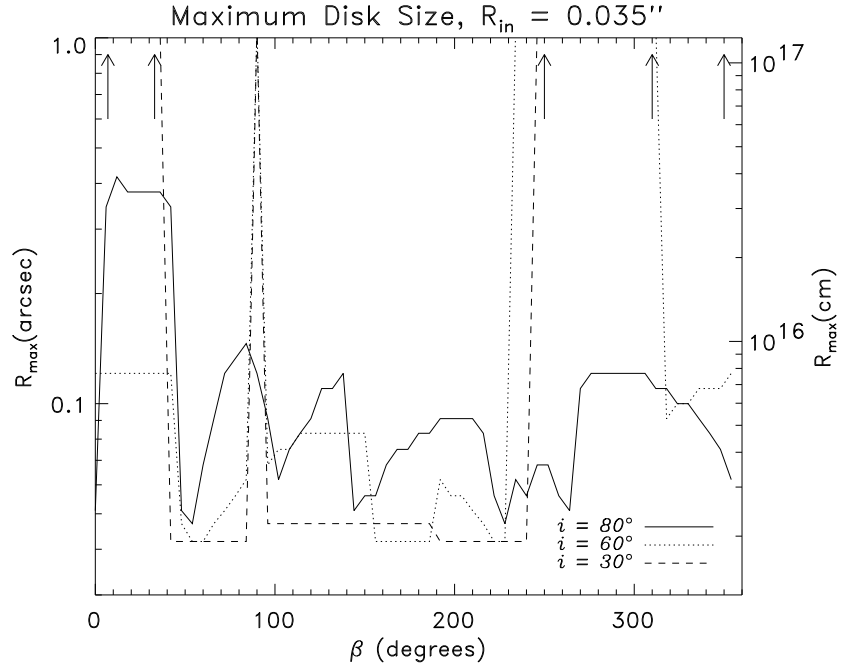


Figure 2.4: Maximum disc outer radius for different orientation angles in the case of a disc with inner radius of  $R_{\text{in}} = 0.035''$ . The maximum value of  $R_{\text{out}}$  is shown as a function of the rotation angle for three different values of the inclination angle (labelled in the Figure). The curves are not smooth because the number of the observed S2 positions is finite; have we had a full continuous coverage of S2 orbit from 1992 to 2002, the respective curves would become smooth functions. Vertical arrows at the top of the plot emphasise the fact that the outer disc radius can be arbitrarily large for the respective set of parameters. In general much larger discs are allowed if  $R_{\text{in}} \gtrsim$  few tens of a milli-arcsecond.

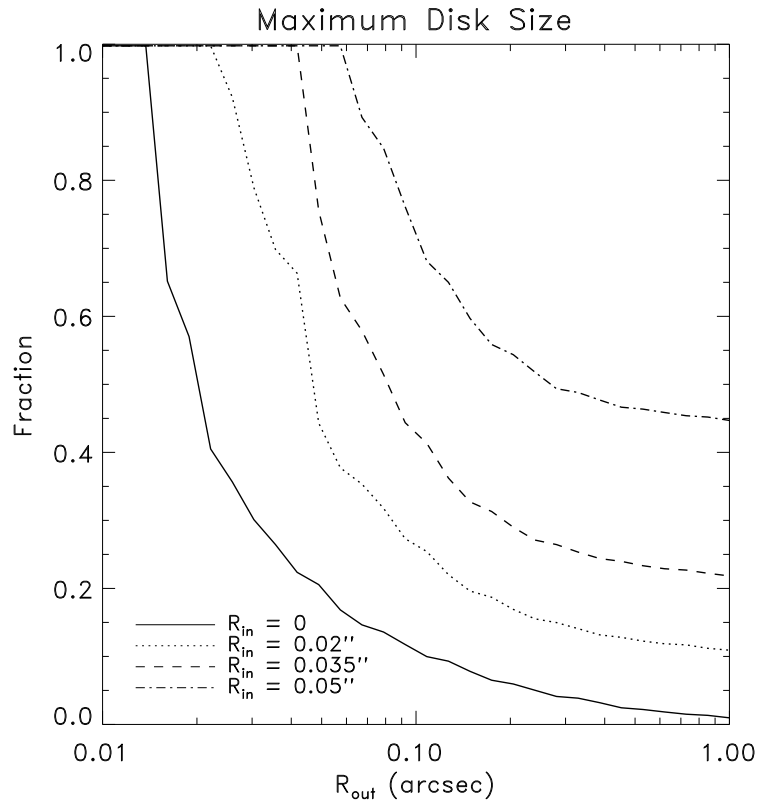


Figure 2.5: Fraction of the parameter space that permits a disc of a given  $R_{\text{out}}$ . The curves are for different values of  $R_{\text{in}}$  as marked in the Figure legend.

for only ‘small’ discs, with outer radii  $R_{\text{out}} \lesssim 0.1''$  (or about  $10^4 R_g \sim 10^{16}$  cm). On the other hand, if the disc has an inner hole due to frequent star passages or other reasons, with  $R_{\text{in}} \gtrsim 0.03''$ , then the eclipses are avoided in a large fraction of the parameter space by discs that have a relatively small inclination angle  $i$ . The outer disc radius in this case may be arbitrarily large.

It is important to point out that if the disc is optically thin, with optical depth  $\tau_K < 1$  in the near infrared  $K$  band, then the *eclipses are only partial* and therefore harder to observe. Due to the results of the next section we will see that this is the most likely situation for the Sgr A\* inactive disc (if there is one).

## 2.3 Disc reprocessed emission

### 2.3.1 Setup

The putative disc is heated by the optical and UV radiation of the member stars of the Sgr A\* stellar cluster. The bulk of the absorbed radiation will be re-emitted as the dust thermal emission in infrared frequencies. This radiation may be observable and thus it is desirable to determine the magnitude of the effect. In general the calculation is not trivial since the disc may be optically thick in some frequencies and yet optically thin in others, and hence a careful treatment of radiation transfer is needed. However, we will consider only the case of a disc optically thick in all frequencies.

#### Stellar spectrum

The star S2 is identified as a massive very bright main sequence star of stellar class between B0 and O8. In this range, the corresponding bolometric luminosity of the star is  $0.5 - 2 \times 10^5 L_\odot$  and the temperature is about 30,000 K (Ghez et al., 2003b). For simplicity, we calculate the ‘model’ spectral luminosity of the star as a pure blackbody with  $T = 30,000$  K and  $L_{\text{bol}} = 10^5 L_\odot$ . Observations of the Sgr A\* star cluster in the  $L'$  band (Genzel et al., 2003b) showed that S2 has an excess of about 0.6 magnitudes (or 30 mJy for S2’s parameters) in that band, compared with the ‘normal’ colours of the surrounding stars. This excess could be due to contamination of the star spectrum by the reprocessed emission of the disc. What we call below the ‘observed spectral luminosity’ in  $L'$  band is then the blackbody emission described above plus the excess measured by Genzel et al. (2003b).

#### The blackbody emission

The reprocessed disc emission is a function of time. The cooling time of the disc is much shorter than the star’s orbital period (usually by orders of magnitude). The reprocessed emission can then be calculated under the steady state assumption. The disc reprocessed spectrum is thus a function of geometry, i.e. the distance between the star and the disc,  $d$ . For convenience in this section,

we introduce a spherical coordinate system in which the disc plane coincides with the  $\theta = \pi/2$  plane, and the star is at the  $\theta = 0$  axis. The star's coordinates are thus  $(r, \phi, \theta) = (d, 0, 0)$ . (Note that the black hole is offset from the centre of these coordinates.)

We assume local black body emissivity for the disc. In this coordinate system the distance from a point  $(r, \phi, \pi/2)$  in the disc to the star is  $\sqrt{r^2 + d^2}$ . We thus treat the star as a point source and the disc as an infinitely thin plane. Clearly this approach is inaccurate for  $d \lesssim R_*$ , but we neglect this due to the very short duration of such a close approach. The effective temperature of a ring with radius  $r$  on the disc surface is

$$T_{\text{disc}}(r) = \left( \frac{L_* d}{4\pi\sigma} \right)^{1/4} \frac{1}{(r^2 + d^2)^{3/8}}, \quad (2.1)$$

where  $L_*$  is the star luminosity and  $\sigma$  is the Stefan-Boltzmann constant. Assuming the black body emissivity and integrating over  $r$ , we arrive at the integrated multicolour black body disc spectrum. If the disc is inclined at angle  $i$ , an additional factor of  $\cos i$  should be used.

### Photo-ionised layer of the disc

This simple approach (equation 2.1) to calculating the disc spectrum is an approximation of the more realistic situation. At the temperatures given by equation 2.1, that are usually  $T_{\text{disc}} \lesssim 10^3$  K, the main agent responsible for the disc opacity and emissivity is dust. In reality the ionising UV flux of the star will create a layer of completely ionised hydrogen on the top of the disc. The dominant role in this layer is played by the gas rather than the dust. Within this thin layer, the recombination rate will balance the influx of ionising photons from the star. Assuming a temperature of the order of  $10^4$  K for the layer, we find that its column depth is

$$N_{\text{H}} \sim 10^{18} n_{11}^{-1} d_{15}^{-2} \text{ cm}^{-2}, \quad (2.2)$$

where  $d_{15}$  is distance between the star and the disc in units of  $10^{15}$  cm, and  $n_{11}$  is the hydrogen nuclei density in units of  $10^{11} \text{ cm}^{-3}$ . This column depth is orders of magnitude smaller than that of the putative inactive disc, which was estimated by Nayakshin et al. (2004) to be in the range  $N_{\text{H}} \sim 10^{22} - 10^{25} \text{ cm}^{-2}$  in order to produce luminous enough X-ray flares (depending on the distance from Sgr A\* and taking model uncertainties into account). The thin layer will re-emit in the optical and the UV the incident stellar radiation. A fraction of the UV flux is emitted back out of the disc, and a fraction is emitted towards the disc, penetrating deeper and ionising deeper layers. The flux re-emitted below the Lyman limit (and below the corresponding thresholds for photo-ionisation of helium, oxygen and other abundant elements) can penetrate much deeper in the disc than the original ionising stellar photons. This radiation will be absorbed chiefly by the dust grains ‘deep’ inside the disc and then be emitted as the blackbody calculated in equation 2.1.

From this discussion it is clear that in reality a fraction of the incident UV radiation is reflected in the optical-UV band. Correspondingly, this fraction of the incident radiation should not be counted in equation 2.1. However, for the stellar spectrum that we assume here, i.e. the blackbody with  $T = 30,000$  K, only about 20% of the energy is emitted at frequencies above the Lyman limit, and therefore it seems that the shielding effect of the ionised layer should not be very large. Similarly, the dust scattering opacity could in certain wavelengths exceed that for the dust absorption, and then a significant fraction of the incident stellar radiation flux could be reflected back with no change in frequency. However we calculated (using Draine & Lee, 1984 optical constants and a Mie code provided by K. Dullemond) the dust opacity for several typical grain sizes and found that this occurs in a rather narrow range of conditions, and hence we neglected this effect.

We also estimated the Brackett  $\gamma$  ( $\lambda = 2.16\mu\text{m}$ ) line flux from this photo-ionised layer of gas. We used the number of ionising photons appropriate for a B0 star, a layer temperature of 10,000 K and the case B approximation (see Osterbrock, 1989). The resulting equivalent width of this line<sup>3</sup> is  $\sim 60$  Å, about twenty times larger than the absorption in the Br $\gamma$  line from the star itself (see Fig. 1 in Ghez et al., 2003b). In addition, we estimated the continuum free-free emission from the photo-ionised layer to yield  $\nu L_\nu \sim 10^{35}$  erg/sec at  $2.2\mu\text{m}$ , which is at the level of a few tenths of S2 spectral luminosity (see Fig. 2.6), above the current uncertainties in the flux of S2 (see Ott et al., 2003). Thus, if such a strong Brackett  $\gamma$  and the free-free continuum emission from the disc were present, they should have been detected by now.

However, the above estimates are extremely sensitive to the star's spectrum. Ghez et al. (2003b) conclude that S2 is an O8-B0 main-sequence star. If we assume that S2 spectral type is B0.5, then the number of photo-ionising photons decreases by a factor of  $\sim 8$ . Then both the line and the continuum disc decrease by the same factor. In addition, the PSF in the  $K_s$  band is comparable to the size of the emitting area of the disc. It is thus possible that a significant fraction of the ionised layer emission would be counted as a background 'local' gas emission. Indeed, (Ghez et al., 2003b) note that the background emission accounts for as much as 50 % of S2's flux. Hence to answer this question quantitatively, one needs to do a much more careful modelling of the disc emission, i.e. convolving the latter with the PSF instead of simply adding the two components.

Finally, due to a much faster disc rotation (compared to  $\sim 220$  km/s for S2; Ghez et al., 2003b) the Br $\gamma$  emission line should be 5-10 times broader<sup>4</sup> than the line from the star, making it more in line with the observed S2 and 'local gas' spectrum (Ghez et al., 2003b).

---

<sup>3</sup>This is so for any distance  $d$  because the line luminosity is  $\propto j_{\text{Br}\gamma} \pi d^2 n_{11} N_{\text{H}} \propto \text{const } j_{\text{Br}\gamma}$  according to equation 2.2

<sup>4</sup>Here we assume that the star-disc separation is of the order of the star's distance to the black hole,  $r_{\text{b}}$ , in which case a large fraction of the disc is illuminated by the star. If instead  $d \ll r_{\text{b}}$ , then the line may be mainly shifted but not significantly broadened.

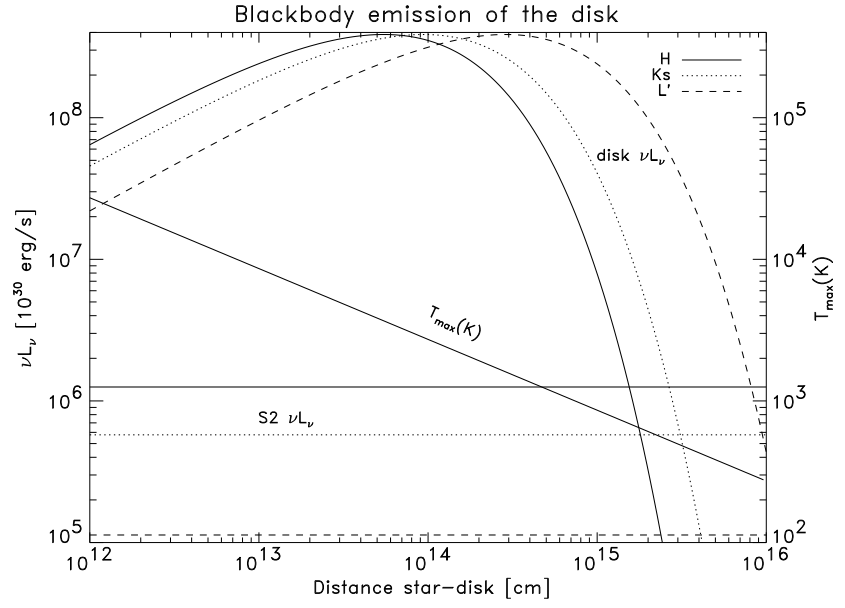


Figure 2.6: Spectral luminosity of the disc ( $\nu L_\nu$ ) illuminated by star S2 in the three near infrared bands (see legend in the Figure) as a function of the star-disc separation  $d$ . The disc is assumed to be face-on to the observer ( $i = 0$ ). The model spectral luminosity (see §2.3.1) of S2 is also shown on the bottom of the plot. The diagonal line shows the maximum gas temperature in the disc for the given distance (the scale is on the right). Note that the star is easily outshined by the disc for  $d \lesssim \text{few} 10^{15}$  cm.



### 2.3.2 Reprocessed emission of an infinite disc

In this section we study the reprocessed disc emission for discs with no inner hole and with an infinitely large outer radius (the disc is then a plane). In Fig. 2.6 we show the disc spectral luminosity, i.e.  $\nu L_\nu$ , (integrated over the  $4\pi$  steradian of the sky) for the frequencies corresponding to the infrared bands  $H$ ,  $K_s$  and  $L'$  ( $1.81$ ,  $1.38$  and  $0.79 \times 10^{14}$  Hz, or  $1.66$ ,  $2.18$  and  $3.80 \mu\text{m}$ , respectively), shown as a function of the star-disc separation  $d$ . The luminosity of S2 in these three bands is also shown for comparison with the horizontal lines on the bottom of the Figure. On the right vertical axis of the plot, the maximum effective temperature in the disc is shown.

Figure 2.6 shows that the contribution of the disc cannot be ignored for distances  $\lesssim \text{few} \times 10^{16}$  cm. S2 radiates in the Rayleigh-Jeans regime in the near infrared, and therefore only a small fraction of the star's bolometric luminosity is emitted at these frequencies. The disc captures a half of the star's bolometric luminosity (mostly optical-UV) and re-processes it into much smaller frequencies. Therefore the near infrared disc emission can be much brighter than the star. The distance of  $10^{16}$  cm is quite large in comparison to S2's pericentre ( $\sim 3 \times 10^{15}$  cm), and is of the order of S2's apocentre. Therefore the reprocessed emission could be expected to be large for S2 for the whole of the year 2002.

Figure 2.6 also indicates that the optically thick disc assumption may actually break down when the star is too close to the disc. Some of the dust species are destroyed (evaporated) when the dust temperature is greater than several hundred Kelvin, and at  $T \sim 1,500$  K the dust can be nearly completely destroyed. Therefore our treatment is not accurate for  $d \lesssim 10^{15}$  cm, where the results will be dependent on the exact disc column depth, dust properties, etc. We overestimate the disc emission at these small distances, and hence the maxima reached by the curves in Figure 2.6 will be in reality smaller by factors of a few to ten. Nevertheless it is clear that the disc emission would still dominate over the S2 emission and this fact will be sufficient for our further analysis.

One important simplifying assumption that we make while performing these calculations is the following. In equation 2.1 it is explicitly assumed that the illuminated side of the disc faces the observer, i.e. that the star is in front of the disc. In the opposite case the results depend on the mean optical depth of the disc,  $\tau$ . Approximately, the radiation emitted from the back side of the disc will be reduced by a factor of  $\sim 1/\tau$ . In what follows we neglect this effect, i.e. we assume that the front and the back side of the disc radiate the same spectrum which is roughly correct for  $\tau$  not too much larger than unity. In the following figures, however, we point out the times when the star was behind the disc; the thermal disc emission at these times should be remembered to be smaller than that indicated in the figures by an amount depending on  $\tau$ . To show the maximum possible effect of this complication, we simply turned off all the NIR emission during an eclipse for one particular calculation (see Fig. 2.8). Our main conclusion – a rather unlikely presence of an *optically thick* disc in Sgr A\* – is unchanged, and thus a better treatment of the back-side illuminated disc is not necessary.

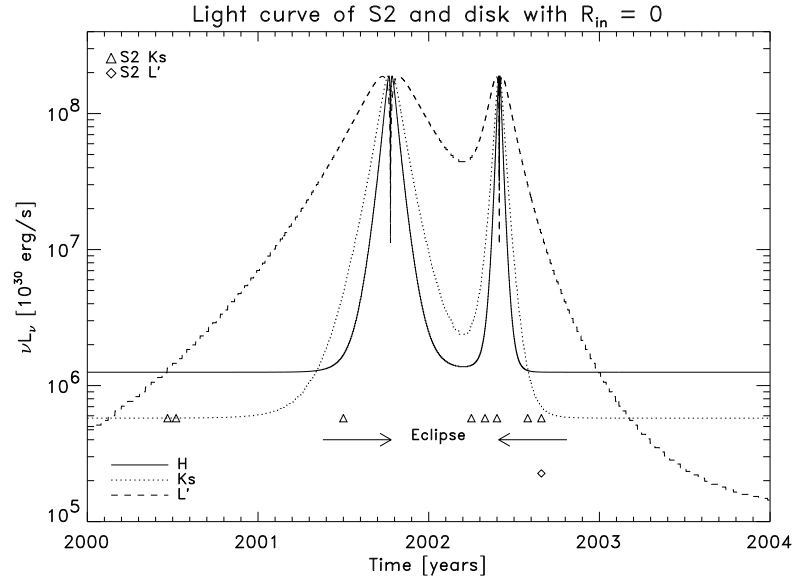


Figure 2.7: NIR light curves of S2 and the disc reprocessed emission for  $i = 60^\circ$  and  $\beta = 300^\circ$ . The triangles show the epochs in which Schödel et al. (2002); Schödel et al. (2003) observed this star. The corresponding ‘observed’ stellar luminosity is the model spectral luminosity in the  $K_s$  band calculated as explained in §2.3.1. The diamond shows the model spectral luminosity of S2 plus the excess in the  $L'$  band as observed (Genzel et al., 2003b; note that there exists only one detection of S2 in  $L'$  band so far).

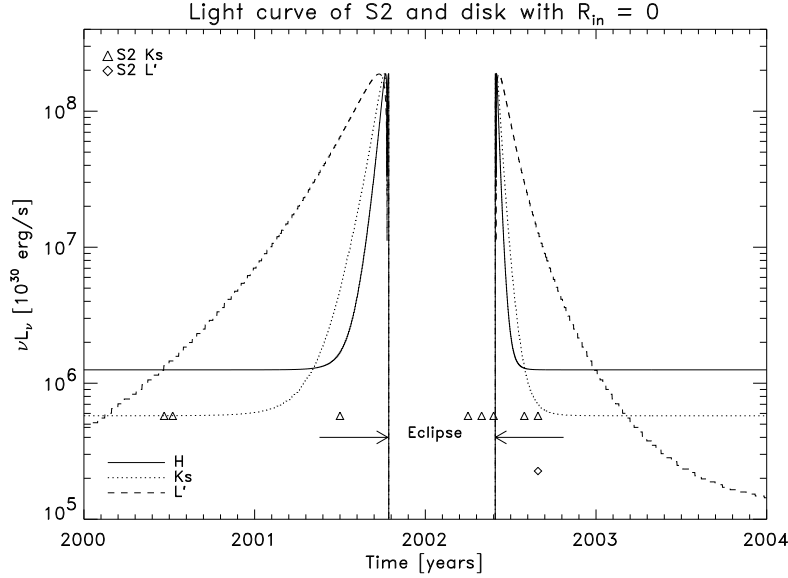


Figure 2.8: Same as Fig. 2.7, but assuming that both the stellar and the reprocessed emission are completely unobservable during the eclipse.

### 2.3.3 The reprocessed disc emission for S2's orbit

We now calculate the combined star plus disc luminosity for S2 (Figure 2.7), first assuming that the disc is inclined at  $i = 60^\circ$  and that rotation angle  $\beta = 300^\circ$ . The triangles show the times when Schödel et al. (2002); Schödel et al. (2003) actually observed the star. The maximum near infrared luminosity reached by the source is the same, roughly half the star's bolometric luminosity, in all the three frequency bands. The maxima are reached nearly simultaneously around the time when the star physically crosses the disc. The very sharp drops in the disc luminosity near the maxima are simply due to the fact that the disc becomes 'too' hot when the star is very close to the surface of the disc (e.g., see Fig. 2.6). In this case the three near infrared bands are on the Rayleigh-Jeans part of the disc blackbody curves and the emission is therefore weak.

The part of the light curve between the two maxima in  $\simeq 2001.8$  and  $\simeq 2002.4$  is the time when the star is eclipsed by the disc so that the disc emission should be actually reduced at these moments as we explained above. In Fig. 2.8 we show the extreme case when the optical depth of the disc is so high that all the emission is absorbed by the disc material during the eclipse. Comparing the Figs. 2.7 and 2.8, we observe that *any optically thick* infinite disc, oriented as in these Figures, is ruled out by the existing data. There has been no change in S2's  $K_s$  band flux down to  $\sim 10 - 20\%$  level for all 10 years of the observations (private communication from R. Schödel).

We test the sensitivity of the result on the disc inclination angle,  $i$ , in Fig.

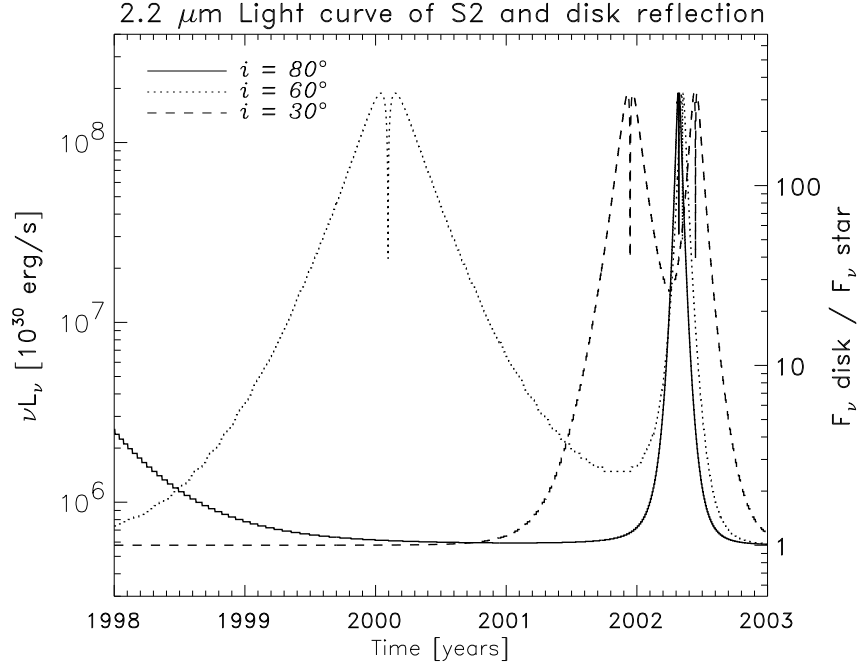


Figure 2.9: Model spectral luminosity of S2 plus the disc reemission at  $2.2 \mu\text{m}$  as a function of time for discs with  $\beta = 80^\circ$  and different inclination angles.  $R_{\text{in}} = 0$  for this Figure.

2.9, where we fix the disc rotation angle,  $\beta = 350^\circ$ , but vary  $i$ . Three different values of  $i$  ( $30^\circ$ ,  $60^\circ$  and  $80^\circ$ ) are chosen. Only the  $K_s$  luminosity of the star plus disc system is shown. The maximum near infrared luminosity reached by the three curves is the same as in Figure 2.7, but the times of the maxima and the width of the curves are different. It is apparent that it is hard to escape the tight observational constraints unless the disc is oriented exactly edge on to the observer.

Finally, we perform a search in the parameter space in a manner similar to that done in §2.2.3. In particular, we make a fine grid in the disc orientation parameter space. For every combination of  $\cos i$  and  $\beta$ , we determine the  $K_s$  luminosity of the disc at the epochs when S2 was actually observed by Schödel et al. (2003). We then pick the maximum of these values. The disc  $K_s$  luminosity found in this way is the maximum luminosity that should have been observed by Schödel et al. (2003) for given  $\cos i$  and  $\beta$ . The result is displayed in Figure 2.10 where we show the ratio of the disc flux to that of the star for the three NIR frequencies, averaged over  $\beta$ . Except for nearly edge-on discs, the reprocessed emission should have been detected by now. Since this effect has not been observed, we can rule out the existence of an optically thick disc with no inner

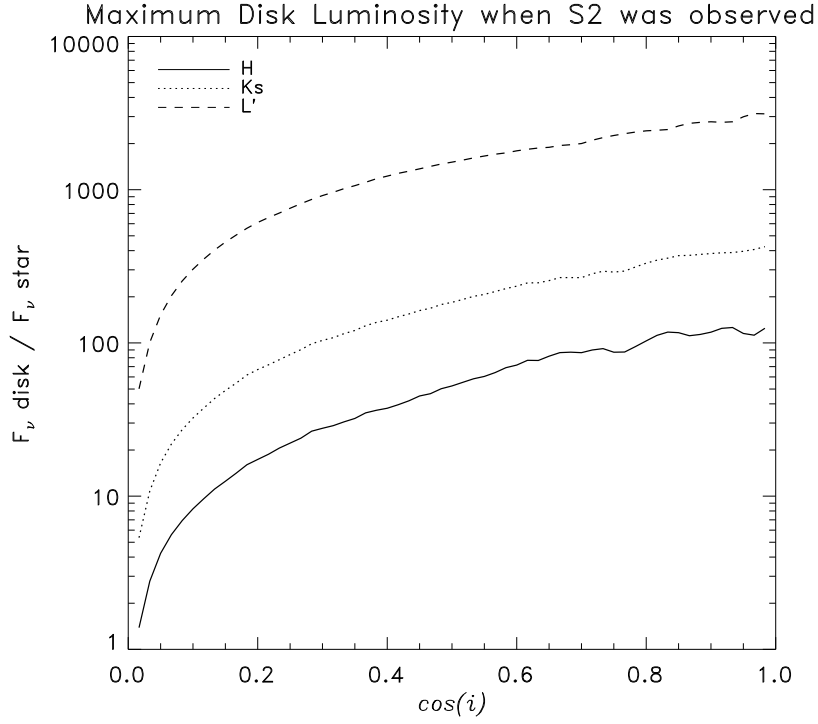


Figure 2.10: Maximum spectral luminosity of the disc in the three NIR bands that should have been detected by Schödel et al. (2003) if an optically thick disc with  $R_{\text{in}} = 0$  was present in Sgr A\*. The luminosity is shown in units of S2 spectral luminosity as a function of the disc inclination angle. Note that the disc is always much brighter than the star in the infrared except for the nearly edge-on orientation.

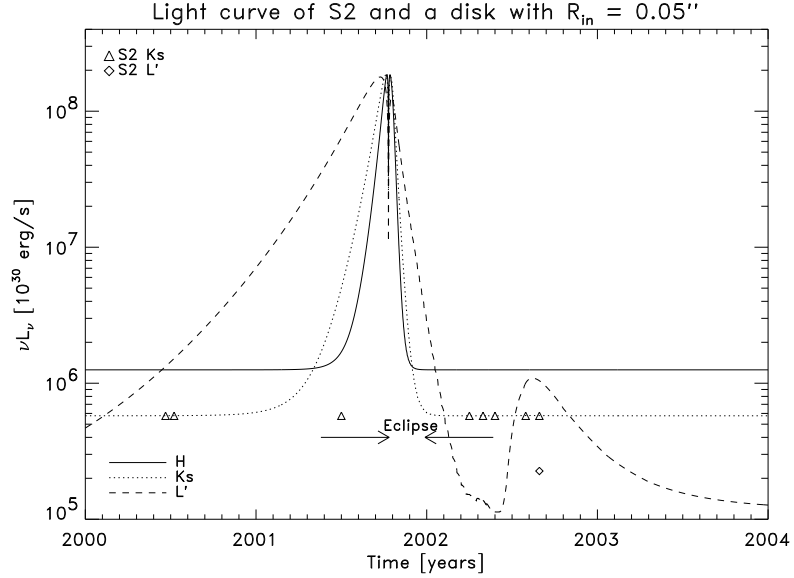


Figure 2.11: Same as Fig. 2.7 but for a disc with an inner hole of  $R_{\text{in}} = 0.05''$ . Note the absence of the second maxima in the  $H$ - and  $K_s$  bands. However the  $L'$  band excess is still much larger than observed.

hole in Sgr A\*.

### 2.3.4 The case of S2 and discs with empty inner regions

We now perform similar calculations but allowing the disc to have an inner hole of a given size  $R_{\text{in}} \neq 0$ . Figure 2.11 shows the light curves in the three frequency bands for the disc inclined at  $i = 60^\circ$  and  $\beta = 300^\circ$ , with  $R_{\text{in}} = 0.05''$ . Comparing the light curves with those shown in Fig. 2.7, the most striking difference is the absence of the second maximum in the  $H$  and  $K_s$  bands. This is due to the fact that there is now only one crossing of the disc with the star – in 2001.8 – while the second crossing shown in Fig. 2.7 does not occur because there is no inner disc for  $R < R_{\text{in}}$ . Nevertheless the strength of the first maximum is such that such a disc is still ruled out.

We then repeated the same calculation (same  $i$  and  $\beta$ ) but with a larger inner hole radius,  $R_{\text{in}} = 0.1''$ . The result is shown in Fig. 2.12. Since the star is relatively far from the disc surface for all of its orbit for these particular disc parameters, there are no eclipses or detectable increases in the  $H$  or  $K_s$  bands. Further, until 2002, the S2 star had not been detected in the  $L'$  band, therefore the light curves in Fig. 2.12 appear to be consistent with the observations. In fact, we feel that by adjusting the disc parameters it is possible to obtain the  $L'$  band spectral excess similar to that observed by Genzel et al. (2003b). We

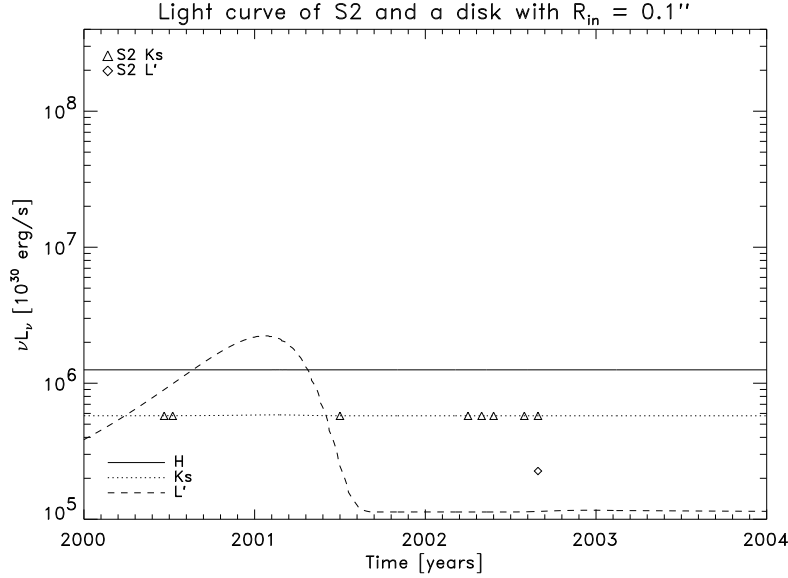


Figure 2.12: Same as Fig. 2.11 but for a larger inner disc hole,  $R_{\text{in}} = 0.1''$ . Note that such a disc does satisfy the observational constraints: there are no eclipses or transient brightening in the  $K_s$  band due to disc re-emission of the star's radiation.

shall explore this in detail in future papers.

### 2.3.5 Summary: constraints due to disc reprocessed emission

We have shown that the reprocessed emission of the disc illuminated by the star is a very powerful constraint on the disc presence and/or properties. In fact, the effect is ‘stronger’ than stellar eclipses that we studied in §2.2 (see also Nayakshin & Sunyaev, 2003). The luminous stars emit most of their radiation in the visible and UV ranges. The disc re-processes this emission in the NIR band which then appears much brighter than the star itself in the same frequency. We have seen that the reprocessed NIR disc emission is up to a factor of 100 higher than that of the star. At the same time eclipses yield an effect of order unity.

Analysing the predicted NIR light curves for S2 we found that an optically thin disc with a very small inner hole  $R_{\text{in}} \simeq 0$  is ruled out. The disc emission would have been seen by now, whereas observations do not show any variability in S2  $K$  band fluxes. We then tested discs with non-zero values of  $R_{\text{in}}$ , and found that only for rather large values of  $R_{\text{in}} \gtrsim 0.1''$  are such discs permitted.

## 2.4 Star cluster asymmetry due to stellar eclipses

In §2.2 we explored the eclipses of the individual stars by the putative optically thick disc. To observe such eclipses one should be able to resolve individual star's orbits, which is extremely difficult and has been made possible only for our Galactic Centre (see Schödel et al., 2003; Ghez et al., 2003a). At the same time, similar eclipses of *unresolved* stars of the cluster should also be occurring, and hence one may hope to detect the disc 'shadow' on the background emission of the nuclear cluster. In doing the calculations below, we will be concerned with the optical-UV emission rather than with the infrared, as we were in the previous sections. Our working assumption is that the visible and UV flux incident on the disc is absorbed and reprocessed into the near infrared emission (see §2.3), reflecting only a small fraction of the radiation in the visible-UV range. Hence we treat the disc as an optically thick absorbing surface in this section.

We will only consider discs with no inner holes, i.e.  $R_{\text{in}} = 0$ , since the instrument resolution (for other than Sgr A\* galactic centres) is usually worse than the actual non-zero value of  $R_{\text{in}}$ . Note that an enhanced emission from the inner hole could in principle be detected, but *its asymmetry* is currently impossible to resolve. In addition, the star cluster is assumed to be spherically symmetric. For this reason the angle  $\beta$  is no longer of importance. Instead we define the  $xyz$  coordinate system, with  $z$  axis directed straight to us, and  $x$  and  $y$  as in Fig. 2.13. The  $x$  axis is positive where the disc is closer to the observer.

We also define the column density of stars along the line of sight,  $N(x, y)$ , as the integral of the star density,  $n(\vec{R})$ , through the line of sight from the disc to the observer, located at infinity,

$$N(x, y) = \int_{z'}^{\infty} n(\vec{R}) dz. \quad (2.3)$$

where  $z' = -\infty$  if the line of sight does not intercept the disc projection, and  $z' = z_{\text{disc}}$ , the respective  $z$ -coordinate of the disc in the opposite case. For exactness, we take the spherically symmetric density profile  $n(R) \propto R^{-\alpha}$  with  $\alpha = 1.4$  for  $R < R_{\text{cusp}} \sim 10''$  given by Genzel et al. (2003b) and consider the case where  $R_{\text{out}} \ll R_{\text{cusp}}$ .

In Fig. 2.13 we show the resulting map of the stellar column density for the disc inclination angle  $i = 80^\circ$ . The projection of the disc shadow is clearly seen. The boundaries of the disc appear as sharp discontinuities in the surface brightness of the star cluster. This effect is strongest near the side of the disc that is closer to the observer (positive  $x$  in Figure 2.13).

Also note that the star cluster image appears anisotropic on all scales smaller than the disc outer radius. This fact allows us to introduce an 'anisotropy measure',  $A$ , defined as

$$A(r) = \frac{\sqrt{\Delta N^2(r)}}{\overline{N}(r)}, \quad (2.4)$$

where  $\overline{N}(r)$  is the angle-averaged number count of stars at projected distance  $r$



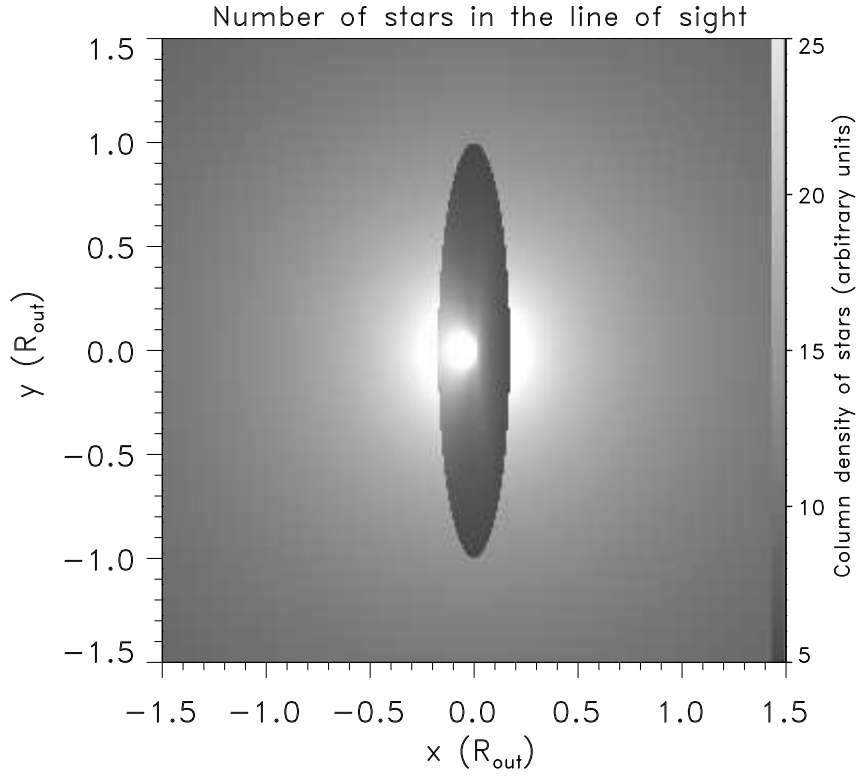


Figure 2.13: Image of the star cluster shaded by a disc with inclination angle  $i = 80^\circ$ . The brighter areas correspond to larger line of sight column density of stars (the scale is shown on the right of the Figure).

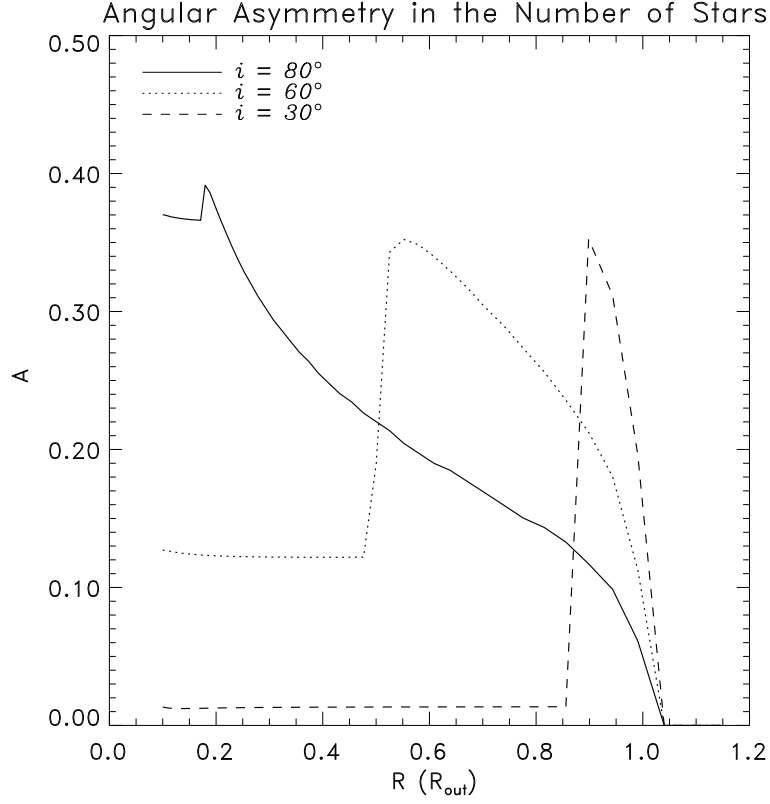


Figure 2.14: Anisotropy measure for a ‘small’ disc ( $R_{\text{out}} \ll R_{\text{cusp}}$ ) and three values of the disc inclination angle,  $i = 80^\circ$  (solid line),  $60^\circ$  (dotted) and  $30^\circ$  (dashed).

from the star cluster centre away:

$$\overline{N(r)} = \frac{1}{2\pi} \int_0^{2\pi} N(r, \phi) d\phi. \quad (2.5)$$

Here we used in the plane of the sky the common polar ( $r - \phi$ ) coordinates centred on the black hole. We also defined  $\overline{N^2(r)}$  in an analogous way and then  $\overline{\Delta N^2(r)} = \overline{N^2(r)} - (\overline{N(r)})^2$ .

The anisotropy measure is independent of the disc orientation in the plane of the sky (i.e. angle  $\beta$ ; see Fig. 2.1). It is also independent of the absolute luminosity of the star cluster. Fig. 2.14 shows the anisotropy measure for three different values of the disc inclination angle as a function of radius  $R$  in units of the disc radius  $R_{\text{out}}$ . For small inclination angles,  $i \lesssim 30^\circ$ ,  $A(R)$  is nearly zero in the innermost part of the disc since there is little variation in  $N(x, y)$  along the circle with  $R < R_{\text{out}} \cos i$ . However for  $R > R_{\text{out}} \cos i$ ,

the projected semi-minor axis of the disc, the anisotropy measure is as high as 0.3, which is due to the high contrast between  $N(R, 0)$  and  $N(0, R)$ . The case of the moderate inclination angle,  $i = 60^\circ$  shows that the anisotropy measure increases in the innermost parts of the cluster, and there is again a maximum around  $R = R_{\text{out}} \cos i$ . This maximum appears to be the feature with which one may attempt to identify the disc inclination angle, if radius  $R_{\text{out}}$  of the disc could be inferred from independent considerations. Finally, the case of a very highly inclined disc,  $i = 80^\circ$ , is mostly a declining curve (after  $R = R_{\text{out}} \cos i$ ).

This method has the advantage that no individual stellar orbits are needed. As the time scales for disc evolution are very long, data collected over many years and even tens of years may be combined to try to resolve the innermost region of the star cluster.

## 2.5 Discussion

In this paper we studied three ways to detect the disc presence in the infrared and optical/UV frequencies, and we then applied them to the particular case of Sgr A\*. We found that the orbit of star S2 alone requires the disc to be optically thin with near infrared optical depth no larger than  $\sim 0.01$ . We now discuss in greater detail the physical motivation for believing there may be a disc in Sgr A\*, and the implications of this paper's results for the disc hypothesis.

### 2.5.1 A cold disc in Sgr A\*?

Sgr A\* is thought to be physically similar to Low Luminosity AGNs (Ho, 1999) since as long as radiative cooling is not important, the dynamics of the accreting gas should be independent of the actual accretion rate (e.g., see review by Narayan, 2002). Ho (2003) noted that cold discs seem to be one of the established features of LLAGN. From spectral energy distributions and from profiles of the double-peaked emission lines, the inner radii of these discs are in the range  $\sim 10^2 - 10^3 R_g$  (see Quataert et al., 1999; Ho, 2003). By analogy, such a disc can be expected to exist in the Galactic Centre.

Furthermore, Nayakshin & Sunyaev (2003) suggested that star-disc crossings may be the process that emits X-ray flares observed in Sgr A\* (Baganoff et al., 2001; Goldwurm et al., 2003). While crossing the disc, the stars drive shocks into the disc material; the gas is heated to temperatures of the order of  $10^7 - 10^9$  K and emits X-rays. Nayakshin et al. (2004) showed that the number of star-disc crossings per day, given by the observed distribution of stars in Sgr A\* (Genzel et al., 2003b) is close to the observed rate of X-ray flaring (Baganoff et al., 2003); the predicted flare duration and multi-frequency spectra are in a broad agreement with the observations. Nayakshin (2003) also suggested that the disc may be an effective cooling surface for the hot winds, and that the hot flow is essentially frozen at large radii, preventing it from piling up at small radii. This suggestion could be a part of the explanation for the observed dimness of

Sgr A\*, although there are other possible explanations (see e.g. the review by Quataert, 2003, and further references there).

Levin & Beloborodov (2003), using data of Genzel et al. (2000), recently concluded that most of the innermost young bright Helium-I stars (that are thought to ‘feed’ Sgr A\* by producing powerful hot winds) line up in a single plane. This result makes it very likely that these hot young stars may have been created from a single large molecular cloud that was compressed to high densities that led to star formation. It is not possible that all of the gas in the molecular cloud would turn into stars; the remainder would have to form a relatively massive gaseous disc, similar to the bright discs of AGN. A tiny not accreted remnant of the original disc could then still be present (Nayakshin, 2003; Nayakshin et al., 2004).

Finally, Genzel et al. (2003b) report discovery of an infrared excess in the spectrum of S2 in 2002 (e.g., see Fig. 2.7) as compared to other similar sources in the region. Namely, S2 appeared to be brighter by  $\sim 0.6$  magnitude in the  $\lambda = 3.8\mu\text{m}$  ( $L'$  band) compared to what is expected from the spectra of other bright nearby stars. Such an excess is usually interpreted as evidence for dust presence around the star (e.g., Scoville & Kwan, 1976). In the absence of the inactive (dusty) disc, the only source of dust would have to be the hot  $T \lesssim 10^9$  K flow itself (Genzel et al., 2003b). While this is not physically impossible, the presence of the dust in a  $T \lesssim 10^9$  K gas is somewhat problematic as the dust can be destroyed by sputtering in such a gas (e.g., Draine & Salpeter, 1979). Our estimates show that all but the largest interstellar grains would be destroyed by the sputtering by the time the gas reaches radii of the order of S2’s pericentre. We suggest that the re-processing of the stellar radiation in a putative disc could be an alternative way to explain the infrared excess of S2. Whereas an optically thick disc that we explored in this paper produces in fact too strong an excess, an optically thin disc (with ‘right’ orientation and  $R_{\text{in}}$  values) appears to be promising in this regard (see Fig. 2.12).

## 2.5.2 Constraints on the disc in Sgr A\*

### Optically thick disc

As we have shown in §2.2, the so far absent eclipses of the star S2 (Schödel et al., 2002; Schödel et al., 2003; Ghez et al., 2003b) require an optically thick disc to have a relatively large inner hole  $R_{\text{in}} \gtrsim \text{few} \times 10^{-2}$  arcsecond (or equivalently  $\text{few} \times 10^{15}$  cm). A hole with these dimensions is not unreasonable (e.g., Nayakshin et al., 2004). However in §2.3 we showed that the disc reprocessed emission yields an even stronger signature than eclipses. We found that the disc with no inner hole and a very large  $R_{\text{out}}$  is incompatible with the observations for any combination of disc orientation angles. We then tested the case of a non-zero value for  $R_{\text{in}}$  and found that *only discs with inner holes as large as  $0.1'' \sim 10^{16}$  cm  $\sim 10^4 R_g$  yield NIR ‘echoes’ that are weak enough to escape the observational constraints.* As such, our results are in complete agreement with the previous results by Falcke & Melia (1997) and Narayan (2002), who also

ruled out the existence of an *optically thick disc with  $R_{\text{in}} = 0$  in Sgr A\**.

### Optically thin disc

It is possible to make rough estimates on how optically thin the disc should be to satisfy the observational constraints. For this we simply assume that the opacity of the grains is gray, in which case the grain temperature should be equal to the effective one (equation 2.1). Then the disc spectral luminosity is that calculated in this paper but scaled down by factor of  $\simeq \tau \ll 1$ , where  $\tau$  is the grey disc optical depth in the NIR. Referring now to Fig. 2.7, we see that in the maximum the  $K_s$  band disc spectral luminosity exceeds that of the star by a factor of several hundred.  $K_s$  flux did not vary within 10 – 20% uncertainty during the last 10 years of S2 observations (private communications from R. Genzel and R. Schödel). On the other hand the background cluster emission accounts for as much as 50% of the flux in  $K_s$  band (Ghez et al., 2003b), and hence we estimate that the optical depth of the disc at  $2.2\mu\text{m}$  should be no larger than  $\tau \sim 10^{-2}$ . However, if  $R_{\text{in}} \neq 0$ , the constraints imposed by the 2002 measured positions can be relaxed and a larger optical depth might be consistent with the observations.

To produce X-ray flares via star-disc interactions as luminous as observed, the mid-plane surface density of the disc was estimated by Nayakshin et al. (2004) at around  $10^{11}$  hydrogen nuclei per  $\text{cm}^3$  (although we note that due to the simplicity of the calculations this value is uncertain by up to a factor of 10). With this the disc surface density,  $\Sigma$ , was estimated as  $\Sigma \sim 1 r_4^{3/2} \text{ g/cm}^2$ , where  $r_4$  is disc radius in units of  $10^4$  gravitational radii,  $R_g$ . For  $R = 0.03'' \simeq 4 \times 10^3 R_g$ , we have  $\Sigma \simeq 0.2 \text{ g/cm}^2$ . Using the standard interstellar grain opacity and dust-to-gas mass ratio, one gets opacity at  $2.2 \mu\text{m}$  of  $\tau_{2.2} \simeq 0.6$  (see Figure 1 in Voshchinnikov, 2002). Such a disc would violate the constraints that we obtained in this paper. Even assuming that Nayakshin et al. (2004) overestimated the mid-plane density by a factor of 10, the NIR opacity still appears to be a little too large.

On the other hand, the dust grains are destroyed with each star's passage. The smallest grains are especially vulnerable to such destruction. Of course when the star leaves the disc, the dust will reform. With the gas densities as high as  $10^{11} \text{ cm}^{-3}$ , the dust grains could grow at a rate as large as  $10^{-3} \text{ cm/year}$  (Nayakshin et al., 2004). In addition, because only the largest grains survive the star passages, the large grains will grow preferentially. Therefore, the combination of the repeated dust destruction and dust growth could create larger grains than in the interstellar medium. Using the optical constants from Draine & Lee (1984) and a simple Mie theory code to compute dust opacity (provided by K. Dullemond), we estimated that for the standard dust-to-gas mass ratio of 0.01 the NIR opacity is reduced to a  $\sim 1/10$ th of its interstellar value at  $2.2 \mu\text{m}$  if the typical grain size is  $a \gtrsim 30\mu\text{m}$ .

### 2.5.3 Star cluster asymmetry due to disc presence

In §2.4 we considered the effects of the disc on the appearance of the integrated star cluster brightness along a given line of sight. The disc was assumed to be optically thick and completely absorbing at the relevant wavelength (i.e. optical or UV). We found that the disc (obviously) imprints a shadow on the star cluster light. We then defined the ‘asymmetry measure’ parameter  $A$ , defined in equation 2.4, which appears to be a convenient indicator of the disc presence. In particular, as a function of radial distance from the star cluster centre,  $A(r)$  has a clearly defined shape with characteristic features that could be used to constrain the inclination of the disc. Observational determination of  $A(r)$  may thus allow one to observationally test the disc presence in the nuclear stellar clusters of nearby galaxies.

## 2.6 Conclusions

In this paper we studied some of the potentially observable signatures of a cold disc presence in our Galactic Centre, and in the centres of other galaxies. Such discs may be the remnants of previously active, i.e. accreting, discs. This work is essentially an expansion of the ideas presented in Nayakshin & Sunyaev (2003) via (i) using the exact and updated S2 star orbit in the study of possible eclipses of S2; (ii) including new effects – disc re-processing and star cluster anisotropy. Our present work is also complementary to that of Nayakshin et al. (2004) who studied X-ray and near infrared flares produced when stars pass through the cold disc.

The strongest of the three effects considered in the paper turned out to be the re-processing of the stellar visible radiation into the near infrared bands (§2.3). We found that if an *optically thick disc* were present in Sgr A\*, the reprocessed emission of the bright star S2 would have been observed by now in all  $H$ ,  $K_s$  and  $L'$  near infrared bands. Since this contradicts to the data, an optically thick disc would have to have a rather large inner radius,  $R_{\text{in}} \gtrsim 0.1'' \sim 10^4 R_g \sim 10^{16}$  cm.

At the same time, the observed  $L'$  band excess in S2’s spectrum in the year 2002 (Genzel et al., 2003b) is most naturally interpreted as a signature of the re-processing of S2 stellar radiation in this band. We estimated that the disc invoked by Nayakshin et al. (2004) would have the ‘right’ dust opacity if the minimum size of the grains in the disc would be about  $30\mu\text{m}$ . Such a large minimum grain size may be the result of the unusually high (by interstellar standards) density in the disc and the too frequent stellar passages through the disc. Therefore, *both the X-ray flares of Sgr A\* and the mid-infrared excess of S2 in 2002 may be the result of the interactions of stars with an optically thin inactive disc.*

## Chapter 3

# A self-gravitating accretion disc in Sgr A\* a few million years ago: is Sgr A\* a failed quasar?

Originally published by Nayakshin & Cuadra in *Astronomy & Astrophysics* **437**, 437

*Sgr A\* is extra-ordinarily dim in all wavelengths requiring a very low accretion rate at the present time. However, at a radial distance of a fraction of a parsec from Sgr A\*, two rings populated by young massive stars suggest a recent burst of star formation in a rather hostile environment. Here we explore two ways of creating such young stellar rings with a gaseous accretion disc: by self-gravity in a massive disc, and by capturing ‘old’ low mass stars and growing them via gas accretion in a disc. The minimum disc mass is above  $10^4 M_\odot$  for the first mechanism and is few tens of times larger for the second one. The observed relatively small velocity dispersion of the stars rules out discs more massive than around  $10^5 M_\odot$ : heavier stellar or gas discs would warp each other too strongly by orbital precession in an axisymmetric potential. The capture of ‘old’ stars by a disc is thus unlikely as the origin of the young stellar discs. The absence of a massive nuclear gas disc in Sgr A\* now implies that the disc was either accreted by the SMBH, which would then imply almost a quasar-like luminosity for Sgr A\*, or was consumed in the star formation episode. The latter possibility appears to be more likely on theoretical grounds. We also consider whether accretion disc plane changes, expected to occur due to fluctuations in the angular momentum of gas infalling into the central parsec of a galaxy, would dislodge the embedded stars from the disc midplane. We find that the stars leave the disc midplane only if the disc orientation changes on time scales much shorter than*

the disc viscous time.

### 3.1 Introduction

The complex chain of events leading to the growth of super-massive black holes (SMBHs) in galactic centres is not yet fully understood (e.g., Rees, 2002). Nevertheless, gas accretion is probably the dominant physical process delivering the matter to the giant black holes (e.g., Yu & Tremaine, 2002). At small radial distances from the SMBH, the standard thin accretion disc (Shakura & Sunyaev, 1973) appears to be an appropriate way to provide the SMBH with gas at rates approaching the Eddington limit. However, at distances larger than  $\sim 10^{-2}$  parsec from the SMBH, standard thin discs face several problems.

First, the time necessary for the gas to inflow into the black hole – the disc viscous time scale – becomes too long (e.g. as large as  $10^8$ – $10^{10}$  years for larger radii). In parallel with this, the (standard accretion) disc mass becomes very large. When the latter exceeds about 1 % of the SMBH mass, local gravitational instabilities develop (e.g., Paczyński, 1978; Kolykhalov & Sunyaev, 1980; Shlosman & Begelman, 1989; Goodman, 2003; Collin & Zahn, 1999). The structure of such discs is unclear (see §3.9) due to uncertainties in theory and a dearth of relevant observations.

Sgr A\* is the closest SMBH (with a mass  $M_{\text{BH}} \approx 3 \times 10^6 M_{\odot}$ ; e.g., Schödel et al., 2002). Although Sgr A\* has remained extremely dim during the entire history of X-ray observations, there are hints that it was much more active in the past. The X-ray and  $\gamma$ -ray spectrum of the giant molecular cloud Sgr B2 is most naturally explained as a time-delayed reflection of a source with a flat AGN-like spectrum (e.g., Sunyaev et al., 1993; Koyama et al., 1996; Revnivtsev et al., 2004). The required luminosity is in the range of  $\sim \text{few} \times 10^{39}$  erg/sec, too high by Galactic standards. Sgr A\* is then strongly suspected of having been brighter in X-rays by some 6 orders of magnitude 300–400 years ago.

Deeper in the past, a few million years ago, few dozen massive stars were formed and are currently at a distance of the order of 0.1–0.3 pc from Sgr A\* (Krabbe et al., 1995; Genzel et al., 2003b; Ghez et al., 2003b). This is surprising given that the tidal force of the SMBH would easily shear even gas clouds with densities orders of magnitude higher than the highest density cores of GMCs observed in the Galaxy.

*In situ* star formation scenarios for the Sgr A\* young massive stars have been numerically studied by Sanders (1998) with a sticky-particle code and also qualitatively described by Morris, Ghez, & Becklin (1999). In particular, one of the simulations done by Sanders (1998) assumed that a cold cloud of gas with radial dimensions of 0.4 pc and with a small angular momentum falls into Sgr A\* gravitational potential starting from a distance of 2.4 parsec. The cloud gets tidally sheared into a thin band of gas which then forms a precessing eccentric ring. Frequent shocks are assumed to lead to strong compression of the gas and star formation.

The existence of such low angular momentum clouds seems to be question-



able. In addition, the initial conditions of the simulations are rather extreme: to be stable against tidal shear (e.g., eq. 1 of Sanders, 1998), the cloud mass should be  $M_{\text{cl}} \gtrsim 7 \times 10^4 M_{\odot}$ , a very large mass for a cloud of 0.4 pc in size. Recent observations (Liszt, 2003) seem to contradict the Sanders (1998) model for the ionised gas streamers. Genzel et al. (2003b) discount current star formation in the mini-spiral, which is believed to be an ionised streamer. Genzel et al. (2003b) also note more generally that ‘if massive stars are forming frequently in dense gas streamers when outside the central parsec and then rapidly move through the central region, one would expect  $\sim 100$  times as many massive stars outside the central region as in the central parsec’, which is not the case observationally.

Alternatively to the *in situ* star formation, Gerhard (2001) proposed that the young massive stars could have been formed outside the central parsec in a massive star cluster. Then, due to dynamical friction with the older population of background stars, the cluster would have been dragged into the central parsec and then dissolved there by the SMBH tidal shear. However, this appears to be only possible (Kim & Morris, 2003; McMillan & Portegies Zwart, 2003) if the cluster is very massive ( $M \gtrsim 10^6 M_{\odot}$ ), or if it is formed very near the central parsec already. In both cases a very dense core for the star cluster is required and appears to be unrealistic. An intermediate mass black hole in the centre of the cluster does allow the star cluster to survive longer against tidal disruption and hence transport the young stars in the central parsec more efficiently (as suggested by Hansen & Milosavljević, 2003). However the numerical simulations of Kim, Figer, & Morris (2004) show that the mass of the black hole has to be unusually large ( $\sim 10\%$ ) compared to the cluster mass for this idea to work in practice.

Levin & Beloborodov (2003) and Nayakshin, Cuadra, & Sunyaev (2004) suggested that the origin of the young stars is a massive self-gravitating accretion disc existing in Sgr A\* in the past. Here we intend to investigate this idea quantitatively and to also look into some related theoretical questions.

We first estimate the minimum mass of such accretion discs to be around  $10^4 M_{\odot}$ , for each of the two stellar rings. In addition, we rule out the possibility that a less massive accretion disc could capture enough of low mass stars from the pre-existing ‘relaxed’ Sgr A\* cusp and then grow them by accretion into massive stars (§3.3).

We then attempt to understand the spatial distribution of the young stars. In particular, we find that the rate of  $N$ -body scattering between the stars (§3.4) of the same ring can explain the observed stellar velocity dispersions in the inner stellar ring if the time-averaged total stellar mass in the ring was  $10^4 M_{\odot}$  or higher. We also find that stellar orbits in both rings should remain close to the circular Keplerian orbits up to this day (if stars were indeed born in a disc). The outer ring is however observed to be geometrically thicker and with a higher velocity dispersion than the inner one. The velocity dispersion of the outer ring may result from the stellar disc warping in the gravitational potential of the inner ring. Such warping sets the upper limit on the disc mass of about  $10^5 M_{\odot}$  (§3.5).

We also question in §3.6 whether it is possible for the disc to leave the newly born stars behind (due to their high inertia) when the disc plane rotates. Dislodging the newly born stars, or proto-stars, from the disc midplane would have significantly reduced the problems faced by accretion discs at large radii since these stars would then stop devouring the disc and instead heat it and speed up the accretion of gas onto the SMBH via star-disc collisions (Ostriker, 1983). However, we find that the disc maintains a firm grip on these stars unless the plane change occurs on a time scale much shorter than the disc viscous time (§3.6).

It is found that young massive stars would not migrate much radially (§3.7) in the disc, meaning that they are probably located at the radius where they were originally formed. Small scale proto-stellar discs around the embedded stars may be gravitationally unstable as well and may create further generations of stars. Hierarchical growth and merging of such objects may result in the creation of ‘mini star clusters’ with the central object collapsing to an intermediate mass black hole (§3.8). This could potentially be relevant to the observations of such objects as IRS13 (Maillard et al., 2004).

Since the combined mass of the stellar material in the observed stellar rings presently is  $\lesssim 10^3 M_\odot$  (Genzel et al., 2003b), there is the interesting question of whether most of the gaseous disc mass has been used to activate the presently dormant Sgr A\* or whether it was reprocessed through star formation and expelled to larger radii via winds and supernova explosions. We believe the latter outcome is more likely since the accretion of gas onto embedded stars is very efficient. We briefly discuss observations that could distinguish between the quasar and the nuclear starburst possibilities (§3.9).

### 3.2 The minimum mass of a self-gravitating disc in Sgr A\* is $10^4 M_\odot$

The standard accretion disc solution (Shakura & Sunyaev, 1973) neglects self-gravity of the disc. Clearly, this solution becomes invalid when the disc becomes strongly self-gravitating, but here we only want to estimate the minimum disc mass at which the self-gravity becomes important. For numerical values of the standard disc parameters, we follow Svensson & Zdziarski (1994) with their parameters  $\xi = 1$  and  $f = 0$  (i.e. no X-ray emitting disc corona is assumed). The dimensionless accretion rate  $\dot{m}$  is defined as  $\dot{m} = \dot{M}/\dot{M}_{\text{Edd}}$ , where  $\dot{M}_{\text{Edd}} = L_{\text{Edd}}/\varepsilon c^2$  is the accretion rate corresponding to the Eddington luminosity and  $\varepsilon \approx 0.06$  is the radiative efficiency of the standard accretion flow.<sup>1</sup>

For large radii ( $r \gg 1$ ) the gas dominated equations are appropriate:

$$\frac{H}{R} = 2.7 \times 10^{-3} (\alpha M_8)^{-1/10} r^{1/20} \dot{m}^{1/5}, \quad (3.1)$$

$$\Sigma = 4.2 \times 10^6 \text{ g cm}^{-2} \alpha^{-4/5} M_8^{1/5} r^{-3/5} \dot{m}^{3/5}. \quad (3.2)$$

---

<sup>1</sup>Note that our definition of  $\dot{m}$  is different from the one Svensson & Zdziarski (1994) use:  $\dot{m}_{\text{SZ}} = 17.5\dot{m}$ .

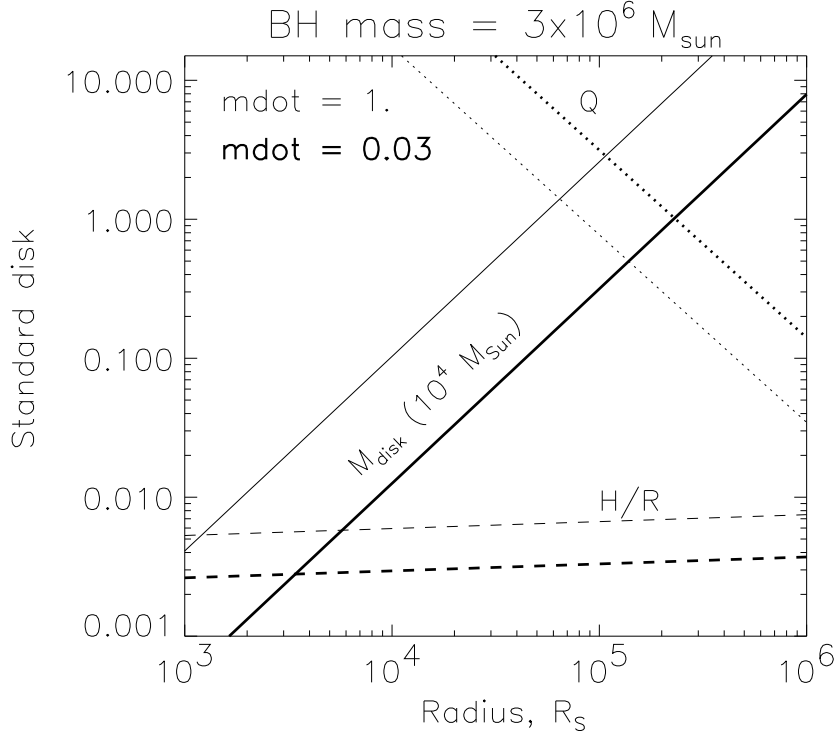


Figure 3.1: The disc mass in units of  $10^4 M_\odot$ , the Toomre instability parameter  $Q$ , and the ratio of the disc height scale  $H$  to radius  $R$  as a function of radius for the standard accretion disc model. The thick curves are plotted for  $\dot{m} = 0.03$ , whereas thin ones are for  $\dot{m} = 1$ . In both cases the disc is unstable to self-gravity at  $R \gtrsim 10^5 R_S$ , where its mass is  $M_d \gtrsim 10^4 M_\odot$ .

$$T = 6.3 \times 10^2 \text{ K } (\alpha M_8)^{-1/5} \dot{m}^{2/5} \left[ \frac{R}{10^5 R_S} \right]^{-9/10}. \quad (3.3)$$

Where  $H$  is the disc vertical height scale,  $R$  is the distance from the SMBH,  $T$  is the midplane gas temperature,  $\alpha$  is the dimensionless viscosity parameter,  $M_8 = M_{\text{BH}}/10^8 M_\odot$ ,  $r = R/R_S$ ,  $R_S = 2GM_{\text{BH}}/c^2$  is the Schwarzschild radius of the SMBH and  $\Sigma$  is the surface density of the accretion disc. These equations assume Thomson electron scattering opacity for simplicity. Figure 3.1 shows some of the disc parameters obtained for  $M_{\text{BH}} = 3 \times 10^6 M_\odot$ ,  $\alpha = 1$ , and two values of the dimensionless accretion rate,  $\dot{m} = 0.03$  (thick lines) and  $\dot{m} = 1$  (thin lines). The mass of the disc as a function of radius is approximated as  $M_d \approx \pi R^2 \Sigma$ .

It is well known that the standard accretion disc becomes self-gravitating at

large radii, when the Toomre (1964) parameter  $Q$  becomes less than unity,

$$Q = \frac{c_s \Omega}{\pi G \Sigma} \approx \frac{H}{R} \frac{M_{\text{BH}}}{M_{\text{d}}} < 1 \quad (3.4)$$

( $c_s$  is the sound speed inside the disc and  $\Omega$  its angular velocity). The radius where  $Q = 1$  yields the minimum mass of the disc needed for the latter to become *locally* self-gravitating<sup>2</sup>.

As can be seen from Fig. 3.1, the disc should weigh at least  $10^4 M_{\odot}$  in order to become self-gravitating. Note that this minimum disc mass estimate is quite robust because  $H/R$  depends on  $\alpha$ , radius and the accretion rate only weakly. This estimate is also conservative. The basic Shakura-Sunyaev model used here does not include irradiation by the central source, which may increase the disc midplane temperature somewhat, leading to a slightly larger  $H/R$ . In addition, trapping radiation by opacity effects would reduce the efficiency of cooling, adding to the stability of the disc against self-gravity.

### 3.3 Capturing low mass stars and growing them by accretion: too slow.

Artymowicz, Lin, & Wampler (1993) noted that stars in the nuclear star cluster on orbits relatively close to the local circular rotation of the accretion disc in quasars will be captured by the disc. The stars can then rapidly grow by gas accretion, and then enrich the accretion disc with heavy elements through stellar evolution. For the problem of the observed young massive stars in the Galactic Centre (GC), the Artymowicz et al. trapping mechanism may be an alternative route to form the stars. The accretion disc does not have to be self-gravitating for the mechanism to work, provided there is enough stars and the time scale for the star trapping is short enough. One may thus hope to reduce the required disc mass.

To within a factor of the order of unity, equation 15 of Artymowicz et al. (1993) yields the number of stars captured by the disc within time  $\Delta t$  as

$$dN_*(R) \sim \frac{\zeta^4}{4} N_*(R), \quad (3.5)$$

where  $N_*$  is the total number of stars in the star cluster within radius  $R$ , and the variable  $\zeta$  is defined by

$$\zeta^4 = 32 C_{\text{d}} \frac{M_* M_{\text{d}}}{M_{\text{BH}}^2} \frac{\Delta t}{P}, \quad (3.6)$$

---

<sup>2</sup>Disc self-gravity is local when the disc mass is much smaller than the SMBH mass. Effectively, regions of disc separated by large radial distances do not communicate with each other via gravity in this regime. When the disc mass becomes comparable to that of the SMBH, the instability becomes global, and a very rapid angular momentum transfer via self-gravity occurs.

where  $P$  is the orbital period and  $M_* = m_* M_\odot$  is the typical mass of the stars in the cluster. For an estimate, we take  $C_d \simeq 3$  and  $q_{-2} \equiv 100M_d/M_{\text{BH}} \lesssim 1$ . Note also that we want to start with abundant stellar seeds, so we assume  $m_* \sim 1$ . At the typical radial position of the young massive stars in Sgr A\*,  $R = 0.1\text{pc} \sim 3 \times 10^5 R_S$ , the circular Keplerian rotation period is

$$P \simeq 10^3 \text{ year} \left[ \frac{R}{3 \times 10^5 R_S} \right]^{3/2} \quad (3.7)$$

Thus,

$$\zeta^4 \simeq 3 \times 10^{-4} m_* q_{-2} \frac{\Delta t}{10^3 P} . \quad (3.8)$$

Now, from results of Genzel et al. (2003b) we estimate that

$$N_*(R) \simeq 10^5 m_*^{-1} \left[ \frac{R}{3 \times 10^5 R_S} \right]^{3/2} \quad (3.9)$$

(we assumed the cusp power-law index  $p = 1.5$  for simplicity; see also equation 15 in Nayakshin et al., 2004). Therefore, the number of stars captured by the disc is

$$dN_* \sim 7 q_{-2} \frac{\Delta t}{10^6 \text{ years}} . \quad (3.10)$$

Note that the radius  $R$  and the average stellar mass  $m_*$  scale out of this relation.

The number of captured stars is somewhat low if we take into account the fact that the  $\sim 12$  ‘Helium’ stars found in each of the rings are only the brightest end of the stellar distribution, and there are probably many more (less massive) stars in the rings (§3.7 in Genzel et al. (2003b)). Therefore one would require  $q_{-2} \gtrsim 3$ –10, that is disc mass  $M_d \sim (1$ –3)  $\times 10^5 M_\odot$ . With this rather high required disc mass, the disc would have to be self-gravitating, and one expects a large number of stars to be born inside the disc. The disc capture mechanism thus fails to reduce the minimum disc mass. Nevertheless, it should not be forgotten completely because of its ability to bring in some *late* type stars into the plane of the disc, e.g. the plane of the young massive stars. This type of star would not be born inside the accretion disc in a time span of just a few million years.

### 3.4 Velocity dispersion of an isolated stellar disc

Stars embedded in accretion discs are often considered in a ‘test star’ regime (e.g., Syer et al., 1991), when each star corotates with the accretion disc. The star’s velocity is then nearly equal to the local Keplerian circular velocity. When number of embedded stars,  $N_* \gg 1$ , two-body interactions between stars will increase their local velocity dispersion,  $\sigma$ , potentially leading to some interesting consequences.

Since the disc velocity field has the radial Keplerian shear, it is the radial velocity dispersion of stars that will grow the fastest. However, when the

anisotropy  $\sigma_r/\sigma_z$  becomes larger than 3, buckling instability will develop and the stellar velocity dispersion will become more isotropic (Kulsrud, Mark, & Caruso, 1971; Shlosman & Begelman, 1989). Thus we assume an isotropic velocity dispersion here for simplicity. The velocity dispersion of stars grows due to  $N$ -body interactions at the rate

$$\frac{d\sigma}{dt} \sim \frac{4\pi G^2 M_* \rho_*}{\sigma^2} \ln \Lambda_* \quad (3.11)$$

where  $\Lambda_* \sim H_* \sigma^2 / GM_*$  is the Coulomb logarithm for stellar collisions;  $H_*$  is the stellar disc height scale, which in general may be different from the gas disc height scale  $H$ .

The growth of velocity dispersions is opposed by the dynamical friction force acting between the stars and the gas. Consider a star moving inside the disc with a relative velocity  $v_{\text{rel}}$  with respect to the local Keplerian velocity,  $v_K$ . Artymowicz (1994) shows that the angular momentum and energy flow between the disc and the star (a small disc perturber in the case of proto-planetary discs), calculated explicitly, coincides within a factor of a few with the hydrodynamical Bondi-Hoyle drag acting on the star during its passage through the disc. The acceleration experienced by the star is thus

$$\vec{a}_d = -4\pi G^2 M_* \rho C_d \frac{\vec{v}_{\text{rel}}}{g^4 (c_s^2 + v_{\text{rel}}^2)^{3/2}}, \quad (3.12)$$

where  $g = \min(1, v_c/v_{\text{rel}})$  and  $v_c = C_d^{1/4} v_{\text{esc},*}$  is of the order of the escape velocity from the star,  $v_{\text{esc},*}$ . In perturbative analytical approaches, such as dynamical friction,  $C_d \gtrsim 1$  is the Coulomb logarithm,  $\ln \Lambda$ , where  $\Lambda$  is the ratio of the disc height scale  $H$  to Bondi (or accretion) radius (e.g., Ostriker, 1983). However, in many circumstances the Bondi-Hoyle formula for accretion rate onto the star produces super-Eddington values. The drag force (e.g.  $C_d$ ) should then be reduced to account for the radiation pressure force. One finds that in the disc geometry the largest contribution to the star-gas friction comes from distances  $\sim H$  from the star. The exact value of  $C_d$  depends on disc opacity and the 3-D velocity of the star, but estimates suggest that  $C_d$  is not much smaller than unity in this case.

Note that when the relative velocity is high, the drag force is just the hydrodynamical drag,  $a_d \propto \pi R_*^2 \rho v_{\text{rel}}^2$ , where  $R_*$  is the stellar radius. For  $c_s < v_{\text{rel}} < v_{\text{esc},*}$ , the classical Chandrasekhar (1943) dynamical friction formula is recovered, with  $a_d \propto v_{\text{rel}}^{-2}$ . Finally, if the relative velocity is smaller than  $c_s$ , we have  $a_d \sim \dot{M}_B v_{\text{rel}}$ , which is about equal to the momentum flux accreted by the star ( $\dot{M}_B$  is the Bondi accretion rate).

While  $v_{\text{rel}}$  is not too large, i.e.,  $g = 1$ , the evolution of the stellar velocity dispersion is approximately given by

$$\frac{d\sigma}{dt} \sim 4\pi G^2 M_* \left[ \frac{\rho_* \ln \Lambda_*}{\sigma^2} - \frac{\rho C_d \sigma}{(c_s^2 + \sigma^2)^{3/2}} \right] \quad (3.13)$$

As long as  $\rho_* \ln \Lambda_* < \rho C_d$ , the star-gas drag will be able to keep the stars on local circular Keplerian orbits in the sense that  $\sigma \ll c_s$ , the gas sound speed,

thus the stars indeed behave as test particles. However, when  $\rho_* \ln \Lambda_* > \rho C_d$ , the stellar velocity dispersion will evolve mainly under the influence of  $N$ -body collisions, and it will increase rapidly.

It may appear that the last fact suggests a natural mechanism to stop the very efficient (see §3.9) accretion of gas onto the embedded (proto-) stars. As the stellar velocity dispersion grows much larger than the gas sound speed, the stars will be no longer embedded in accretion discs as they would spend most of their orbits outside the main body of the accretion disc. In addition, even when the stars are crossing the disc, the relatively high value of  $v_{\text{rel}}$  means that the accretion rate onto stars will be strongly reduced. However, the effect is important only when  $\rho_* > \rho$  (assuming  $\ln \Lambda_* \sim C_d$ ), that is when the stellar density is already larger than the gas density. Therefore, before this effect may become important, about a half of the initial gas mass should already be consumed by the stars. The accretion onto the stars is curbed by the  $N$ -body dispersion effects too late, when the disc is already partially consumed by the stars.

For Sgr A\*, we can estimate the expected  $H_* \sim R\sigma/v_K$ . The relaxation time, defined as the time needed for the stellar disc to thicken to height  $H_*$  can be found from equation 3.11:

$$\frac{t_{\text{rel}}}{t_{\text{dyn}}} \sim \left[ \frac{H_*}{R} \right]^4 \frac{M_{\text{BH}}^2}{4M_{\text{d}*}M_* \ln \Lambda_*}, \quad (3.14)$$

where  $M_{\text{d}*}$  is  $\pi R^2 H_* \rho_*$ , the mass of the stellar disc. Equation 3.14 yields

$$\frac{t_{\text{rel}}}{t_{\text{dyn}}} \sim 2500 \frac{10^4 M_\odot}{M_{\text{d}*}} \frac{10 M_\odot}{M_*} \left[ \frac{H_*/R}{0.1} \right]^4 \ln \Lambda_*^{-1}. \quad (3.15)$$

With  $t_{\text{dyn}} \sim 300$  years, we have  $t_{\text{rel}} \sim 10^6$  years. Hence the geometrical thickness of the rings, and the ratio of velocity dispersion to the local Keplerian velocity,  $\sigma/v_K$ , are expected to be of the order of 0.1 for the two young stellar rings in the GC. The individual stellar velocities should thus still be close to the local *circular* Keplerian values if the origin of the stars is in the gaseous disc.

Levin & Beloborodov (2003) estimate the geometrical thickness of the inner stellar disc in Sgr A\* to be of the order of  $H_*/R = 0.1$ . This ratio is however larger but is not quantified for the outer disc found by Genzel et al. (2003b). From their figure 15 we estimate that  $H_*/R \sim 0.3$  for the outer, counter-rotating, disc.

One may try to invert equation 3.15 to constrain the initial stellar mass of the discs in the GC by using the observed velocity dispersions (Genzel et al., 2003b) in the rings. Unfortunately the limits are not very stringent due to the strong dependence of  $t_{\text{rel}}$  on  $H/R$ . A disc mass as high as  $M_{\text{d}} \sim 3 \times 10^5 M_\odot$  could still be consistent with the observations for the inner stellar ring. Interestingly, for the outer stellar ring, the velocity dispersion is too high to be explained by the  $N$ -body effects unless the ring mass is unrealistically high.

### 3.5 Destruction of stellar rings by orbital precession: the maximum disc mass.

Genzel et al. (2003b) found that most of the young innermost stars lie in one of *two* stellar rings. There is no noticeable difference in the estimated age of the two groups of stars. The rings are bound to interact gravitationally with one another, and this could lead to observable disc distortions.

In particular, stellar orbits precess around the axis of symmetry in an axisymmetric potential (e.g., §3.2 in Binney & Tremaine, 1987). We represented one of the discs by the Kuzmin potential

$$\Phi_K(R, z) = -\frac{GM_d}{\sqrt{R^2 + (a + |z|)^2}}, \quad (3.16)$$

where  $a$  is the disc radius,  $R$  is the radius in the cylindrical coordinates and  $z$  is the perpendicular distance from the disc. We then numerically integrated stellar orbits, starting from nearly circular Keplerian orbits unperturbed by the disc presence. The orbits remain approximately circular, and conserve the inclination angle  $i$  between the orbital plane and the disc plane (because the  $z$ -component of the angular momentum is rigorously conserved in the axisymmetric potential). The stellar orbital plane precesses with respect to the disc at a rate

$$\dot{\phi} = C_p q P^{-1} \cos i, \quad (3.17)$$

where  $C_p$  is a constant (for a given orbit and given geometry) of order unity. Angle  $\phi$  here is the azimuthal angle of the lines of the nodes for the orbit in cylindrical coordinates used to define the Kuzmin potential. The precession rate scaling (equation 3.17) is natural since for small  $q$  the effect is linear in  $q$  as can be seen for orbits nearly co-planar with the disc (when  $i \approx 0^\circ$ ); for  $i = 90^\circ$  there should be no plane precession due to symmetry.

The value of  $C_p$  depends on the value of  $a$  with respect to the radius of the nearly circular stellar orbit; for  $a$  of order the radius,  $C_p \sim 1$ . Setting  $i = 74^\circ$  as appropriate for the two GC stellar rings (Genzel et al., 2003b), we obtain

$$\Delta\phi \simeq C_p \frac{q}{0.003} \frac{t}{10^3 P}. \quad (3.18)$$

The important point to note is that nearly circular orbits of stars at different radii from the SMBH will precess by different amounts  $\Delta\phi$ . Therefore such a precession leads to a warping of the stellar disc. After a time long enough to yield  $\Delta\phi \gtrsim 1$  somewhere in the disc, the initially flat stellar disc will be disfigured and will not be recognisable as a disc at all by an observer.

An approximate upper limit on the *time-averaged* mass of each of the two stellar rings in Sgr A\* can be set. Clearly the exact value of this limit should be obtained numerically with  $N$ -body experiments and comparison with the quality ( $\chi^2$ ) of the fits to the two observed planes (Levin & Beloborodov, 2003; Genzel et al., 2003b). Such a study is underway. Due to an observational uncertainty



in the radial dimensions of the rings' inner and outer radii, and theoretical uncertainty in the distribution of gaseous mass (i.e.  $\Sigma(R)$ ) in the accretion disc, it is possible to reduce  $C_p$  from its maximum value for some values of parameters. Nevertheless, a rather robust value for the upper mass of the discs appears to be

$$\max M_d \approx 10^5 M_\odot . \quad (3.19)$$

### 3.6 Rotating the accretion disc midplane: do stars remain embedded?

The accretion disc midplane orientation can in principle change as a result of a new mass deposition coming with a different orientation of the angular momentum vector. In such a rotation, would the newly born stars remain embedded in the disc and follow its rotation or would they stay behind in the 'old' accretion disc midplane due to their high inertia? The answer to this question is important for AGN discs in general as embedded stars can significantly influence the accretion process (e.g., Goodman & Tan, 2004; Nayakshin, 2004).

By orders of magnitude, one can estimate the time needed to turn the accretion disc plane around on a significant angle to be

$$t_{\text{rot}} \sim \frac{M_d}{\dot{M}_c} \sim t_{\text{visc}} \frac{\dot{M}}{\dot{M}_c} , \quad (3.20)$$

where  $\dot{M}_c$  is the mass condensation rate onto the accretion disc. If the accretion and condensation processes are in an approximate steady state,  $\dot{M}_c = \dot{M}$ ,  $t_{\text{rot}} \sim t_{\text{visc}}$ . The latter is

$$t_{\text{visc}} \sim \frac{R}{v_K} \alpha^{-1} \left( \frac{R}{H} \right)^2 , \quad (3.21)$$

and can be fairly long. Thus in general the disc plane orientation changes rather slowly.

#### 3.6.1 Forces keeping the stars embedded

Two forces mediating interaction between a star and a gaseous disc are the gravity of the disc as a whole, and the friction acting on a star *moving* inside the disc at a certain velocity with respect to the local circular Keplerian speed. If stars lag behind the rotating disc plane, the characteristic relative velocity at which the star and the gas would be separated is  $\sim v_K/t_{\text{rot}}$  and is very small compared to the sound speed in the gas (if  $t_{\text{rot}} \sim t_{\text{visc}}$ ). At small relative velocities the dynamical friction of a star 'leaving' the gas disc is very small too (see equation 3.12), and a simple estimate shows that the dynamical friction force can be safely neglected in what follows.

Therefore the binding force to consider is the direct gravitational attraction between the disc and the star. Near the disc midplane, the infinite plane

approximation can be used for the disc gravity. The gravitational attraction force of the gaseous disc for a star that left the disc midplane (i.e., the star-disc midplane separation  $|z| \gtrsim H$ ) is

$$a_{\text{pl}} = 2\pi G \Sigma, \quad (3.22)$$

where  $\Sigma$  is the local disc surface density. Comparing this acceleration with the centrifugal acceleration of the star moving in a circular Keplerian orbit around the central black hole,  $a_c = v_K^2/R$ ,

$$\frac{a_{\text{pl}}}{a_c} = \frac{2M_d}{M_{\text{BH}}}. \quad (3.23)$$

### 3.6.2 Critical rotation time

Suppose that the accretion disc midplane turns at a rate given by the time scale  $t_{\text{rot}}$ . Define a critical rotation time scale,  $t_{\text{rc}}$ , such that for disc plane changes occurring on time scales shorter than  $t_{\text{rc}}$ , the stars are dislodged from the gas disc. For  $t_{\text{rot}} > t_{\text{rc}}$ , on the contrary, the stars remain bound to the disc. Clearly, we get the critical time scale when  $a_{\text{pl}} = a_{\text{rot}} \equiv v_K/t_{\text{rot}}$ , where  $a_{\text{rot}}$  is the ‘rotation acceleration’ of the turning disc midplane. We obtain for the critical rotation time

$$t_{\text{rc}} = \frac{M_{\text{BH}}}{2M_d} t_{\text{dyn}}. \quad (3.24)$$

Figure 3.2 shows the critical rotation time scales (dotted curves) along with other important time scales for the standard accretion disc model with same parameters as used for Fig. 3.1 and for a 10 Solar mass star. The thick line curves are for  $\dot{m} = 0.03$ , whereas the thin curves are for  $\dot{m} = 1$ . The accretion and migration time scales will be discussed in §3.7 below.

Note that  $t_{\text{rc}}$  is longer than  $t_{\text{dyn}}$  but is much shorter than  $t_{\text{visc}}$ . This implies that if accretion disc plane changes occur on a viscous time scale, the stars would remain bound to the disc. Only very fast plane changes could dislodge the stars from the disc midplane.

### 3.6.3 The case of Sgr A\*

We have just shown that it is fairly difficult to separate the stars and the accretion discs in slow disc plane rotations or deformations. For the Sgr A\* case, this implies that either (i) there were two separate accretion disc creation events that created the two differently oriented rings; or (ii) the accretion disc itself was extremely warped so that its inner part was oriented almost at the right angle with respect to the outer disc part.

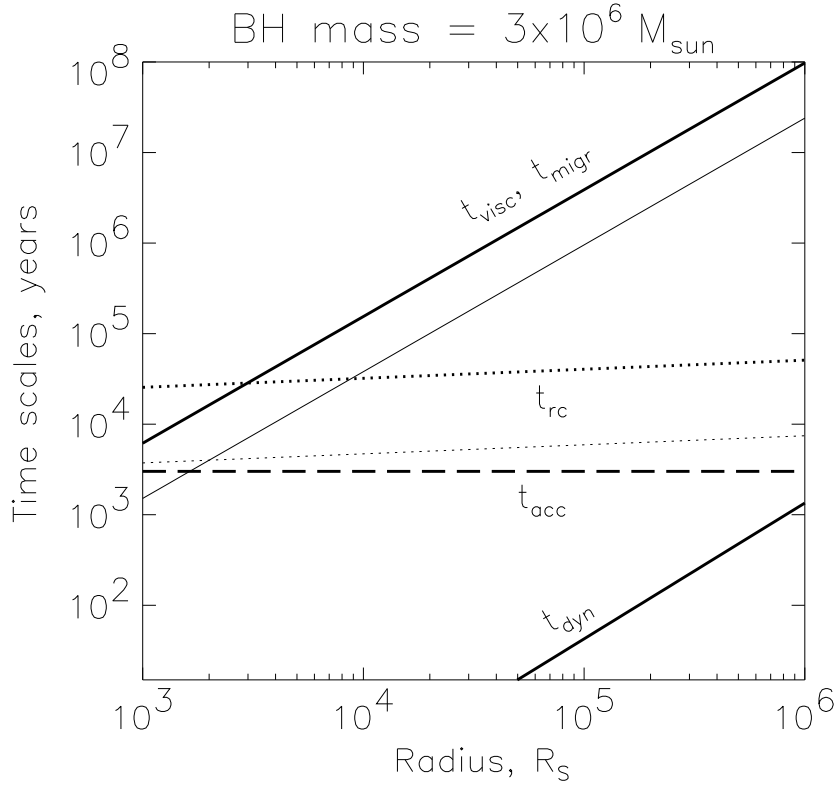


Figure 3.2: Time scales for a 10 Solar mass star embedded in the standard accretion disc with parameters as in Fig. 3.1. As before, thick curves correspond to  $\dot{m} = 0.03$ , whereas thin ones are for  $\dot{m} = 1$ . The solid lines show the viscous and the dynamical time scales for the disc, as labelled in the figure. The star is massive enough to open up a gap and hence migrates inward on the viscous timescale ( $t_{\text{migr}} = t_{\text{visc}}$ ). The dashed and dotted lines are the accretion and the critical rotation time scales, respectively. For chosen parameters, the former one is independent of  $\dot{m}$  (see text in §3.7 for detail).

### 3.7 Accretion onto embedded stars

The Hill's radius  $R_H$ ,

$$R_H = \left[ \frac{M_*}{3M_{\text{BH}}} \right]^{1/3} R, \quad (3.25)$$

defines the sphere around the star where the dynamics of gas is dominated by the star rather than the SMBH. The accretion of gas onto a star is believed to be similar to the growth of terrestrial planets in a planetesimal disc (Lissauer, 1987; Bate et al., 2003). For  $R_H > H$ , gas accretion onto the star is quasi two-dimensional. The accretion rate is determined by the rate at which differential rotation brings the matter into the Hill's sphere,

$$\dot{M}_* = \dot{M}_H \sim 4\pi R_H H \rho v_H \sim 4\pi R_H^2 \rho c_s, \quad (3.26)$$

where  $\rho = \Sigma/2H$  is the mean disc density. We used the fact that the characteristic gas velocity (relative to the star) at the Hill's distance from the star,  $v_H$ , is  $v_H = R_H |d\Omega/d\ln R| \sim c_s (R_H/H)$  since the angular velocity for Keplerian rotation is  $\Omega = c_s/H$ . Equation 3.26 is valid as long as  $R_H > H$  since in the opposite case the gas thermal velocity becomes important and the accretion would proceed at the Bondi accretion rate ( $\dot{M}_B$ ; e.g., Syer et al., 1991). Of course  $\dot{M}_*$  cannot exceed  $\dot{M}_{*,\text{Edd}} \simeq 10^{-3} r_* \simeq 10^{-3} M_\odot/\text{year } m_*^{1/2}$ , the Eddington accretion rate onto the star<sup>3</sup>. We thus estimate

$$\dot{M}_* = \min \left[ \dot{M}_H, \dot{M}_B, \dot{M}_{*,\text{Edd}} \right]. \quad (3.27)$$

One can then define the accretion time scale for a star embedded in a disc:

$$t_{\text{acc}} \equiv \frac{M_*}{\dot{M}_*}. \quad (3.28)$$

Figure 3.2 shows the accretion time scale (dashed line) for a  $10 M_\odot$  embedded star. Although we considered two values for the accretion rate onto the SMBH,  $\dot{m} = 0.03$  and  $\dot{m} = 1$ , as in Figure 3.1,  $t_{\text{acc}}$  turns out to be the same for both of these because the accretion rate is close to the Eddington value.

An important point from Figure 3.2 is that accretion onto embedded stars is able to double the stellar mass in a few thousand years. Therefore, growing stars as massive as  $100 M_\odot$  in a million years in a disc with gas mass  $M_d \gtrsim 10^4 M_\odot$  appears possible. [One potential uncertainty here is the reduction in the accretion rate onto the embedded stars once these stars are massive enough to clear out a radial gap in the accretion disc. Results of Bate et al. (2003), Figure 9, show that this reduction can be very large. However, in the case of an AGN disc with *many* embedded stars, the dynamics of the star-gas interaction is likely going to be different from the case of a 'test' star or planet. The accretion disc will then be divided into many rings between stars on nearly circular radial orbits. If the orbits are close enough (number of stars  $N_* \gg 1$ ), then the gas in a

<sup>3</sup>We assumed that  $r_* = (R_*/R_\odot) \approx (M_*/M_\odot)^{1/2}$ . Note that equation 10 in Nayakshin (2004) contains a typo.

ring will experience alternating inward and outward pushes from the two stars closest to it and hence the radial gap can in fact be closed, enabling unhindered accretion. The issue deserves future study.]

We also estimated the radial migration time scale,  $t_{\text{migr}}$ , using the prescription for the radial migration velocity based on the numerical calculations of Bate et al. (2003). For the parameters chosen, the 10  $M_{\odot}$  stars, and any stars more massive than that, open up a gap in the accretion disc and their radial migration is identical to the viscous flow of matter in the gas disc. Thus  $t_{\text{migr}} = t_{\text{visc}}$  (two solid curves in Figure 3.2). The migration time scale is very long, indicating that stars will remain close to where they were born in accretion discs with parameters close to that of the standard disc for Sgr A\*. A more realistic self-gravitating disc would not change this conclusion significantly since the migration time scale only gets longer when the midplane disc density decreases as a result of disc swelling due to gravitationally induced turbulence.

### 3.8 Growth of ‘mini star clusters’ and intermediate mass black holes in accretion discs

Goodman & Tan (2004) have recently suggested that it is possible to grow super-massive stars in AGN accretion discs. The maximum mass of a star in this case is the gas disc mass in a ring with width of the order of the Hill radius of the star,  $R_{\text{H}} = R(M_*/3M_{\text{BH}})^{1/3}$ . This is the ‘isolation’ mass,  $M_{\text{i}} \simeq M_{\text{d}}^{3/2} M_{\text{BH}}^{-1/2}$ ,

$$M_{\text{i}} \approx 550 M_{\odot} \left[ \frac{M_{\text{d}}}{10^4 M_{\odot}} \right]^{3/2} \left[ \frac{3 \times 10^6 M_{\odot}}{M_{\text{BH}}} \right]^{1/2}. \quad (3.29)$$

The stability of super-massive stars is briefly summarised in §2 of Goodman & Tan (2004). The super-massive star could collapse directly into a black hole if the star is more massive than 300  $M_{\odot}$  (Fryer et al., 2001).

However, the Hill accretion rate estimate assumes that all of the disc mass delivered by the differential rotation into the Hill radius around the star is accreted onto the star. Even without the gap, this is not obvious because the gas still has to lose most of its angular momentum before it can reach the stellar surface (e.g., Milosavljević & Loeb, 2004). Furthermore, quite frequently the accretion rate onto the star estimated in this way exceeds the Eddington accretion rate onto the star (as is the case for Figure 2). Milosavljević & Loeb (2004) have shown that the fringes of the small-scale disc around the embedded stars themselves become self-gravitating and may therefore also form stars or planets. It is thus possible to grow in situ star clusters. The maximum total mass of such a cluster should be close to the isolation mass.

A qualitative confirmation of these ideas can be found in numerical simulations of a related physical problem by Tanga et al. (2004). These authors simulate the growth and clustering of planetesimals in a proto-stellar disc. They find a hierarchical growth of clusters of particles and find that these ‘clusters’ are intrinsically stable structures. This is likely because of the abundant supply

of gas into the Hill sphere: there is always plenty of gas to interact with the particles (gravitationally bound objects in the AGN case) that continue to get more and more bound to the central object in the mini-cluster.

This mechanism of growth of intermediate mass black hole (IMBH) and star cluster bound to it may be relevant to the observations of the IRS13 cluster near Sgr A\* (Maillard et al., 2004). The ‘dark’ mass in the IRS13 is estimated to be  $\gtrsim 10^3 M_\odot$ . Equation 3.29 shows that an initial mass of the disc is of the order of several times  $10^4 M_\odot$  would have been sufficient to ‘in situ’ grow an object massive enough to become the IRS13 cluster.

### 3.9 Discussion

We have considered here the formation of massive stars in a self-gravitating accretion disc for conditions appropriate for the central  $\sim 0.2$  pc of our Galaxy. Formation of an accretion disc (instead of a narrow ring) would be a likely outcome of a cooling instability for a hot gas since the gas would realistically have a broad range of the angular momentum values. Additionally, a cloud with an initial size of a parsec or larger, tidally disrupted and shocked, should settle in a disc of a size comparable to its initial radius. There is of course a direct observational test which would distinguish between the accretion disc versus the compact infalling cloud idea of Sanders (1998) – one simply has to establish whether the orbits of the young stars in the two stellar rings are nearly circular or they are strongly eccentric. As we showed in §3.4, stars born in an accretion disc in Sgr A\* would still retain their nearly circular orbits.

The standard theory of gravitational instability for a thin disc (Toomre, 1964; Paczyński, 1978) predicts that the minimum mass of the gas in the disc that would make it gravitationally unstable for the parameters appropriate to our Galactic Centre is  $\sim 10^4 M_\odot$  (§3.2). It would be interesting to compare the predicted stellar mass resulting from star formation in such an accretion disc with the current stellar content of the rings. Unfortunately theoretical uncertainties for the efficiency of star formation in self-gravitating discs are too large. Shlosman, Begelman, & Frank (1990) have shown that if the cooling time of a self-gravitating disc is shorter than  $t_{\text{dyn}} = \Omega^{-1}$ , then the disc will fragment and form stars and/or planets. For longer cooling times, it was argued that the disc does not fragment (Shlosman et al., 1990). Numerical simulations with a constant cooling time by Gammie (2001) confirmed this, and have shown that the disc settles into a stable state where the cooling is offset by the energy input generated by gravitational instabilities (see also Paczyński, 1978). Yet for disc temperatures of the order of  $10^3$  Kelvin, the opacity is strongly dependent on the temperature. Johnson & Gammie (2003) showed that in the non-linear stage of the instabilities, the local cooling time may be orders of magnitude smaller than that found in the unperturbed disc model. However AGN discs are usually hotter than this and hence the non-linear effect should be weaker.

Nevertheless, we believe that the Sgr A\* accretion disc was likely consumed almost entirely in the star formation episode rather than accreted by the SMBH.

There is no doubt about star formation here: there are dozens of the brightest and quite massive stars in each of the stellar rings with 3-D velocity measurements. There are additional numbers of dimmer stars that have only 2-D velocities measured but are strongly suspected of belonging to these same rings (Genzel et al., 2003b, §3.7). The accretion time scale of the embedded stars is very short (§3.7 and Figure 3.2) compared to the disc viscous time scale. We have also shown in this paper that neither disc plane rotations, warps, or the stellar  $N$ -body scattering (unless there is already more mass in the stars than in the gas, see also Cuadra & Nayakshin, 2005) can ‘shake’ the stars off the disc midplane. In addition, each massive star opens up a radial gap in the accretion disc around it. These stars would not let *the standard* accretion disc transfer the gas into the SMBH simply because they are in the way of the gas flow.

While the standard accretion disc equations are not applicable to the region where the disc becomes self-gravitating, the stellar accretion time scale is shorter than the viscous time by 3–4 orders of magnitude. We experimented with a prescription for the accretion disc equations that introduces turbulent energy and pressure in addition to the thermal ones to keep the disc marginally stable (i.e.,  $Q \gtrsim 1$ ), and found that the turbulent energy content must be unrealistically high to reduce the accretion rate onto the stars sufficiently.

We have also found (§3.4) that the geometrical thickness of the inner 2–4'' stellar ring, and the stellar velocity dispersion, could be explained by  $N$ -body scattering between the members of the same ring if the initial stellar mass was as high as  $10^4 M_\odot$ . However, the outer 4–7'' projected distance ring (Genzel et al., 2003b) is too thick to result from the internal scattering. We believe that a better explanation is stellar ring warping due to a non-spherical gravitational potential (§3.6), e.g. due to the presence of the inner ring. Estimating the rate at which the rings become distorted, we tentatively set an upper limit on the *time-averaged* total mass of each of the gas-star discs (rings) at around  $10^5 M_\odot$ . Future numerical  $N$ -body modelling and direct comparison to stellar orbits may tighten this limit.

We hope that future observations of the stellar mass content in the two rings in Sgr A\*, and also observations of the inner Galaxy ISM budget, could be used to constrain the initial mass of the gaseous accretion disc and its further fate. As we have shown, the gaseous disc mass should have been in the range of  $1\text{--}10 \times 10^4 M_\odot$ , 10 to 100 times higher than the present day mass in the observed stellar rings (Genzel et al., 2003b). If most of the disc gas was used to make stars, then more of these stars and/or their remnants should be found in the future in the inner  $\sim 0.2$  pc of the Galaxy. In addition, one may look for evidence of a hot, high metallicity bubble in the inner 1 kpc of the Galaxy produced by stellar winds and supernova explosions.

If instead the gas was mostly accreted by Sgr A\*, then there should be evidence of a past quasar phase. The required accretion rate,  $\sim 10^4\text{--}10^5 M_\odot/10^6 \text{ yr} = 10^{-2}\text{--}10^{-1} M_\odot \text{ year}^{-1}$  is comparable with the Eddington accretion rate for Sgr A\*,  $\dot{M}_{\text{Edd}} \sim 0.03 M_\odot \text{ yr}^{-1}$ , corresponding to perhaps  $L_X \lesssim 10^{43} \text{ erg sec}^{-1}$  or even more. This would have to be a very rare event in Sgr A\*'s recent life since the recent star formation episode appears to be an isolated event in

Sgr A\*'s past (Krabbe et al., 1995). In addition, such star formation and accretion events should also be rare in nearby galaxies, since these either have no detectable AGN or have very weak ones with an X-ray luminosity usually less than  $L_X \lesssim 10^{40}$  erg sec $^{-1}$  (e.g., Zang & Meurs, 2001; Pellegrini, 2005). A past bright AGN phase should also leave a hot buoyant radio bubble in the Milky Way halo, as accretion onto the SMBH is widely believed to go hand in hand with super-luminous jet outflows. Future observations will hopefully constrain Sgr A\* accretion activity a few million years ago.

### 3.10 Conclusions

Our main results are as follows:

1. The minimum mass of each of the discs needed to form the observed young stars by self-gravity is around  $10^4 M_\odot$ .
2. The observed stellar velocity dispersions in the outer ring are too large to result from  $N$ -body interactions between stars belonging to the same ring. The orbital precession of stars caused by the potential of the other disc can explain the observed disc thickness and velocity dispersion if the time-averaged stellar and gaseous mass in the inner disc is in the range  $3\text{--}10 \times 10^4 M_\odot$ .
3. A few million years ago, Sgr A\* had a good chance to become a very bright AGN with a bolometric luminosity  $L \sim 10^{44}\text{--}10^{45}$  erg/sec, but was robbed of most of its gaseous fuel by nuclear star formation in a self-gravitating accretion disc. Nevertheless, even if only a few percent of the available disc fuel was captured by Sgr A\*, the SMBH in our Galactic Centre was as bright as  $L \sim 10^{42}\text{--}10^{43}$  erg/sec.

We have also shown that capture of stars from the ‘old’ relaxed isotropic Sgr A\* star cluster (the cusp; see Genzel et al., 2003b) by the accretion disc is inefficient unless the gaseous disc mass was as high as  $10^5 M_\odot$ . In addition, the role of possible accretion disc midplane changes was estimated. It was found that the embedded stars inertia would have been efficient in taking the stars out of the body of the discs only if the disc plane change its orientation on time scales much shorter than the disc viscous time.



## Chapter 4

# Accretion of cool stellar winds on Sgr A\*: another puzzle of the Galactic Centre?

Originally published by Cuadra, Nayakshin, Springel & Di Matteo in *Monthly Notices of the Royal Astronomical Society* **360**, L55

*Sgr A\* is currently being fed by winds from a cluster of gravitationally bound young mass-losing stars. Using observational constraints on the orbits, mass loss rates and wind velocities of these stars, we numerically model the distribution of gas in the  $\sim 0.1$ – $10''$  region around Sgr A\*. We find that radiative cooling of recently discovered slow winds leads to the formation of many cool filaments and blobs, and to a thin and rather light accretion disc of about an arcsecond scale. The disc however does not extend all the way to our inner boundary. Instead, hot X-ray emitting gas dominates the inner arcsecond. In our simulations, cool streams of gas frequently enter this region on low angular momentum orbits, and are then disrupted and heated up to the ambient hot gas temperature. The accreting gas around Sgr A\* is thus two-phase, with a hot component, observable at X-ray wavelengths, and a cool component, which may be responsible for the majority of time variability of Sgr A\* emission on hundred and thousand years time-scales. We obtain an accretion rate of a few  $\times 10^{-6} M_{\odot} \text{ year}^{-1}$ , consistent with Chandra estimates, but variable on time-scales even shorter than hundred years. These results strongly depend on the chosen stellar orbits and wind parameters. Further observational input is thus key to a better modelling of Sgr A\* wind accretion.*

## 4.1 Introduction

Sgr A\* is identified with the  $M_{\text{BH}} \sim 3 \times 10^6 M_{\odot}$  super-massive black hole (SMBH) in the centre of our Galaxy (e.g., Schödel et al., 2002; Ghez et al., 2003b). By virtue of its location, Sgr A\* may play a key role in the understanding of Active Galactic Nuclei (AGN). Indeed, this is the only AGN where recent observations detail the origin of the gas in the immediate vicinity of the SMBH capture radius (e.g., Najarro et al., 1997; Paumard et al., 2001; Baganoff et al., 2003; Genzel et al., 2003b). This information, missing for all other AGN because of too great a distance to them, their large luminosity, or both, is absolutely necessary if the accretion problem is to be modelled self-consistently.

Arguably the most famous puzzle of Sgr A\* is its low luminosity with respect to estimates of the accretion rate at around the capture radius, i.e. at distances of order  $1'' \sim 10^5 R_{\text{S}} \sim 0.04$  pc, where  $R_{\text{S}}$  is the Schwarzschild radius of Sgr A\*. Two methods have been deployed to obtain these estimates. From *Chandra* observations of the Galactic centre region, one can measure the gas density and temperature around the inner arcsecond and then infer an estimate of the Bondi accretion rate of  $\dot{M} \sim 10^{-6} M_{\odot} \text{ year}^{-1}$  (Baganoff et al., 2003). However, unlike in the classical textbook problem (Bondi, 1952), hot gas is continuously created in shocked winds expelled by tens of young massive stars near Sgr A\*, and there is neither a well defined concept of gas density and temperature at infinity, nor one for the gas capture radius.

The other method addresses this problem by direct modelling of the gas dynamics of stellar winds, assuming that the properties of the wind sources are known. Three dimensional simulations of wind accretion around Sgr A\* were performed by Coker & Melia (1997), who randomly positioned ten mass-losing stars a few arc-seconds away from Sgr A\*. They presented two different runs in which the stars were distributed in either a spherically isotropic or a flattened system. Rockefeller et al. (2004) used a particle-based code with more detailed information on stellar coordinates and wind properties. However, in both cases the stars were at fixed locations, whereas in reality they follow Keplerian orbits around the SMBH. The accretion rate on to Sgr A\* predicted by both studies was estimated at  $\sim \text{few} \times 10^{-4} M_{\odot} \text{ year}^{-1}$ . Finally, Quataert (2004) studied the problem in the approximation that there is an infinite number of wind sources distributed isotropically around Sgr A\* in a range of radii. His model yields an accretion rate estimate of  $\sim \text{few} \times 10^{-5} M_{\odot} \text{ year}^{-1}$ .

Due to recent impressive progress in the observations of Sgr A\*, we now know much more about the origin of the gas feeding the SMBH. Stellar wind sources are locked into two rings that are roughly perpendicular to each other (Paumard et al., 2001; Genzel et al., 2003b). In addition, the wind velocities of several important close stars were revised downward from  $\sim 600 \text{ km s}^{-1}$  (Najarro et al., 1997) to only  $\sim 200 \text{ km s}^{-1}$  (Paumard et al., 2001), making the Keplerian orbital motion much more important.

Motivated by these points, we performed numerical simulations of wind accretion on to Sgr A\* including optically thin radiative cooling and allowing the wind-producing stars to be on Keplerian orbits. In this Letter we report our

most important findings: (i) the slow stellar winds are susceptible to radiative cooling once they are shocked in the hot bubble inflated by the fast winds; (ii) a disc/ring is formed on  $\sim$  arcsecond scale; (iii) cool gas blobs frequently enter the inner arcsecond on low angular momentum orbits, are torn apart and thermalized, and then mixed with the hot gas there. Gas is thus distinctly two-phase in the inner region, with the cold phase being invisible to *Chandra*. (iv) The resulting ‘accretion rate’ (see §4.4) is of order several  $\times 10^{-6} M_{\odot} \text{ year}^{-1}$ , consistent with *Chandra* estimates, but is highly variable. This warrants a somewhat worrying question: how representative is the current low luminosity of Sgr A\*? Summarising these points, it appears that the accretion flow on to Sgr A\* and other low luminosity AGN cannot be fully understood based on observations of hot X-ray emitting gas alone.

## 4.2 Analytical estimates

The density of hot gas  $1.5''$  away from Sgr A\* is about  $n_e = 130 \text{ cm}^{-3}$  (Baganoff et al., 2003), and the gas temperature is  $T_g \approx 2 \text{ keV}$ . The pressure of the hot gas is thus  $p_{\text{th}} = n_e T_g \approx 3 \times 10^9 \text{ K cm}^{-3}$ . The temperature resulting from collisions of stellar winds with wind velocity  $v_w = 10^8 v_8 \text{ cm s}^{-1}$  is

$$T = 1.2 \times 10^7 \mu_{0.5} v_8^2 \text{ Kelvin}, \quad (4.1)$$

where  $\mu_{0.5}$  is the mean molecular weight in units of half the proton mass. This temperature is to a large degree compatible with the  $T_g \simeq 1.2 \text{ keV}$  measured by *Chandra* at slightly larger radii. The optically thin cooling function, dominated by metal line emission, is  $\Lambda \approx 6.0 \times 10^{-23} T_7^{-0.7} (Z/3)$ , where  $T_7 = T/10^7 \text{ K}$ , and  $Z$  is the metal abundance relative to Solar (Sutherland & Dopita, 1993). The cooling time is thus

$$t_{\text{cool}} = \frac{3kT}{\Lambda n} \approx 10^4 \mu_{0.5}^{1.7} v_8^{5.4} p_*^{-1} \text{ years}, \quad (4.2)$$

where  $p_* = nT/p_{\text{th}}$ . The dynamical time near this location is  $t_{\text{dyn}} = R/v_K \simeq 60 (R'')^{3/2}$  years, where  $R''$  is the radial distance to Sgr A\* in arc-seconds and  $v_K$  is the Keplerian velocity at that distance. This shows that cooling is of no importance for the gas originating in the winds with outflow velocity  $v_8 \sim 1$ . However, if the wind velocity is, say,  $v_w = 300 \text{ km s}^{-1}$ , then  $t_{\text{cool}}$  is only roughly 15 years, which is shorter than the dynamical time. Therefore one could expect that slower winds may be susceptible to radiative cooling in the high pressure environment of Sgr A\*. In reality the gas velocity is the sum of the wind velocity and the stellar orbital motion. At a distance of  $2''$ , for example, the Keplerian circular velocity is about  $440 \text{ km s}^{-1}$ . With respect to the ambient medium, the leading wind hemisphere will move with velocity  $v_8 \sim 1$ , whereas the opposite one will move even slower than  $v_w$ . This shows that even for winds with velocities  $v_w \gtrsim 500 \text{ km s}^{-1}$ , lagging regions of the wind may still be affected by cooling.

### 4.3 Method and initial conditions

A full account of our numerical method along with validation tests will appear in Cuadra et al. (2006). Here we only briefly describe the method. We use the SPH/ $N$ -body code GADGET-2 (Springel et al., 2001; Springel & Hernquist, 2002) to simulate the dynamics of stars and gas in the gravitational field of the SMBH. This code, developed for cosmological simulations, takes into account the (Newtonian)  $N$ -body gravitational interactions of all particles and also follows the hydrodynamics of the gas. We use the cooling function cited in §4.2 with  $Z = 3$ , and set the minimum gas temperature to  $10^4$  K.

We model the SMBH as a heavy ‘sink’ particle (Springel et al., 2005; Di Matteo et al., 2005), with its mass set to  $3.5 \times 10^6 M_\odot$ . For scales of interest, the black hole gravity completely dominates over that of the surrounding stars and gas. The inner boundary condition is specified by requiring the gas passing within the radius  $R_{\text{in}}$  from the SMBH to disappear in the black hole. In addition, particles at distances larger than the ‘outer radius’  $R_{\text{out}}$  are of little interest for our problem and are simply eliminated.

Stars are modelled as collisionless particles moving in the potential of Sgr A\*. The stars emit new gas particles that are initialised with the minimum temperature and a mass  $m_{\text{SPH}} = 5 \times 10^{-7} M_\odot$ . The initial particle velocity is the sum of the orbital motion of the star, and a random component. The latter is equal in magnitude to the wind velocity and its direction is chosen randomly to simulate isotropic winds in the frame moving with the star.

Following results of Paumard et al. (2001), we assume that ‘narrow line stars’ produce winds with velocity  $v_w = 300 \text{ km s}^{-1}$ , whereas the ‘broad line stars’ produce winds with  $v_w = 1000 \text{ km s}^{-1}$ . We refer to the former as LBV stars, and to the latter as WR stars. The radial extent of the inner stellar ring is from  $2''$  to  $5''$ , and the inner and outer radii of the outer ring are  $4''$  and  $8''$ , respectively. The rings are perpendicular to each other for simplicity (Genzel et al., 2003b, conclude that the rings are inclined at  $i \approx 74^\circ$  to each other). We argue that the total number of wind sources is likely to be higher than those that have been resolved so far. On average they would clearly have to be less powerful than estimated by Najarro et al. (1997). We therefore use 20 wind sources in total, with each star losing mass at the rate of  $\dot{M}_* = 4 \times 10^{-5} M_\odot \text{ year}^{-1}$ . Note that this is still a factor of  $\sim 2 - 3$  below the observationally estimated total mass loss rate from the Sgr A\* star cluster, but some of the wind sources are likely to be outside  $R_{\text{out}}$  and thus should not be included here. Typically, the time-step of the calculation is  $\sim 0.18$  years, so the mass loss rate above implies that  $\sim 20$  SPH particles are created around each star per time-step. The stars are distributed in rings uniformly in radius but randomly along the azimuthal angle. Stars in the same ring rotate in the same direction, of course, as they follow circular Keplerian orbits. We populate the inner ring with 6 LBVs and 2 WRs, and the outer one with 3 LBVs and 9 WRs.

To increase the resolution in the inner region, we split the SPH particles that get closer than  $10 R_{\text{in}}$  to the SMBH. To avoid numerical problems, the splitting is performed at a randomly chosen time - of the order of the dynamical

time at that radius - after the particle entered the inner  $10 R_{\text{in}}$ . Then the particle is divided into  $N_{\text{split}} = 5$  new ones that are placed randomly within the smoothing length of the original one. The mass of the old particle is equally divided between the new ones, while the temperature and velocity are kept constant. The rest of the SPH properties are updated self-consistently by the code. Other simulations, without splitting, show the same overall results as the one presented here (Cuadra et al., 2006).

The values for the inner and outer boundary conditions are  $R_{\text{in}} = 0.07''$  and  $R_{\text{out}} = 9''$ . We start with a negligible gas density inside the computational domain and then fill it up self-consistently with stellar winds. We ran the simulation for about 4,000 years. Realistic longer simulations would have to include a highly complex gas density field on larger scales around Sgr A\* and frequent supernovae (see below), which we leave for future investigations. The total number of SPH particles,  $N_{\text{SPH}}$ , initially increases steeply with time until the hot winds fill up the whole inner sphere. Later, the number of particles continues to increase due to the fact that most of the slow wind particles are bound. By the end of the simulation we reach  $N_{\text{SPH}} = 1.7 \times 10^6$ .

## 4.4 Results

### 4.4.1 Gas morphology.

Figure 4.1 shows the column density of gas and the stellar wind sources in the inner  $6''$  of the computational domain. The inner and outer rings are viewed at inclination angles of  $40^\circ$  and  $50^\circ$  in the Figure, respectively. The inner ring rotates clockwise in this projection, while the outer one rotates in the opposite sense.<sup>1</sup>

As fast stellar winds fill the available space, the slower ones are shocked and cool radiatively. Dense shells are formed around the shocks. These shells are torn into filaments and blobs. Different parts of the shells have different velocities and thus angular momenta, creating many cool gas blobs with different velocities. Some are directed to outer radii and have velocities large enough to escape from the computational domain. Others receive velocities directing them inward. At smaller radii the density of blobs is higher, thus they collide, and settle in the plane established by the inner LBVs. The blobs are also sheared by the differential Keplerian rotation, and a gas disc is born at radii somewhat smaller than that of the stellar orbits. The blobs typically consist of a few hundred SPH particles, many more than the minimum 40 neighbours used in the SPH kernel averaging for these simulations.

We find that the disc does not extend all the way inwards, as the inner arcsecond or so is dominated by the hot X-ray emitting gas. Surprisingly, the hot component originates from both fast and slow winds. Cool filaments that enter the inner region appear to be torn by differential rotation and then shock-

---

<sup>1</sup>An animated movie of this simulation is available at <http://www.mpa-garching.mpg.de/~jcuadra/Winds>.

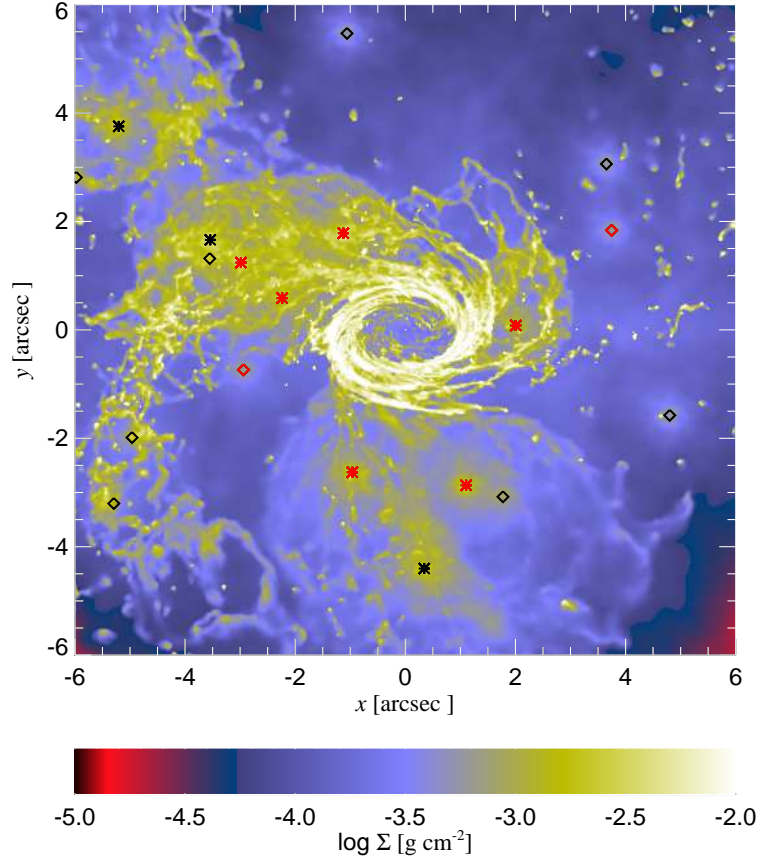


Figure 4.1: View of the gas column density and of the stars (overlaid) in the inner 6'' cube of the computational domain, after about 3,000 years. The ‘LBV’ stars within the slice are marked as stars, while the ‘WR’ stars are shown as diamonds. Stars painted in red and black belong to the inner and the outer rings, respectively.

heated to the ambient temperature as they interact with the hot gas. Since the disc mass is miniscule by AGN standards, the disc is constantly violently affected by the stars from the other ring. Streams and blobs of cool gas are kicked high up above the disc midplane due to interactions with winds from stars crossing the disc. These blobs rain down on to the disc, and some are brought into the sub-arcsecond region of the flow.

#### 4.4.2 Accretion on to Sgr A\*.

The ‘accretion rate’,  $\dot{M}_{\text{BH}}$ , on to Sgr A\* is defined in our simulations as the rate at which SPH particles enter the sphere with radius  $R_{\text{in}}$ , and is plotted versus time in Fig. 4.2. Solid and dotted lines correspond to time bins of 10 and 200 years, respectively. The latter seems to be a reasonable estimate for the viscous time-scale of the hot accretion flow at around  $R_{\text{in}}$ . The average rate we obtain, a few  $\times 10^{-6} M_{\odot} \text{ year}^{-1}$ , is in good agreement with the Bondi estimate (Baganoff et al., 2003), and is one to two orders of magnitude lower than what previous studies found (cf. §4.1). However, factors of a few variability in the accretion rate are immediately obvious. This variability can be tracked down to the arrival of individual cool gas blobs or filaments in the innermost region. Since the density of the hot gas in the vicinity of Sgr A\* is never zero, the accretion rate never decreases to zero.

It must be stressed that the real  $\dot{M}_{\text{BH}}$  further depends on intricate physical details of the inner accretion flow that we cannot resolve here. Some of the gas entering  $R \leq R_{\text{in}}$  is unbound and some may become unbound later on as result of viscous heating in the flow (Blandford & Begelman, 1999). Therefore, the accretion rate measured in our simulations is best understood to yield the outer boundary conditions for the inner accretion flow, and as such should be a more physically complete estimate of that than the commonly used Bondi accretion rate based on *Chandra* observations of hot X-ray emitting gas only.

The number of particles in the inner  $1''$  (comparable to the Bondi radius estimate for this problem) is about 70,000. This ensures that we have enough resolution at the inner boundary. On average,  $\sim 4$  SPH particles are accreted at each time-step.

#### 4.4.3 Existence of cold disc in sub-arcsecond region of Sgr A\*.

The cold ‘disc’ found in our simulations is constantly being created but it is also likely to be destroyed from time to time. Its mass can be estimated as  $M_{\text{disc}} = \dot{M}_{\text{cw}} t = 10 M_{\odot} (\dot{M}_{\text{cw}}/10^{-3} M_{\odot} \text{ year}^{-1}) t_4$ , where  $t_4 = t/10^4$  years and  $\dot{M}_{\text{cw}}$  is the mass outflow rate of cool stellar winds. A supernova occurring within the inner 0.5 pc of the Galaxy would easily destroy such a disc. The number of young early type stars in the Sgr A\* cluster is likely to be in the hundreds, and some have already reached the WR stage (e.g. Paumard et al., 2001; Genzel et al., 2003b). Assuming that the most recent star formation event occurred a few million years ago, one would then estimate the SN rate in Sgr A\*’s inner star

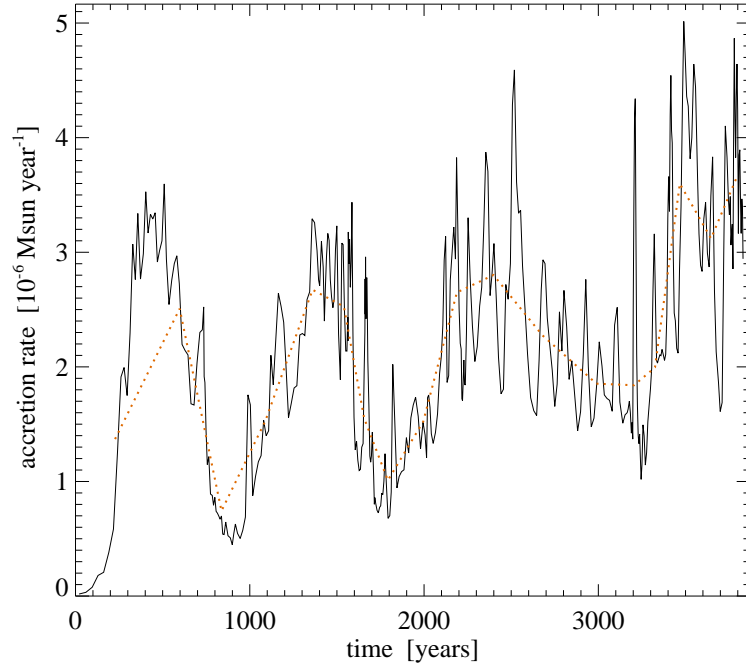


Figure 4.2: Accretion rate on to Sgr A\* versus time, averaged in bins of 10 years (solid) and 200 years (dotted). Both are expected to be only rough indicators of the actual accretion rate since much of the gas captured may still be unbounded inside  $R_{\text{in}}$  and/or has to be processed in the inner accretion flow that we do not resolve.



cluster to be at least  $\sim 10^{-4}$  per year. For comparison, the viscous time at a radius of  $1''$  is  $10^6 - 10^7$  years at best (e.g. fig. 2 in Nayakshin & Cuadra, 2005). Furthermore, there is much more cold material on scales of several arcseconds and beyond that may be plunging on to Sgr A\* (Paumard et al., 2004). Arrival of this mass in the inner arcsecond could also destroy the disc.

Therefore it is likely that the cool disc of  $\sim$  arcsecond scales does not smoothly extend inside the sub-arcsecond region of Sgr A\*. However, occasionally we observe cool gas blobs to directly fall into the capture ‘sphere’ in the simulation. It is also conceivable that events started by a supernova shell passage, or by an infall of additional cool material, could also leave a remnant in the form of a cold disc. Thermal conduction between the two phases could lead to evaporation of a cold accretion disc via the Meyer & Meyer-Hofmeister (1994) mechanism, which is unfortunately model dependent due to our poor knowledge of the magnetic field geometry and strength.

Nayakshin & Sunyaev (2003) suggested, mainly based on the presence of X-ray flares in Sgr A\*, that there is a cool disc at  $\sim 0.01-0.1''$  scales and beyond. The required mass of the disc was estimated to be smaller than a Solar mass. However, observations of NIR flares (Genzel et al., 2003a) put the flares at no more than a few milli-arcseconds away from the radio position of Sgr A\*, which is somewhat problematic for this model. Also, the NIR flare spectra appear to strongly favour a synchrotron (i.e. SMBH jet) origin. Further, no eclipses or star ‘brightenings’ expected when bright stars approach the disc (Cuadra et al., 2003) have been observed so far. Summarising, there is currently no observational motivation to favour the existence of such a disc in Sgr A\*, although it is also difficult to rule out its presence (unless the disc extends to the SMBH horizon; Falcke & Melia, 1997).

Concluding, we suggest that there cannot be a smooth transition of the larger scale cool disc into the inner sub-arcsecond regions of Sgr A\*. Nevertheless, the issue of the current existence of a cool disc or its periodic appearance and disappearance is an open subject for future work.

#### 4.4.4 Note on the importance of initial conditions.

While this work appears to be the most detailed (to date) numerical attempt to model the accretion of stellar winds on to Sgr A\*, observational uncertainties in the stellar orbits and wind mass loss rates and velocities still leave a lot of room for uncertainties in the final results. The latest observations (R. Genzel & T. Paumard, priv. comm.) reveal that the narrow emission line stars might be more equally divided between the two discs than what we have assumed here. In this case, the disc-like structure would form at a larger scale and be probably not as conspicuous. Similarly, if the mass loss rate of the ‘LBV’ stars is smaller, the cool disc becomes obviously less massive. In addition, mass-loss rates of LBV stars have been observed to vary by more than an order of magnitude within a few years (e.g., Leitherer, 1997). This effect would bring further variability and uncertainty to the results.

Another important ingredient, still missing in our approach, is the inclusion

of cooler gas filaments observed to be (possibly) infalling on to Sgr A\* on several to tens of arcsecond scales from Sgr A\*. These structures, referred to as the ‘mini-spiral’ (Scoville et al., 2003; Paumard et al., 2004), would undoubtedly change some of our results.

Finally, like all previous numerical investigations (Coker & Melia, 1997; Rockefeller et al., 2004; Quataert, 2004), we have entirely neglected the contribution of the wind producing stars on orbits inside the central 2''. While the most important wind sources are all located outside of this region (Najarro et al., 1997; Paumard et al., 2001), the weaker OB stellar winds inside the inner region may still contribute. For example, if their wind loss rates are about the inferred accretion rate, these stars (that appear to be on more randomly oriented orbits, see Eisenhauer et al., 2005) could potentially destroy the disc in the inner arcsecond.<sup>2</sup>

Future observations of the wind properties and stellar orbits near Sgr A\* are key to produce an increasingly more realistic model of the accretion flow on to Sgr A\*.

## 4.5 Discussion and Conclusions

AGN accretion discs are less well understood than discs in X-ray binaries on comparable relative scales, because we do not have good observational constraints on the origin of gas accreting on to the SMBH. Sgr A\* is becoming the only exception to this as observations improve. In this paper we made an attempt to realistically simulate the outer  $\sim 0.1\text{--}10''$  region of the gas flow on to Sgr A\*. The resulting gas flow is far more complex than thought earlier based on studies that included non-radiative fast stellar winds from stars either fixed in space or distributed in a spherically-symmetric fashion. The presence of cool gas in the sub-arcsecond region, as found here, may considerably complicate the interpretation of observational constraints on the accretion of Sgr A\*. Although, as discussed above, this does depend on still somewhat poorly known details of stellar orbits and wind parameters.

The average accretion rate in our simulation, a few  $\times 10^{-6} M_{\odot} \text{ year}^{-1}$ , is consistent with the estimates of Baganoff et al. (2003) and 1–2 orders of magnitude lower than what previous models found (Coker & Melia, 1997; Rockefeller et al., 2004; Quataert, 2004). However, this accretion rate changes by factors of a few in time-scales shorter than hundred years. Then how representative is the current low luminosity state of Sgr A\*, if the feeding of the inner region is indeed so turbulent and time-variable as our simulation suggests? After all, observations of X-ray/ $\gamma$ -ray echoes from nearby molecular clouds indicate that Sgr A\* might have been much more luminous some  $\sim 300$  years ago (Sunyaev

---

<sup>2</sup>Note that an extreme case of this was already studied analytically assuming a ballistic trajectory approximation by Loeb (2004). He showed that if the inner ‘S’-stars (e.g., Ghez et al., 2005; Eisenhauer et al., 2005) produce wind outflow rates as strong as  $\sim 10^{-6} M_{\odot} \text{ year}^{-1}$ , then their winds alone could provide enough fuel for Sgr A\* emission. However, most of the ‘S’-stars now appear to be of intermediate to later B-type, suggesting their winds could be orders of magnitude weaker than assumed by Loeb (2004).

et al., 1993; Koyama et al., 1996; Revnivtsev et al., 2004). Another aspect of the same issue is that ‘accretion’ of a cool blob in our simulations is not yet a true accretion event. If the blob manages to survive in the hot gas and settles to a disc or a ring at say  $\sim 10^3 R_S$ , it may circle Sgr A\* for a long time without being noticed. Further uncertainty in these results is the interaction between the hot and the cold gas via thermal conduction. If a cold blob enters the inner region of the hot flow, and is evaporated there, how will this affect the flow there? These and other related questions are to be resolved in future work if we want to reach a full understanding of the accretion process on to Sgr A\*.



## Chapter 5

# Galactic Centre stellar winds and Sgr A\* accretion

Originally published by Cuadra, Nayakshin, Springel & Di Matteo in *Monthly Notices of the Royal Astronomical Society* **366**, 358

We present a detailed discussion of our new 3D numerical models for the accretion of stellar winds on to Sgr A\*. In our most sophisticated models, we put stellar wind sources on realistic orbits around Sgr A\*, we include recently discovered ‘slow’ winds ( $v_w \sim 300 \text{ km s}^{-1}$ ), and we account for optically thin radiative cooling. We test our approach by first modelling only one phase ‘fast’ stellar winds ( $v_w \sim 1000 \text{ km s}^{-1}$ ). For stellar wind sources fixed in space, the accretion rate is of the order of  $\dot{M} \simeq 10^{-5} M_\odot \text{ yr}^{-1}$ , fluctuates by  $\lesssim 10\%$ , and is in a good agreement with previous models. In contrast,  $\dot{M}$  decreases by an order of magnitude for wind sources following circular orbits, and fluctuates by  $\sim 50\%$ . Then we allow a fraction of stars to produce slow winds. Much of these winds cool radiatively after being shocked, forming cold clumps and filaments immersed into the X-ray emitting gas. We investigate two orbital configurations for the stars in this scenario, an isotropic distribution and two rotating discs with perpendicular orientation. The morphology of cold gas is quite sensitive to the orbital distribution of the stars. In both cases, however, most of the accreted gas is hot, producing a quasi steady ‘floor’ in the accretion rate, of the order of  $\sim 3 \times 10^{-6} M_\odot \text{ yr}^{-1}$ , consistent with the values deduced from Chandra observations. The cold gas accretes in intermittent, short but powerful accretion episodes which may give rise to large amplitude variability in the luminosity of Sgr A\* on time scales of tens to hundreds of years. The circularisation radii for the flows are about  $10^3$  and  $10^4$  Schwarzschild radii, for the one and two-phase wind simulations, respectively, never forming the quasi-spherical accretion flows suggested in some previous work. Our work suggests that, averaged over time scales of hundreds to thousands of years, the radiative and mechanical luminosity of Sgr A\* may be substantially higher than it is

*in its current state. Further improvements of the wind accretion modelling of Sgr A\* will rely on improved observational constraints for the wind velocities, mass loss rates and stellar orbits.*

## 5.1 Introduction

Sgr A\* is believed to be a super-massive black hole (SMBH) of mass  $M_{\text{BH}} \simeq 3.5 \times 10^6 M_{\odot}$  in the very centre of our Galaxy (e.g., Reid et al., 1999; Schödel et al., 2002; Ghez et al., 2003b). Winds from young massive stars with velocity  $v_w$  around  $1000 \text{ km s}^{-1}$  are known to fill the inner parsec (e.g., Hall et al., 1982) with hot plasma. The total mass loss rate from these stars is  $\sim 10^{-3} M_{\odot} \text{ yr}^{-1}$  (e.g., Genzel et al., 1994; Najarro et al., 1997), and a fraction of this gas should be accreting on to the SMBH (e.g., Melia, 1992). The observed luminosity is however many orders of magnitude smaller than what is predicted from the classical Bondi-Hoyle theory (Bondi, 1952). There are two possible explanations for this discrepancy: either a much smaller amount of gas actually accretes on to the SMBH or accretion proceeds in a low-radiative efficiency mode. The current consensus appears to be that both of these factors are important for reducing Sgr A\*'s luminosity (Narayan, 2002). From theoretical arguments, it is unlikely that the accretion flow is exactly spherical, and instead it is plausible that a rotating flow forms in which the resulting viscous or convective heating unbinds much of the gas, severely reducing the accretion rate (Blandford & Begelman, 1999; Quataert & Gruzinov, 2000). It is also likely that electrons are not as hot as the ions, thus resulting in a greatly diminished radiative efficiency of the flow (Narayan & Yi, 1994).

Observations of Sgr A\* in the radio and in the X-ray bands constrain the accretion rate at tens of Schwarzschild radii distance from the SMBH to values of the order of  $\dot{M}_{\text{in}} \sim \text{few} \times 10^{-7} M_{\odot} \text{ year}^{-1}$  (Bower et al., 2003; Nayakshin, 2005a). This is significantly smaller than the  $\sim 3 \times 10^{-6} M_{\odot} \text{ year}^{-1}$  accretion rate estimated based on *Chandra* observations at  $\sim 10^5$  Schwarzschild radii (Baganoff et al., 2003), confirming that gas outflows are important. For the sake of closer testing accretion flow theories, it is important to establish the exact amount of gas captured by Sgr A\* to compare to  $\dot{M}_{\text{in}}$ . Note that this exercise can be done only for Sgr A\* at present, since all other AGN are much farther away, and hence Sgr A\* is a unique test object in this regard.

The first three dimensional numerical simulations of Sgr A\* wind accretion were performed by Ruffert & Melia (1994), who studied feeding the black hole from a uniform large scale gas flow. This work was extended by Coker & Melia (1997), who used discrete gas sources, ten mass-losing stars semi-randomly positioned a few arc-seconds away from Sgr A\*, to model the wind emission. Due to numerical difficulties inherent to fixed grid codes, the orbital motions of the stars could not be followed, and thus they were fixed in space. The authors argued that such an approach is valid since the wind velocities, as best known at the time, are larger than the circular Keplerian motions of the stars in these locations. Moreover, if the stellar orbits are isotropically distributed,

and all stars are identical, then the net angular momentum is nearly zero. More recently, Rockefeller et al. (2004) used a particle-based code, making also use of more detailed information on stellar coordinates and wind properties. However, the stars once again were kept at fixed locations.

Recent near-IR data of the nuclear star cluster in Sgr A\* show that the stellar wind sources are located in two ring- or disc-like distributions that are roughly perpendicular to each other (Paumard et al., 2001; Genzel et al., 2003b), implying that shocked gas has a non-zero net angular momentum. This is likely to be important for understanding the structure of the accretion flow. In addition, integral field spectroscopy of the central parsec implies stellar wind velocities of only  $\sim 200 \text{ km s}^{-1}$  (Paumard et al., 2001); much less than the values of  $\sim 600 \text{ km s}^{-1}$  previously estimated. These new data imply that stellar orbital motions are more important than previously thought. Moreover, these slow winds, when shocked, are heated to around  $10^6 \text{ K}$  as opposed to the temperature of  $1 - 2 \times 10^7 \text{ K}$  for the hotter  $\sim 1000 \text{ km s}^{-1}$  winds. This former slow phase of Sgr A\* stellar winds is therefore susceptible to radiative cooling (Cuadra et al., 2005) and thus it is expected to form a *cold* gas flow on to Sgr A\* in addition to the usually studied hot non-radiative phase.

Motivated by the new observations and the above ideas, we performed numerical simulations of wind accretion on to Sgr A\* including optically thin radiative cooling and allowing the wind-producing stars to be on circular Keplerian orbits. Some preliminary results of our study have already been presented by Cuadra et al. (2005). Here we report on specific tests of our new methodology and provide further details on our results. While this study sheds new light on physics of accretion of stellar winds on to Sgr A\*, it is clear that improved observational determinations of stellar mass loss rates, wind velocities, stellar orbits, and also of orbits and distribution of the cooler gas phase filling in the inner parsec will be the key for further improving our understanding of the Galactic centre region.

The paper is structured as following. We describe our numerical method in Section 5.2, and give results of simulations with single, fast wind velocity in Section 5.3, including a comparison with analytic models. In Section 5.4, we then describe our results for simulations with fast and slow ('two-phase') winds, followed in Section 5.5 by an analysis of fiducial *Chandra* observations of our simulated systems. We give a detailed discussion of our results in Section 5.6, and conclude in Section 5.7.

## 5.2 The Numerical Method

We use the SPH/*N*-body code GADGET-2 (Springel et al., 2001; Springel, 2005) to simulate the dynamics of stars and gas in the (Newtonian) gravitational field of Sgr A\*. This code solves for the gas hydrodynamics via the smoothed particle hydrodynamics (SPH) formalism. The hydrodynamic treatment of the gas includes adiabatic processes, artificial viscosity to resolve shocks, and optically thin radiative cooling with the cooling function  $\Lambda \approx 6.0 \times 10^{-23} (T/10^7 \text{ K})^{-0.7} \text{ erg}$

$\text{s}^{-1} \text{cm}^{-3}$  (Sutherland & Dopita, 1993).

The SMBH is modelled here as a heavy collisionless particle with gravitational smoothing length of  $0.01''$ . In addition it acts as a sink particle: gas passing within the inner radius  $R_{\text{in}}$  disappears, giving up its mass and momentum to the black hole (Springel et al., 2005; Di Matteo et al., 2005). The inner radius in our model is a free parameter, but for most tests we pick it to be  $\lesssim 0.1''$ , much smaller than the capture, or Bondi radius,  $R_{\text{capt}} = GM_{\text{BH}}/(c_s^2 + v_w^2)$ , where  $c_s$  is the gas sound speed and  $G$  the gravitational constant. For the case of Sgr A\*, X-ray observations yield  $R_{\text{capt}} \sim 1''$  (Baganoff et al., 2003).

At least 99% of the ‘wind’ (gas) particles escape from the region of interest, the inner  $\sim 10''$ , into the Galaxy. Following these particles in a region which we do not model properly here becomes prohibitively expensive, and is of limited interest for the problem at hand. Therefore we eliminate SPH particles that reach an ‘outer radius’  $R_{\text{out}}$ . We found that setting  $R_{\text{out}}$  larger than the distance from the outermost wind source to the SMBH is appropriate for our purposes.

Stellar winds are modelled via ‘emission’ of new gas (SPH) particles by the star particles from which these winds emanate. Ejection of particles is done typically in bursts of about 30 particles per star and occurs in time intervals of 0.2–1 yr. For each group of new SPH particles a random isotropic velocity distribution is generated. For tests with moving stars, the full initial particle velocity is the sum of its random isotropic part (in magnitude equal to the specified wind velocity  $v_w$ ) and the stellar 3-D velocity. The new particles are given initial temperature of  $10^4$  K, which is also the minimum temperature the gas is allowed to have in the simulations. As we are not interested in resolving the wind structure close to stellar surface, we also give the particles small spatial ‘kicks’ along their velocities. Baring this, we would have to resolve extremely small scale structures around stellar surfaces which is not feasible numerically. The rest of the SPH properties (pressure, density, entropy, etc.) are then calculated and followed self-consistently by the code.

## 5.3 Models with fast winds

A realistic modelling of Sgr A\* wind accretion requires several steps of varying complexity and importance for final results. In this section we shall start by considering the ‘single-phase’ case when the properties of all the wind sources are identical. We are interested in the dependence of the results on the number of sources, their distribution and their orbital motion, as well as on the choice of our free parameter  $R_{\text{in}}$ .

### 5.3.1 Fixed stars

A very useful test for our numerical methods is the comparison with analytical results. Quataert (2004) presented an analytical 1-D (spherical) model for the hot gas in the Galactic Centre. He distributed wind sources in a spherical shell between radii  $2\text{--}10''$  with stellar number density  $n_*(r) \propto r^{-\eta}$ , where  $\eta$  is a free



parameter varying between 0 and 3. The winds are further assumed to shock and be thermalized locally. Essentially, this model is a spherical wind/Bondi accretion model with distributed wind sources, and as such it presents a very convenient test bed for our numerical methods.

In the context of our numerical models, the ‘on the spot’ thermalization of winds is identical to having an infinite number of wind sources, since then the mean distance between them is zero and winds are thermalized immediately. In practice, we ran simulations with 200 stars isotropically and randomly distributed in the same range of radii, with a density profile given by the  $\eta = 2$  power-law. Our first objective is to test the sensitivity of the results to different values for the inner radius,  $R_{\text{in}} = 0.1, 0.4, 1''$ . The outer boundary is set at  $R_{\text{out}} = 15''$  for these tests. We ran tests with larger values for  $R_{\text{out}}$  and found that the results depend little on this value as long as it includes all the wind sources. The total mass loss rate of stars is set to  $\dot{M}_{\text{w}} = 10^{-3} \text{ M}_{\odot} \text{ yr}^{-1}$ , and the wind velocity is  $v_{\text{w}} = 1000 \text{ km s}^{-1}$ .

We ran these simulations until time  $t \sim 2100 \text{ yr}$ , at which the system is in a quasi-steady state. The number of SPH particles in the steady state is  $\simeq 10^6$ . To improve statistics, the radial profiles of quantities of interest are averaged over the last 10 snapshots covering the time interval  $t \approx 1800 - 2100 \text{ yr}$ . The resulting density profiles are shown in Fig. 5.1, together with the result from Quataert (2004) (the model with  $\eta = 2$ )<sup>1</sup>. Except for the flattening at radii approaching  $R_{\text{in}}$ , where the SPH particle density is under-estimated due to our ‘capture all’ boundary condition there, the curves are in good agreement.

Figure 5.2 shows the average radial velocity as a function of radius for the same runs. The radial velocity curves differ more from the Quataert (2004) curve (solid line) than the density curves. Our vacuum inner boundary condition forces the gas next to  $R_{\text{in}}$  to inflow with velocity approaching the gas sound speed. Clearly, when  $R_{\text{in}}$  is large, this inflow velocity is larger than that of the Bondi (1952) solution at that point. Hence simulations with large values of  $R_{\text{in}}$  will over-estimate the accretion rate on to the SMBH (we discuss this point in more detail below). If instead  $R_{\text{in}}$  is a factor of at least several smaller than  $R_{\text{capt}}$ , we expect to closely match Quataert (2004)’s results because by that point the inflow speed of the Bondi (1952) solution is approaching the local sound speed. This should be achieved in the simulation with the smallest inner boundary ( $R_{\text{in}} = 0.1''$ ). While we do obtain very similar gas densities (Fig. 5.1), the inflow velocity is significantly lower in our simulation than in the analytical solution. We find that, even with 200 sources, the accretion flow is still strongly anisotropic in the sub-arcsecond region. Indeed, most of the wind is unbound, with as little as  $\sim 1\%$  accreting on to Sgr A\*. Thus, out of 200 sources, only the  $\sim 10$  innermost stars are important for accretion. This can be seen through the gas velocity profile: the radial velocity changes its sign just above the inner radius of the wind-source region. In addition, as will become clear later, the incomplete thermalization of the winds does lead to some excess energy in the

---

<sup>1</sup>We multiplied Quataert (2004)’s density by a factor 2, since his models were actually computed for  $\dot{M}_{\text{w}} = 5 \times 10^{-4} \text{ M}_{\odot} \text{ yr}^{-1}$  (Quataert, priv. comm.).

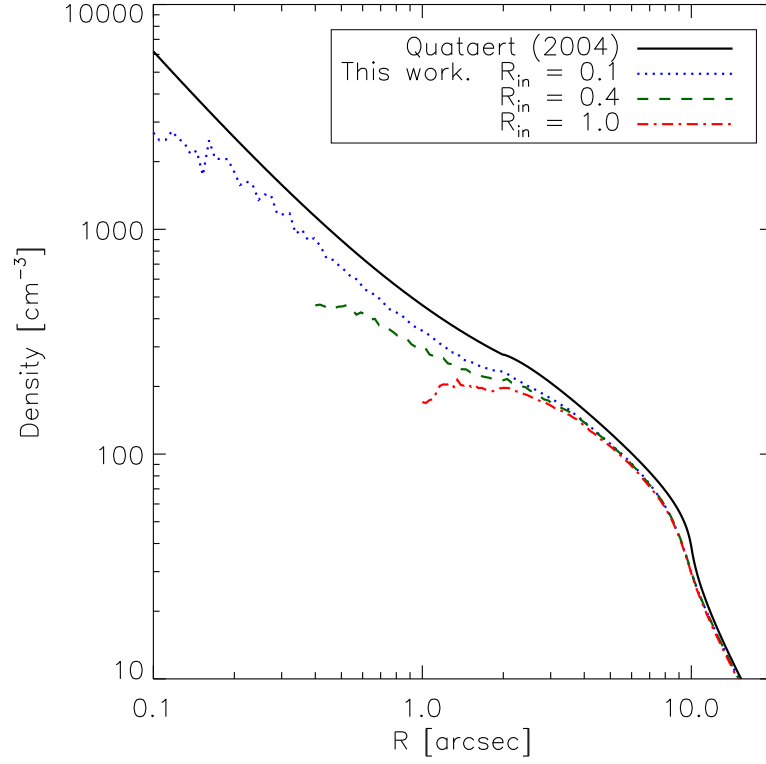


Figure 5.1: Radial density profiles of the gas in simulations with 200 fixed stars, distributed isotropically. The black solid curve shows the model of Quataert (2004). Note that our curves (coloured lines) reproduce his solution rather well down to about twice  $R_{\text{in}}$ . The values of  $R_{\text{in}}$  for the different simulations are given in the inset.

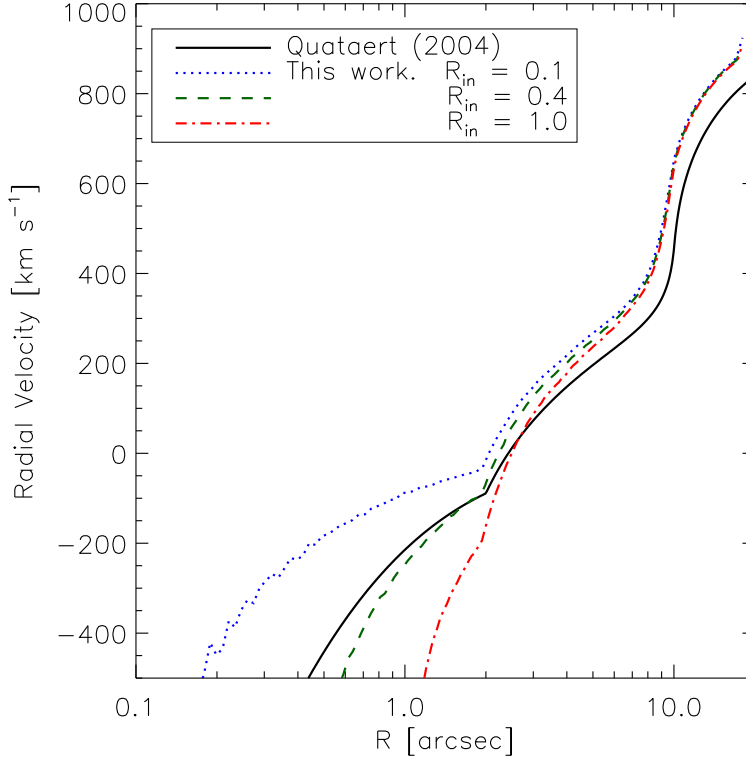


Figure 5.2: Radial velocity profiles of the gas in the calculations with 200 fixed stars distributed isotropically. Note that for larger capture radius the gas inflows faster. Because of the finite number of sources, the outflow velocity of our simulations is slightly larger than that in Quataert (2004).

wind, and thus *not all* of the gas within the nominally defined accretion radius is actually bound. Some of the gas at  $R < R_{\text{capt}}$  may therefore have a positive radial velocity.

Effects that are due to the finite number of stars should also manifest themselves in cooler temperature profiles at large radii compared to the Quataert (2004) results. There is a finite distance the winds will travel before they will experience a shock that will heat the gas up to the expected temperature. Therefore, for comparison purposes, we also defined an ‘effective 1-dimensional’ temperature  $T_{1d} = T + (m_p v_{\text{nr}}^2)/(10k_B)$ , where  $m_p$  is the proton mass and  $k_B$  is the Boltzmann constant. The quantity  $\vec{v}_{\text{nr}} = \vec{v} - \langle |\vec{v} \cdot \hat{r}| \rangle \hat{r}$  is the local gas velocity minus the mean radial velocity at the given radius. In a strictly spherically symmetric model (with an infinite number of stars) the non-radial velocity  $\vec{v}_{\text{nr}}$  would of course be zero, with the corresponding energy converted into thermal energy

of the gas. Therefore  $T_{1d}$  is the quantity to compare with the temperature derived by Quataert (2004). Figure 5.3 shows radially averaged  $T_{1d}$  profiles, and, for the case  $R_{in} = 0.4''$ , we also show the actual uncorrected gas temperature  $T$  (lower green curve), also averaged in radial shells. Note that the difference between  $T_{1d}$  and  $T$  is only significant at radii greater than  $1''$  because inside this radius the gas is relatively well mixed, i.e. shocked. On the contrary, the average gas temperature in the outflow region (close to our outer boundary condition) is significantly smaller than the spherically-symmetric limit. The reason for this is that some of the wind from the outermost stars is actually never shocked as it escapes from the computational domain. The same reason is also responsible for the differences in the radial velocity curves (Fig. 5.2): all of our solutions outflow slightly faster at  $R \lesssim R_{out}$  than do the winds of Quataert (2004).

The accretion rate,  $\dot{M}_{BH}$ , in our simulations is defined as the total mass entering the sphere of radius  $R_{in}$  per unit time. We find that the accretion rate increases initially while winds fill in the available space, but after less than 1,000 years  $\dot{M}_{BH}$  reaches a steady state value. The final value will of course depend on the choice of  $R_{in}$ . For the simulations described above, we get accretion rates  $\dot{M}_{BH} \approx 1.5, 3.5$  and  $7 \times 10^{-5} M_{\odot} \text{ yr}^{-1}$ , for  $R_{in} = 0.1, 0.4$ , and  $1''$  respectively. The increase of  $\dot{M}_{BH}$  with  $R_{in}$  implies that a significant fraction of the gas that is ‘accreted’ in the simulations with large  $R_{in}$  would not have done so had we been able to resolve the smaller scale flow. As far as the exact accretion rate values are concerned, smaller  $R_{in}$  is better, but, since a smaller  $R_{in}$  requires shorter integration steps, one has to make a pragmatic compromise and choose a value of  $R_{in}$  that allows simulations to be run in a reasonable time.

The accretion rates that we obtain are comparable with the Quataert (2004) result for  $\eta = 2$ ,  $4.5 \times 10^{-5} M_{\odot} \text{ yr}^{-1}$ . However, the most reliable of the tests, with  $R_{in} = 0.1''$ , shows an accretion rate a factor of 3 lower than the semi-analytical result. We interpret this as another manifestation of the incomplete spherical symmetry due to the finite number of stars in our simulations. We found that even at radii as small as  $0.3''$  there are large deviations from the mean in the gas velocity in the same radial shell. In addition, a fraction of the gas has significant specific angular momentum. To test these points further, we ran an additional simulation with  $R_{in} = 0.1''$ , but with 40 wind sources, which is more realistic as far as Sgr A\* wind accretion is concerned but should enhance the discreteness effects when compared with Quataert (2004). The results we obtain are in general similar, but the effects produced by the finite number of sources are indeed enhanced. For example, the density in the inner region is  $\sim 50\%$  lower than in the simulation with 200 stars, producing a corresponding lower accretion rate (see green curves in Figs. 5.5 and 5.6).

We find that our derived accretion rate values are about one order of magnitude lower than those of Coker & Melia (1997). The differences are however due to a different physical setup rather than numerics. Coker & Melia (1997) used  $v_w = 700 \text{ km s}^{-1}$ , whereas we used  $v_w = 1000 \text{ km s}^{-1}$  here. This difference in wind velocity alone accounts for a factor of  $\approx 3$  difference in  $\dot{M}_{BH}$ . Furthermore, their total mass loss rate from the young stars is higher than ours by a factor of 3. If we take into account these differences, our simulation with the smallest

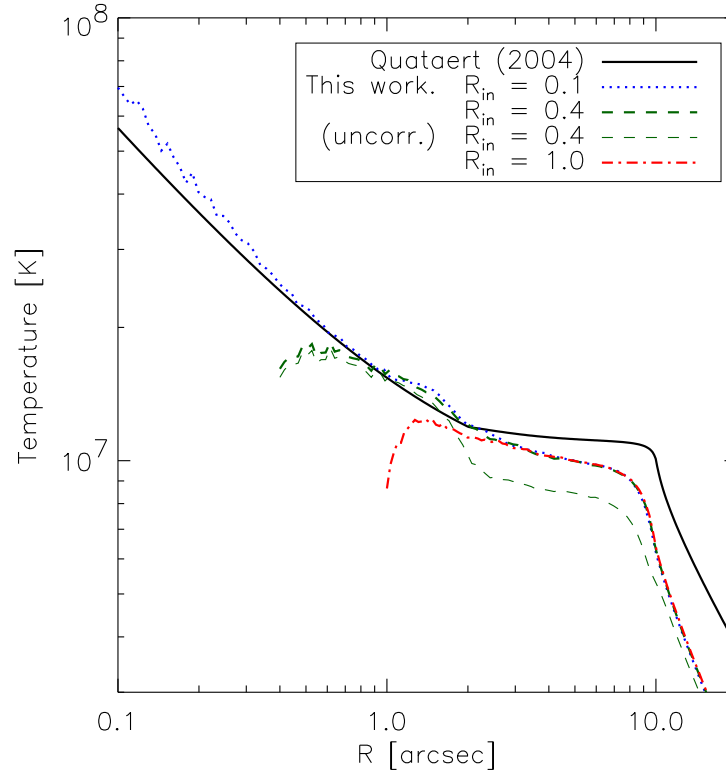


Figure 5.3: The ‘1-d’ temperature profiles of gas for the simulation with 200 fixed, isotropically distributed stars. The definition of  $T_{1d}$  includes gas bulk motions that would be absent in the case of exact spherical symmetry;  $T_{1d}$  is to be compared with the semi-analytical curve of (Quataert, 2004, solid). The ‘raw’ gas temperature, uncorrected for the bulk gas motions, is given for the case of  $R_{in} = 1''$  (lower red curve).

capture radius and 40 fixed stars appears to be consistent with the results of Coker & Melia (1997). Finally, the work of Rockefeller et al. (2004) did not directly focus on the accretion on to Sgr A\*. They were mainly interested in the dynamics of gas on parsec-scales. The accretion rate they quote is likely to be over-estimated because of the large value of  $R_{\text{in}} \approx 2''$  they use.

### 5.3.2 Stars in orbits around Sgr A\*

The next step towards a more realistic model is to allow the stars to follow orbits in Sgr A\*'s gravitational potential. We do this in two idealised configurations: a spherically symmetric and a disc-like system (for the latter, the stellar disc is somewhat thick, with  $H/R \sim 0.2$ , as seems to be the case observationally). In both cases, we put 40 stars in circular orbits around the SMBH. We use the same stellar density profile as in Section 5.3.1,  $n_*(r) \propto r^{-2}$ , and boundary conditions  $R_{\text{in}} = 0.1''$ ,  $R_{\text{out}} = 18''$ .

The significant difference with respect to the simulations discussed in Section 5.3.1 is that now the gas particles have a significant net angular momentum. To quantify this we create radial profiles of the average angular momentum, defined as the modulus of the average angular momentum vector in a shell,  $l(r) = |\langle \vec{r} \times \vec{v} \rangle|$ . Since we measure distances in arc-seconds and velocities in units of circular Keplerian velocity at that distance, a circular orbit at  $r = 1''$  has  $l(1'') = 1$  in these units. Note that  $l(r)$  should vanish for an isotropic orbital distribution of wind sources, even if each individual gas particle has a high angular momentum. Figure 5.4 shows the  $l(r)$  profiles for the simulations described in this section, and for the one with 40 fixed stars from Section 5.3.1.

When the stars are confined to a disc (red curve), the gas has on average roughly the local Keplerian angular momentum at the ‘wind source’ region, simply because the stars are on Keplerian circular orbits with the same angular momenta direction. If the orbits are randomly oriented (blue), the angular momenta of the gas should cancel out owing to the symmetry. However, the cancellation is incomplete due to the finite number of sources. Finally, in the case where the stars are fixed (green), the angular momentum is negligible, as it should.

Comparing the angular momentum in the three simulations in the sub-arcsecond region, we see that all simulations yield similar results. In all the cases the gas in this region is rotating significantly slower than the local Keplerian rotation, indicating that centrifugal support is not important for the gas. This is somewhat surprising given the vastly different angular momentum curves at larger radii and is not a result of viscous transport processes, because a physical viscosity was not included in the simulations<sup>2</sup>. This result rather seems to indicate that only the gas with originally low enough angular momentum makes it into the innermost region and is subsequently accreted, as already discussed by Coker & Melia (1997). The fraction of the stellar wind with low

---

<sup>2</sup>Note that the fact that the gas is significantly sub-Keplerian in the region justifies our neglect of angular momentum transport by viscosity.

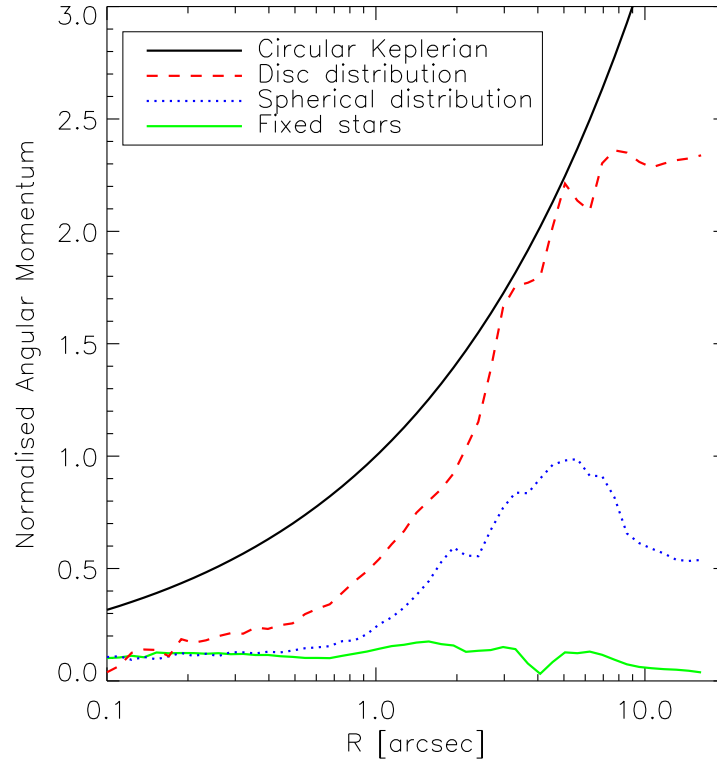


Figure 5.4: Angular momentum averaged on radial shells,  $l(r)$ , in the simulations with 40 stars in circular orbits (red and blue lines) and in fixed positions (green). For comparison we also show the value of the angular momentum of a circular orbit (black).

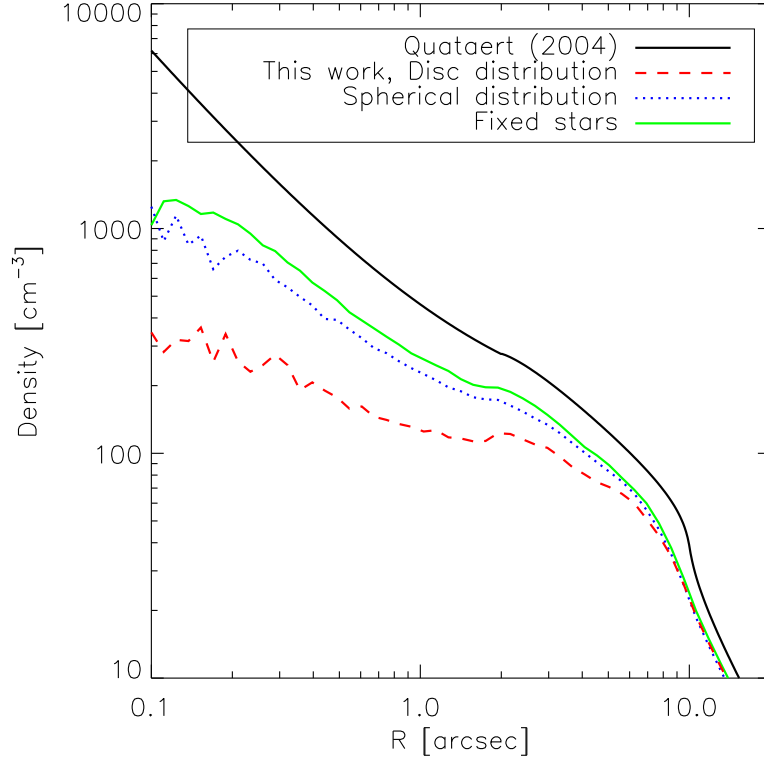


Figure 5.5: Density profiles of the gas in the calculations with 40 stars for different orbital configurations. The presence of significant angular momentum prevents the gas from inflowing, resulting in a lower density in the inner part.

angular momentum however varies greatly between the simulations, which in turn explains the different accretion rates.

Note that, once again due to the finite number of stellar sources, there is a distribution in the values of the gas angular momentum for any given radius. Some of the gas at  $R \sim 0.5''$ , for example, has a roughly Keplerian angular momentum which prevents it from accreting. This gives rise to shallower density profiles, as seen in Fig. 5.5, and is particularly important in the disc simulation (red curve), where the density is 2–3 times lower at  $1''$  than in the case with fixed stars. Note that in this case, the density value at  $1''$  is in better agreement with densities implied by *Chandra* observations (Baganoff et al., 2003). Correspondingly, the mass supply to the central black hole also decreases: we find that in the simulation with stars located in a disc, the average accretion rate is only  $\sim 2 \times 10^{-6} M_{\odot} \text{ yr}^{-1}$ , about 5 times lower than the value found with fixed stars.



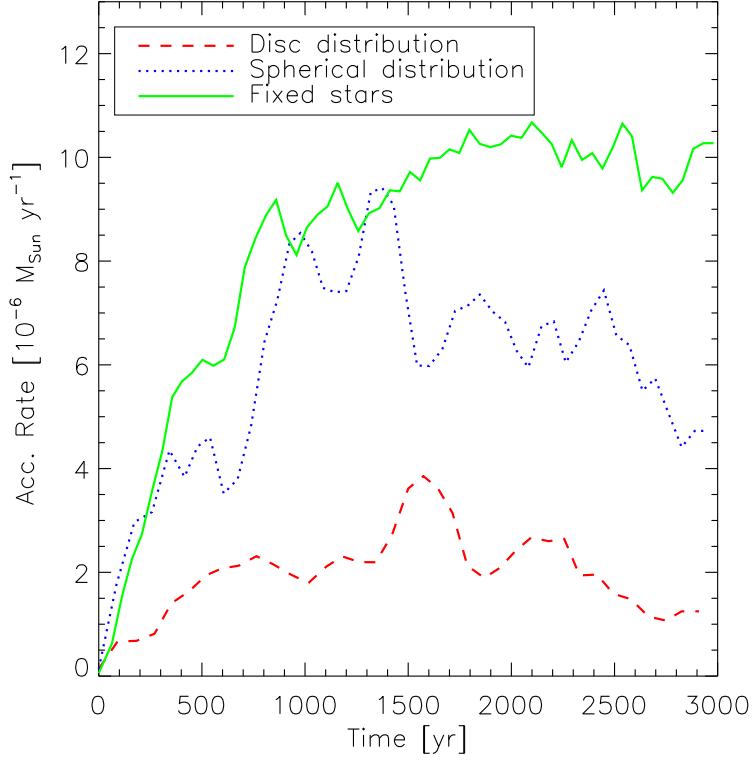


Figure 5.6: Accretion rate as a function of time in the simulations with 40 stars for different orbital configurations. The rotation of the stars produces a lower but variable accretion rate.

In addition to these effects, stellar motions yield a significant variability in the accretion rate. Figure 5.6 shows the accretion rate as a function of time for the same three simulations. In all the simulations, the accretion rate increases initially, as the stellar winds fill up the space. In the run with fixed stars, the accretion rate is practically constant after this initial increase. In contrast, when stars are allowed to follow orbits, the geometry of the stellar system changes with time (both in the isotropic and disk-like configurations), and so does the fraction of gas that can flow to the inner region. We should emphasise that this factor of  $\sim 30-70\%$  variability occurs in the two rather simple and still idealised stellar wind systems. In the more realistic situation, the variability would be enhanced further because we expect (i) yet smaller number of wind sources, (ii) a more diverse set of stars with different mass loss rates, (iii) non-circular stellar orbits, (iv) intrinsic stellar wind variability for luminous blue variable stars, etc.

## 5.4 Fast and slow (two-phase) winds

The next ingredient we add to our treatment of accretion of stellar winds on to Sgr A\* is the presence of slow winds. Previous models have considered only wind velocities  $\gtrsim 600 \text{ km s}^{-1}$ , as measured by Najarro et al. (1997). However, Paumard et al. (2001) showed that several of the inner stars with important mass-loss rates emit winds with velocities as low as  $\sim 200 \text{ km s}^{-1}$ . This has important consequences, because the slow winds are expected to cool and form clumps (Cuadra et al., 2005).

We use 20 wind sources in total, with each star loosing mass at the rate of  $\dot{M}_* = 4 \times 10^{-5} M_\odot \text{ year}^{-1}$ . To resemble the two observed populations of luminous blue variable candidates, ‘LBVs’, and Wolf–Rayet stars, ‘WRs’, we assume that stars in our simulations can have either  $v_w = 300 \text{ km s}^{-1}$  or  $v_w = 1000 \text{ km s}^{-1}$ , characteristic values for the two populations respectively. The values for the inner and outer boundary conditions are  $R_{\text{in}} = 0.07''$  and  $R_{\text{out}} = 9''$ . We run the simulations for  $\approx 4,000 \text{ yr}$ , then the number of particles reaches  $N_{\text{SPH}} \approx 1.5 \times 10^6$ .

For the distribution of the stars we adopt two different configurations. First, we place the stars into two discs in order to reproduce the distribution reported by Genzel et al. (2003b). We also place most of the LBVs in the inner disc, following Paumard et al. (2001). However, the stellar orbits are still only roughly known and the latest observations suggest that the LBVs may actually be distributed more evenly among both stellar systems (Genzel, priv. comm.). For these reasons, we consider a second simulation where the stars are distributed isotropically. The real distribution of the mass-losing stars should be somewhere in between these two extreme cases.

The simulations presented here differ from the work of Cuadra et al. (2005) in that we do not split particles that get relatively close to the SMBH. The splitting was used to increase the resolution in the inner part. However, further tests showed that some loss of accuracy can occur in our present implementation of this approach, so that it failed to really show a convincing practical advantage.

### 5.4.1 Stellar wind sources placed in two discs

Here we attempt to model the Sgr A\*–stellar wind system by setting up the stellar source distribution in a way that resembles the observations of the inner parsec in the GC (Paumard et al., 2001; Genzel et al., 2003b). Our approach is the same as the one described by Cuadra et al. (2005), therefore we describe it only briefly here.

The stars are distributed uniformly in radius and in two perpendicular rings. All stars follow circular Keplerian orbits. The radial extent of the rings is from  $2''$  to  $5''$  and  $4''$ – $8''$  for the inner and outer one respectively. Out of the 20 wind sources, we assume that 6 LBV-type and 2 WR-type stars are in the inner ring, and the outer ring is populated by 3 LBVs and 9 WRs.

### Large scale structure of the gas flow

Figure 5.7 shows the resulting morphology of the gas 2.5 thousand years into the simulation. The inner ring, mainly composed of LBVs that are shown by asterisks, is viewed face-on in the left panel, and edge-on in the right one. The inner ring stars are shown with the red coloured symbols whereas the outer disc stars are painted in black. The inner stars are rotating clock-wise in the left panel of the figure, and the outer ones rotate counter clock-wise in the right panel.

Cool dense regions in the gas distribution (shown as bright yellow regions in Fig. 5.7), are mainly produced by winds from LBVs. When shocked, these winds attain a temperature of only around  $10^6$  K, and, given the high pressure environment of the inner parsec of the GC, quickly cool radiatively (Cuadra et al., 2005). LBV winds form bound clouds of gas, often flattened into filaments due to the SMBH potential and the symmetry of the problem. As more filaments are formed in the inner region, they start overlapping and eventually form a disc that lies almost at the plane  $z = 0$ . The orientation of the disc plane is very close to that of the inner stellar ring, which at first may appear surprising given that there are 3 other LBV stars at the larger stellar disc. However, the escape velocity from the outer ring is of the order of the stellar winds velocity for the LBVs, and thus a large fraction of the slow wind from the outer ring escapes the computational domain and never influences the inner cold disc orientation.

The fast winds contribute to the inhomogeneity of the cold gas. This is well illustrated by one of the two WR-stars placed in the inner ring at  $(x, y) \approx (2, 2.5)$  in the right panel of Fig. 5.7. The wind from this star has more mechanical power than all of the winds from the other LBVs in the simulation ( $L_{\text{mech}} \propto \dot{M}_* v_w^2$ ). It cuts the combined wind of four neighbouring LBVs into two bands of gas. These two streams of gas are further stretched out by tidal shear from the SMBH and then chopped into smaller cool blobs by the interaction with the winds of the outer ring.

The three LBVs placed in the outer ring add complexity to the morphology of the cool gas as they produce cool gas streamers moving in a plane different from that of the inner one. One of these stars is at  $(x, z) \approx (-5.5, -1)$ . It produces most of the cool blobs of gas seen at the left of the right panel. Also note that the LBV at  $(x, z) \approx (4, 1)$  is uplifting a significant amount of the cooled wind from the inner LBVs. On the other hand, the WRs by themselves do not produce much structure, as seen for instance from the two stars located at the upper left corner on the right panel. The fast winds they produce have temperatures  $\gtrsim 10^7$  K after shocking, and do not cool fast enough to form filaments.

Figure 5.8 shows the average gas temperature in a slice  $z = \pm 0.5''$  (left panel) and in a slice  $y = \pm 0.5''$  (right panel) of the inner  $6''$  region<sup>3</sup>. The clumps and the disc are cold as a result of radiative cooling, and before they collide the stellar winds have a low temperature as well. However, close to the stars the

---

<sup>3</sup>To avoid low-density hot regions from dominating the map, we column-averaged  $\log T$  rather than simply  $T$ .

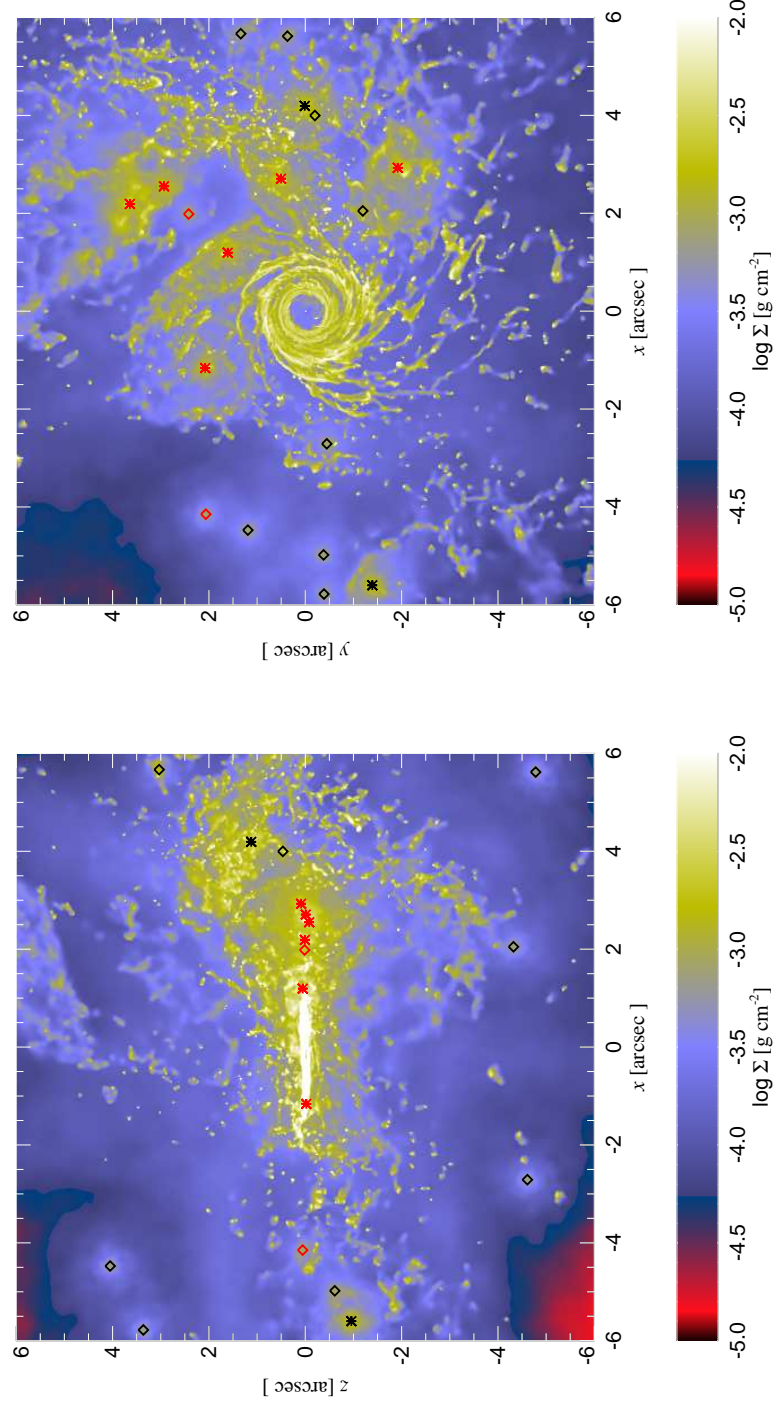


Figure 5.7: Left panel: Column density of gas in the inner  $6''$  of the computational domain 2,450 years after the beginning of the simulation. Stars of the inner disc are shown as red symbols, while the ones on the outer disc appear in black. Asterisks mark slow wind stars (LBVs), whereas diamonds mark stars producing fast winds (WRs). The inner stellar ring is face-on while the outer one is seen edge-on (plane  $y = 0$ ). Right panel: same as on the left, but the outer stellar ring is now seen face-on while the inner one appears edge-on ( $z = 0$ ).

temperature appears higher than it would have been in reality. This is an artifact of the injection of a finite number of SPH particles per time-step into the wind, which creates some small-scale structure in the density and pressure profiles, leading to energy dissipation. This effect is however of minor importance since the temperature in these regions is still relatively low compared to the maximum temperatures that the gas can attain in a shock. In other words, the energy of the winds is still strongly dominated by the bulk motion of the gas rather than thermal energy.

The diffuse gas filling up the rest of the space is hot, with temperature  $\sim 10^7$  K, comparable to that producing X-ray emission detected by *Chandra*. Gas cooler than that would be invisible in X-rays due to the finite energy window of *Chandra* and the huge obscuration in the Galactic plane.

### Structure of the inner flow

Figure 5.9 depicts the structure of the inner flow later in the simulation, at  $t = 4.0 \times 10^3$  years. At this late time, the cool disc becomes heavier and larger in the radial direction than seen in Fig. 5.7. The inner  $\sim 0.3''$  region is still devoid of cool gas except for a few filaments. This is due to two reasons. First, the angular momentum of the slow winds from the innermost stars is not zero, even for the wind directed in the opposite direction of the stellar motion. The Keplerian circular velocity at  $2''$  is  $v_K \approx 440$  km/sec, whereas the wind velocity is  $v_w = 300$  km/sec. Thus wind with even the minimum angular momentum would circularise at  $r \sim 2'' \times (v_K - v_w)^2 / v_K^2 \sim 0.2''$ . However, due to interactions of this gas with the gas with higher angular momentum, the minimum disc radius is actually a factor of  $\sim 2$  higher. Second, the inner empty region of the disk is not filled in by the radial flow of cold gas through the disc because the viscous time scale of the cold disc is enormously long compared with the duration of the simulation (e.g. Nayakshin & Cuadra, 2005). Gas clumps having low angular momentum infall into the inner arcsecond, but this does not occur frequently enough to fill in that region, and most of these clumps appear to be disrupted and heated in collisions. The long viscous time-scale is also the reason why the filaments do not merge forming a smooth disc at larger radii. The individual filaments that give shape to the disc are still distinguishable in the figure.

The mass of the cold disc is actually quite small, i.e. only  $\approx 0.2 M_\odot$ . It is instructive to compare this number with the mass of the wind produced by the ‘LBV’ stars in  $4 \times 10^3$  years, which turns out to be  $1.4 M_\odot$  for this simulation. Obviously most of the cold gas escapes from the simulation region. However, some of this gas does not have a true escape velocity. Had we simulated a larger region, a fraction of this cold gas could return to the inner region on highly eccentric orbits, producing further variability and complexity in the morphology of the cold gas and accretion history of Sgr A\*.

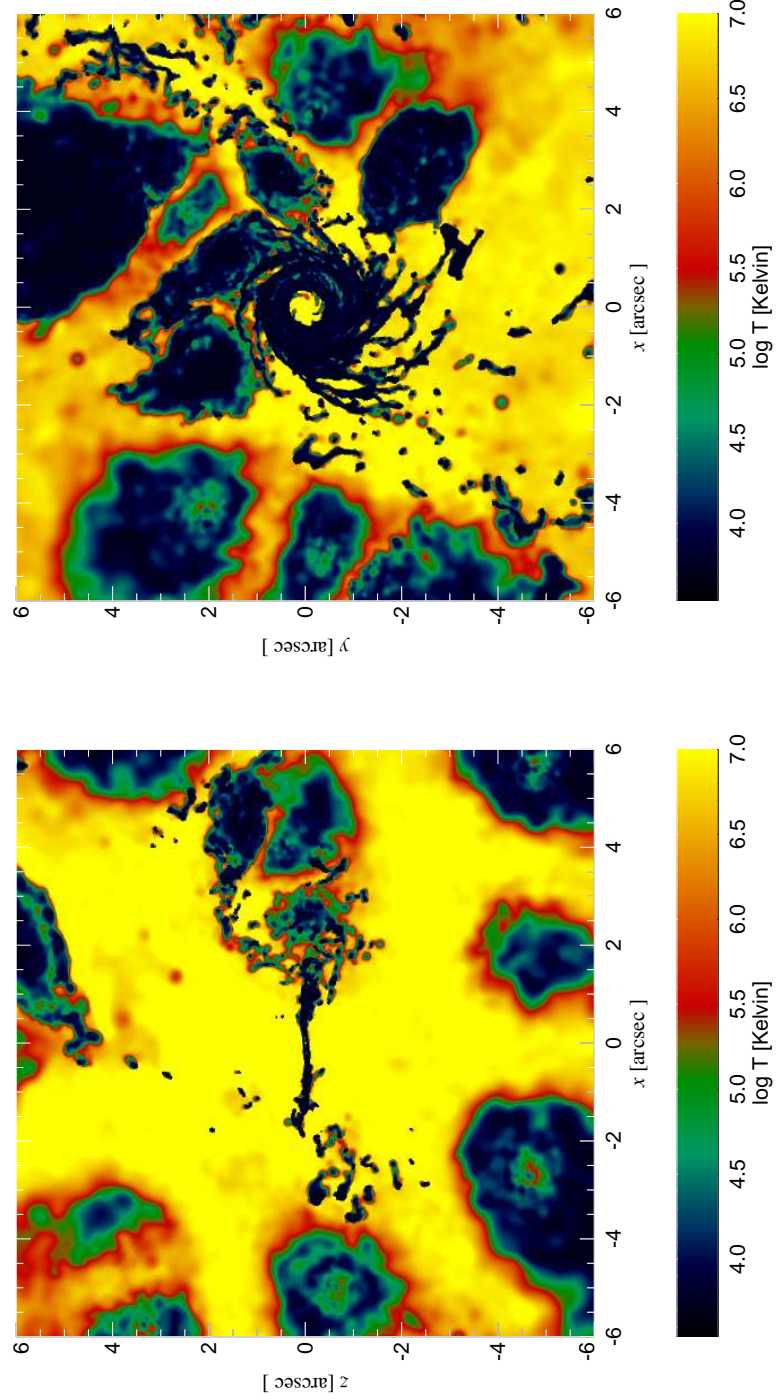


Figure 5.8: Similar to Fig. 5.7, but showing 1''-thick cuts of the gas temperature. Stars are not shown for clarity. The left panel shows a slice between  $z = -0.5''$  and  $+0.5''$ , whereas the right one shows the gas temperature in the range  $-0.5'' < y < +0.5''$ . The minimum temperature in the simulation is set to  $10^4$  K. In reality gas would cool even further, likely to a few hundred K.

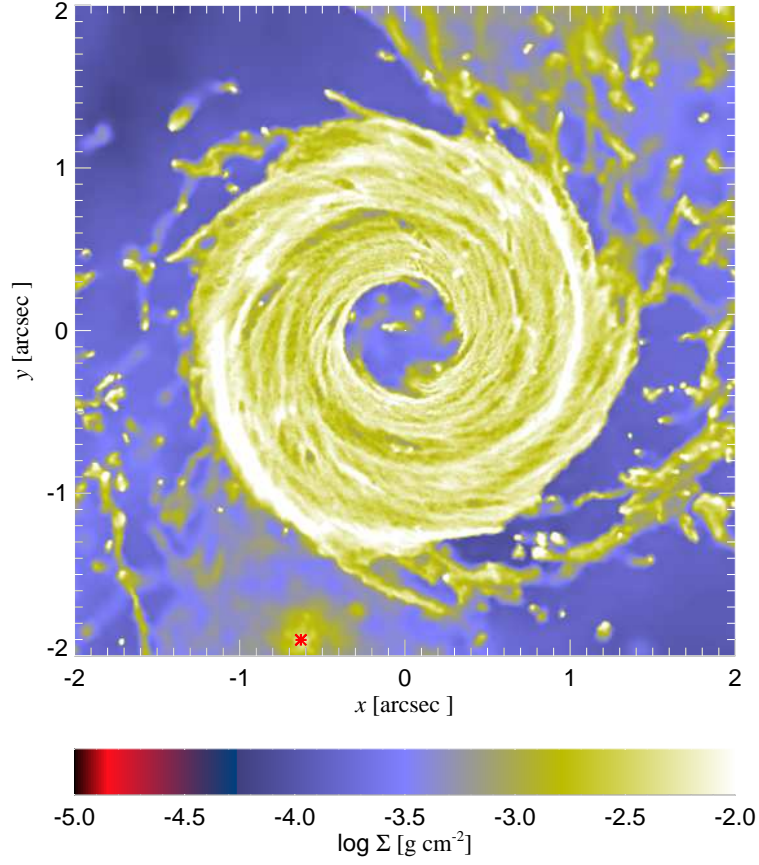


Figure 5.9: Top view of the inner  $2''$  cube at time  $t = 4.0 \times 10^3$  years. Note that the disc grew larger in radial extent but the inner region is still devoid of cool gas except for a few clumps.

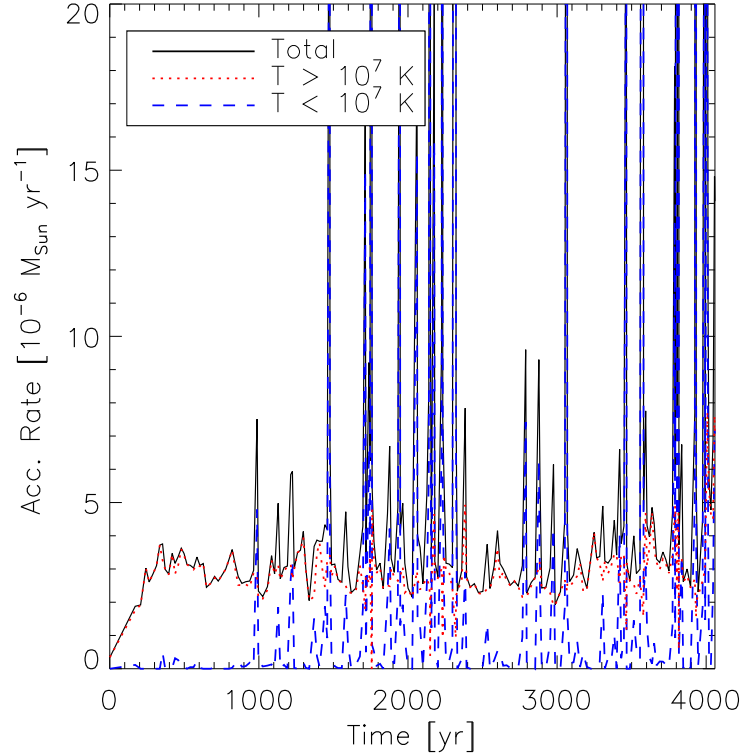


Figure 5.10: Accretion rate on to the SMBH as a function of time (black line). This rate is then divided into that of hot gas (red) and that of low temperature gas (blue). Note that the time-averaged accretion is dominated by the hot component that is quasi-constant; the accretion of cold gas is episodic and highly variable, but smaller overall.

#### Accretion on to Sgr A\*

As described in Section 5.2, all gas particles entering the inner boundary of the computational domain, in this case  $R_{\text{in}} = 0.07''$ , are presumed to be instantaneously accreted by Sgr A\*. In practice, such accretion would happen on the viscous time scale of the flow, which depends on the viscosity  $\alpha$ -parameter (Shakura & Sunyaev, 1973), the gas temperature and the circularisation radius. When taking these factors into account, we would expect a time-scale of at least 10 yr for the accretion of hot gas. For this reason, in Fig. 5.10, we plot the accretion rate smoothed over a time-window of duration  $\Delta t \approx 10$  years.

Figure 5.10 also shows the accretion rate of hot ( $T > 10^7$  K, red line) and cold ( $T < 10^7$  K, blue line) gas separately. The accretion rate of hot gas is



fairly constant, and has a value  $\dot{M}_{\text{BH}} \approx 3 \times 10^{-6} \text{ M}_{\odot} \text{ yr}^{-1}$ , consistent with the *Chandra* estimates (Baganoff et al., 2003). In addition to this component, the intermittent infall of cold clumps produces most of the variability in the accretion rate. The cold gas falls into the innermost regions due to two factors: (i) it is initially created on low angular momentum trajectories, and/or (ii) it acquires such orbits through collisions with other cold gas clumps.

For further analysis we define the local mass inflow and outflow rates integrated on shells at a given radius. Figure 5.11 shows both of these quantities, for all the gas (thin lines), and for the hot gas only ( $T > 10^7 \text{ K}$ , thick lines). The profiles were measured in a similar fashion as those in Section 5.3 by stacking 10 snapshots at  $t \approx 2.5 \times 10^3 \text{ yr}$ . For the hot gas, the outflow practically cancels the inflow between  $0.4''$  and  $2''$ . Only the gas with low enough angular momentum and thermal energy accretes in this region, the rest escapes into the outflow. This effect is completely absent in a spherically symmetric flow such as the Bondi (1952) solution.

The true accretion flow in our simulation starts at  $R \approx 0.4''$ , where the inflow rate becomes approximately constant and the outflow is negligible. This radius would be a better definition of the effective capture radius.

The profiles that include all the gas (thin lines) are dominated by cold gas in the disc at  $R \approx 0.3\text{--}1.3''$ . We find that the mean eccentricity for this gas is  $e \approx 0.1$ . This deviation from circular velocity, together with the relatively high mass of the disc explain the ‘noise’ in the inflow/outflow profiles in this region. However, the inflow dominates, and its net rate is much larger than the accretion rate at  $R_{\text{in}}$ , so an important fraction of the gas actually stays in the disc, making it grow in mass. For larger radii the inflow becomes negligible and the outflow rate reaches approximately the total mass loss rate of the wind sources,  $\dot{M}_{\text{w}} = 10^{-3} \text{ M}_{\odot} \text{ yr}^{-1}$ .

### 5.4.2 Simulation with isotropic orbits

With the aim to test how the results depend on the assumed stellar orbits we run a simulation with exactly the same set-up as in the previous subsection, but instead of placing the stars into the two rings, we oriented the stars’ circular orbits randomly. The distribution of angular momentum vectors is obviously isotropic for this case.

Figure 5.12 shows the column density of the gas at  $t = 2.4 \times 10^3$  years after the beginning of the simulation. For this simulation, no conspicuous disc is formed. Instead, we find that only a small ring on scales of  $\sim 0.5''$  is formed. The ring has the same angular momentum direction than the innermost star (an LBV). Its radial scale is smaller than the inner boundary of the disc formed in Section 5.4.1, because in this simulation the gas that formed the ring interacts with a larger quantity of gas with different angular momenta, loosing its own.

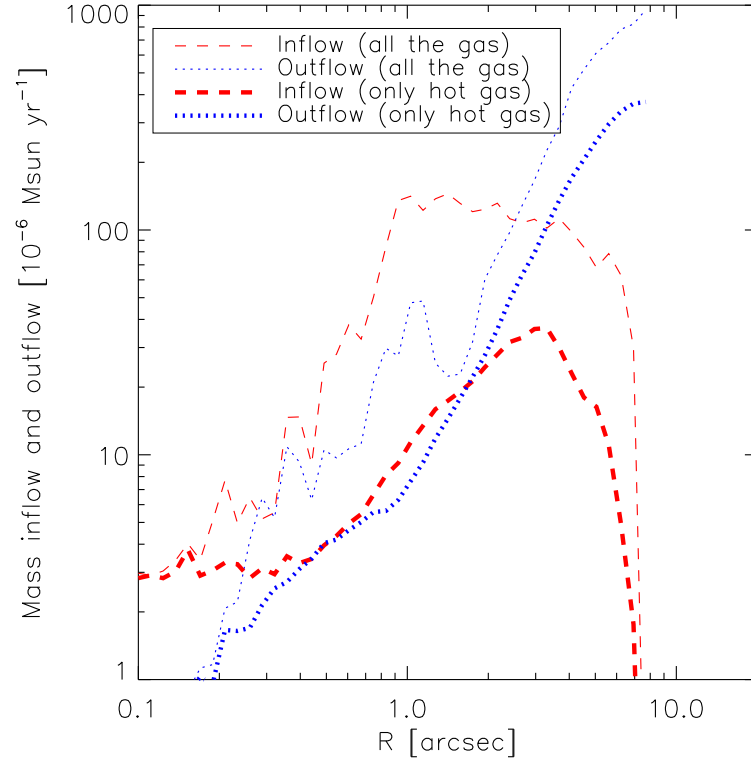


Figure 5.11: Mass inflow (red curves) and outflow (blue) as a function of radius. The thick lines show the profiles for the hot gas only, while the thin lines include all the gas.

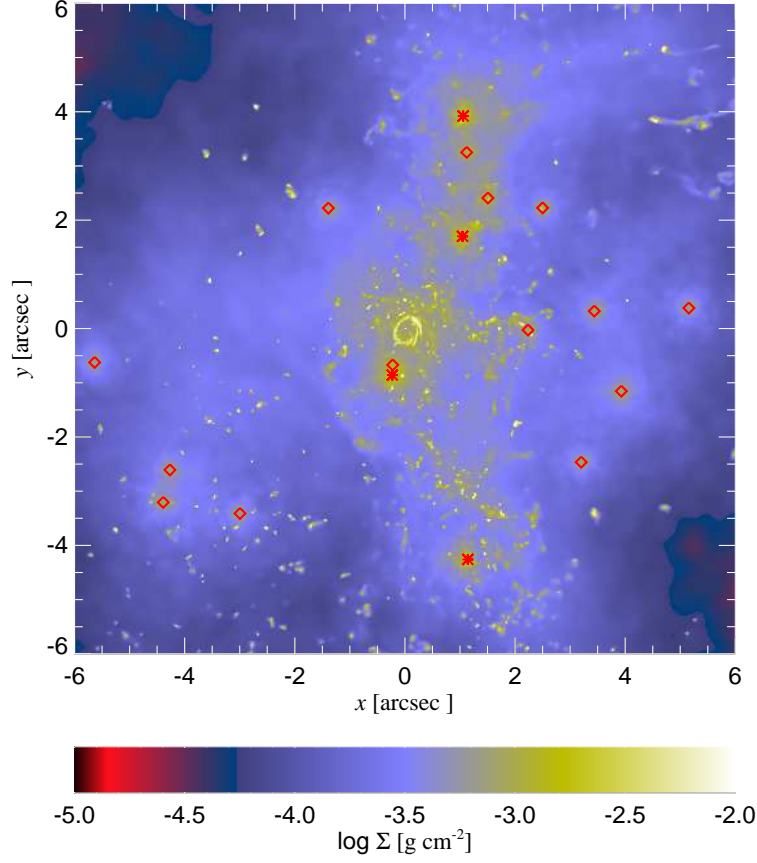


Figure 5.12: Gas column density map for a simulation with 20 stars, chosen as in Section 5.4.1 but with orbits that have a random angular momentum vector.

### 5.4.3 Comparison of both simulations

The prominent disc-like structure that we find in the simulation with two stellar discs appears to be inconsistent with some of the current observations. In infrared images (e.g., Scoville et al., 2003; Paumard et al., 2004) complex structures of cold gas are indeed seen, but they are not in a disc configuration. In addition, the cold gas structures are typically observed on larger scales than what we find in our simulation. The most likely reason for the discrepancies between these recent observations and our model may be ascribed to the specific initial conditions we used. In particular, placing many LBVs in the same plane at a short distance from the SMBH may be particularly favourable for the development of a disc. Completely different is the case in which the stellar orbits are oriented randomly (Section 5.4.2). The distribution of angular momenta vectors is obviously isotropic for this case, so there is no obvious preference for a particular plane where a disc would form. The tiny ring formed there perhaps could be missed observationally or not formed at all if closest slow wind stars are in reality farther away than we assumed for the simulation.

Nevertheless, in both simulations we get a two-phase medium in the inner region, and a comparable accretion rate. These are robust results, dependent only on the velocities we have chosen. The specific gas morphology, instead, depends strongly on the orbital geometry of the initial source distribution.

The angular momentum profiles (defined as in Section 5.3.2) of gas in the simulations with isotropic orbits (blue) and with two discs (red) are shown in Fig. 5.13. In the isotropic case the angular momentum is low at the wind source region. In contrast, the gas angular momentum is much higher in the two stellar disc simulations at the same range of radii. Somewhat surprisingly, the angular momentum content of hot gas in the inner arcsecond is actually quite similar for the two simulations. This can be traced to the hydrodynamical interaction of the hot gas with the cold gas, whose net angular momentum is much higher. Indeed, the angular momentum profiles of all the gas (cold and hot), shown with thin curves in Fig. 5.13, are nearly Keplerian in the inner arcsecond region.

### 5.4.4 Comparison of the two-phase and one phase simulations

At this point it is also instructive to highlight some of the systematic differences between the ‘one-phase’ (fast winds only) and the ‘two-phase’ simulation results. The angular momentum profiles of the one-phase and two-phase simulations are shown in Figs. 5.4 and 5.13, respectively. While in the one-phase simulations the angular momentum of gas near the capture radius was always much lower than the local Keplerian value, the two-phase simulations show almost Keplerian rotation near the inner boundary. As explained in Section 5.4.3, this is caused by the interaction between the hot and the cold gas phases. Only the part of the fast wind that has a low angular momentum accretes from the hot phase, because its pressure support against SMBH gravity is already high. In contrast, cold gas has little pressure support and hence even gas with a rather high

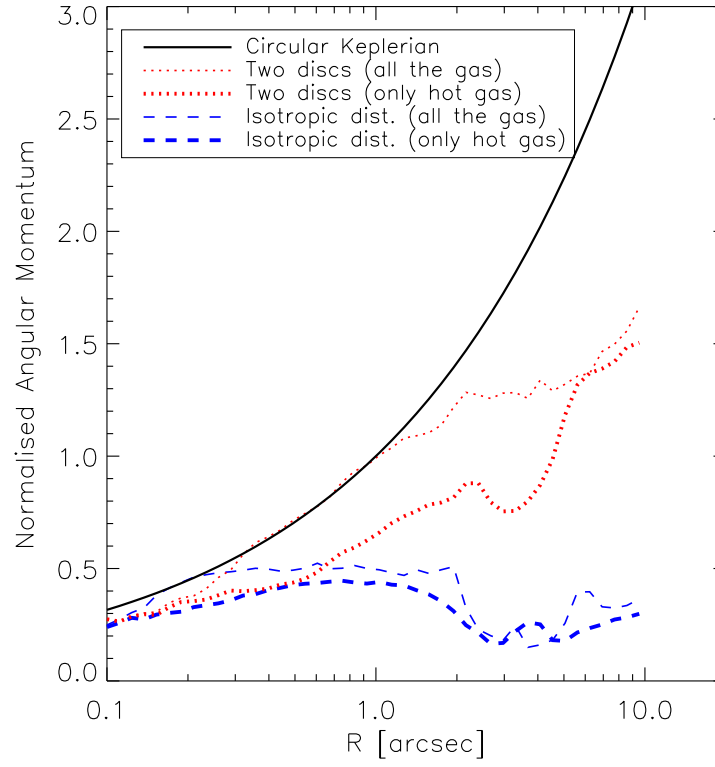


Figure 5.13: Angular momentum profiles of the simulations with isotropic orbits (blue, Section 5.4.2) and with two discs (red, Section 5.4.1). For comparison, the value of a Keplerian circular orbit is shown as well (black line).

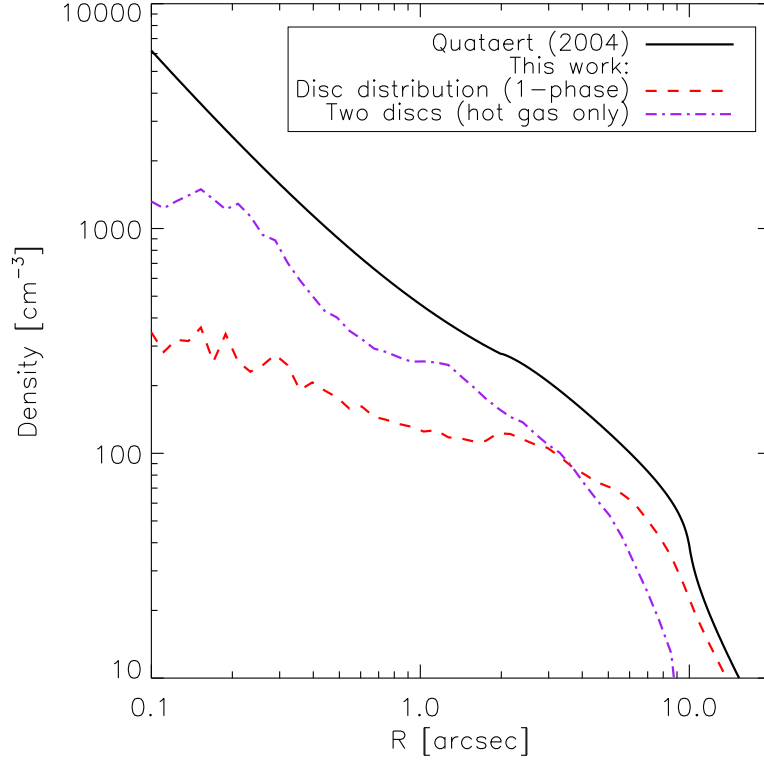


Figure 5.14: Hot gas density profiles of ‘one-phase’ simulations with stars arranged in disc orbits (red dashed line, Section 5.3.2) and two-phase simulations with two discs of stars (violet dot-dashed, Section 5.4.1). Note that the two-phase simulation yields a much more centrally concentrated profile.

angular momentum can be captured into the central arcsecond by Sgr A\*. This also implies that such two-phase accretion flows are more strongly rotating, or more precisely, that their circularisation radii are larger (see Section 5.6.5).

The other notable difference between the one and two phase simulations is that the latter produce much more concentrated radial density profiles for hot gas (Fig. 5.14). Due to the presence of slow winds and thus more prominent radiative cooling, the two-phase simulations yield less pressure support for the gas. A larger angular momentum is then needed to support the gas against gravity, as pointed out above. However this extra support is apparently insufficient and the radial density profile plunges in quicker in the two-phase case than it does in the one phase case. Interestingly, despite using a different setup and including different physics, our two-phase hot gas density curve is by and large similar in shape to that of Quataert (2004), although yielding a lower accretion

rate.

## 5.5 What would Chandra see?

Having obtained maps of the gas density and temperature distributions, we calculate the expected X-ray emission of each pixel. We use an optically thin cooling function  $\Lambda(T)$  (see Section 5.2), modified to crudely model the effects of the interstellar absorption. As is well known, the column depth of the cold ISM to Sgr A\* is very high,  $N_{\text{H}} \sim 10^{23}$  hydrogen atoms  $\text{cm}^{-2}$  (e.g., Baganoff et al., 2003), and hence *Chandra* receives hardly any photons with energy less than  $\sim 2$  keV. Therefore, gas cooler than  $T \sim 10^7$  Kelvin will contribute very little to the X-ray counts. We then use

$$\Lambda_{\text{mod}}(T) = \frac{\Lambda(T)}{1 + (T_{\text{cut}}/T)^5}, \quad (5.1)$$

where  $T_{\text{cut}} = 10^7$  Kelvin.<sup>4</sup> Below we consider X-ray emission from two of our simulations.

Figure 5.15 shows a resulting X-ray map for the simulation with fast winds only (Section 5.3), with 40 stars in a rotating disc configuration. The map shows the luminosity (normalised to one arcsec) integrated over pixels of  $0.5''$ , which is about the *Chandra* pixel size (clearly we could have produced much finer simulated X-ray images of the GC). Remarkably, the density of the hot gas in the inner arcsecond is so low that stellar winds actually dominate the X-ray map. This is due to two factors. First, the stellar density is greater for stars located in a (relatively thin) disc than it is for the same stars spread around a spherical shell at the same radial distance. As a result, the stars are closer to each other and the shocked gas density is higher. Second, the large angular momentum of the gas prevents most of it from flowing into the inner arcsecond of this simulation (see Figs. 5.4 and 5.5), thus reducing the X-ray emission from the centre.

Figure 5.16 depicts the light curves of the radial annuli ( $R < 1.5$ , 3 and  $6''$ , respectively) for the simulation corresponding to Fig. 5.15. Clearly, the central region never dominates the X-ray emission. Also, variability is rather mild and occurs on time scales of hundreds of years.

Figure 5.17 shows the more ‘realistic’ simulation which includes both fast and slow winds with stars located in two rather than one ring. Note that the scale of the colour bar on the bottom is 10 times higher than that used in Fig. 5.15. In sharp contrast with Fig. 5.15, the central source clearly stands out now at a level consistent with that observed by *Chandra*. This difference is caused by a much stronger concentration of the hot gas in the centre in this latter model, discussed in Section 5.4.4.

Figure 5.18, shows the light curves corresponding to Fig. 5.17 and can be directly compared with Fig. 5.16. We note that in the more ‘realistic’ simulation

---

<sup>4</sup>A very sharp rollover in temperature is justified by the very strong dependence of photo-electric absorption cross section on photon energy.

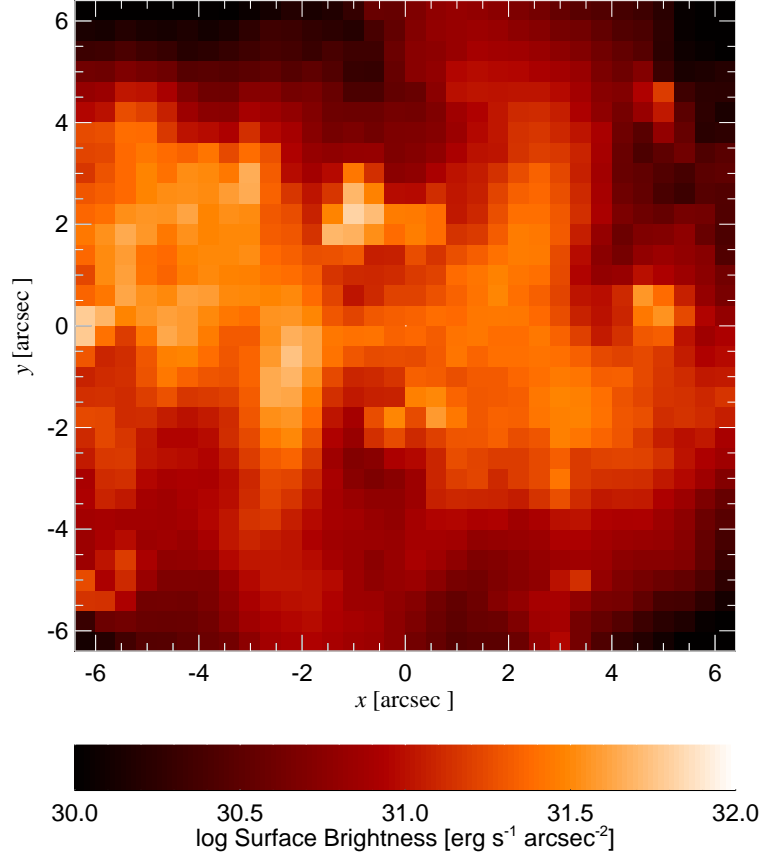


Figure 5.15: Simulated *Chandra* view of the inner  $12''$  by  $12''$  for the simulation with fast winds only (Section 5.3), with 40 stars arranged in a disc configuration. The corresponding density profile was shown in Fig. 5.5 (dashed red curve). Note the strong and highly extended emission from stellar wind shocks. No central source associated with Sgr A\* is actually visible.



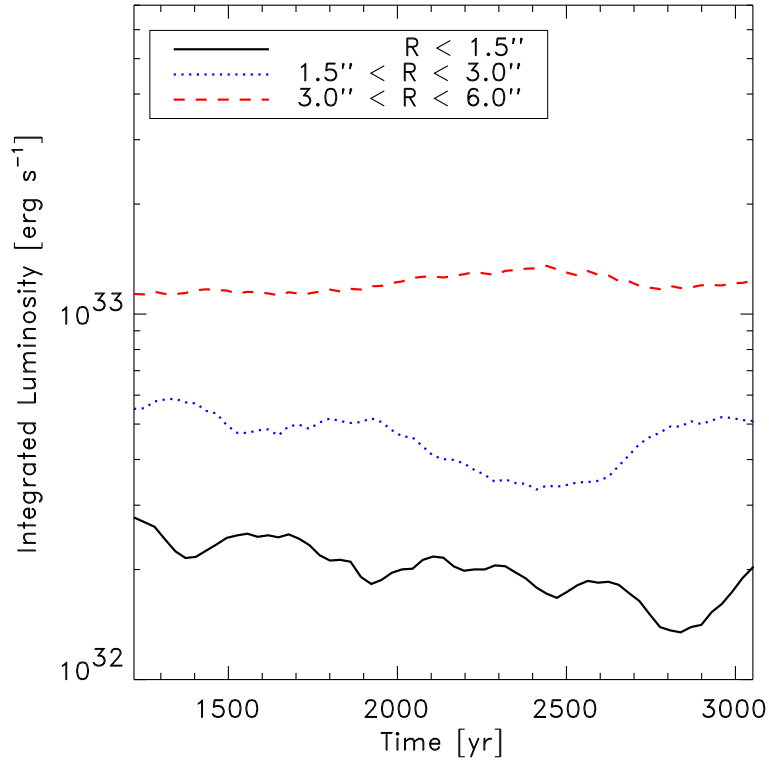


Figure 5.16: Light curves of three radially selected regions, as indicated in the inset. Variability is due to changes in the relative positions of the stars. The luminosity of the inner region is correlated with the accretion rate, because both are determined by the density in the inner arcsecond.

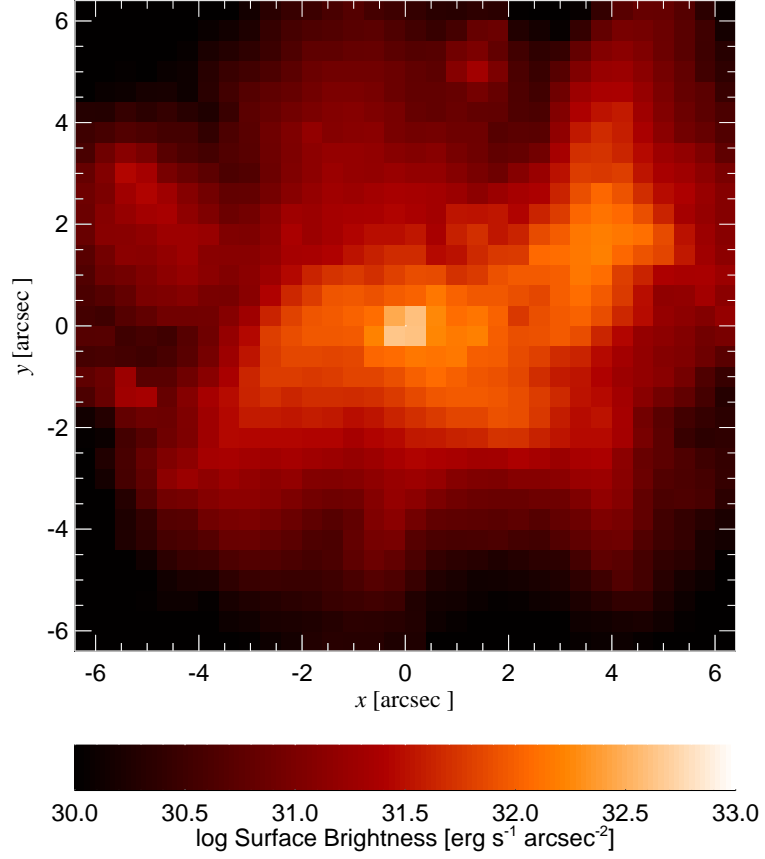


Figure 5.17: Simulated *Chandra* view of the inner 12'' by 12'' for the simulation shown in Fig. 5.7. The rings of stars are inclined at a 45° angle to the line of sight in this figure. Note that the central arcsecond clearly stands out in X-rays, but the emission is spatially extended, perhaps slightly more than in the real Sgr A\* observations by *Chandra*.

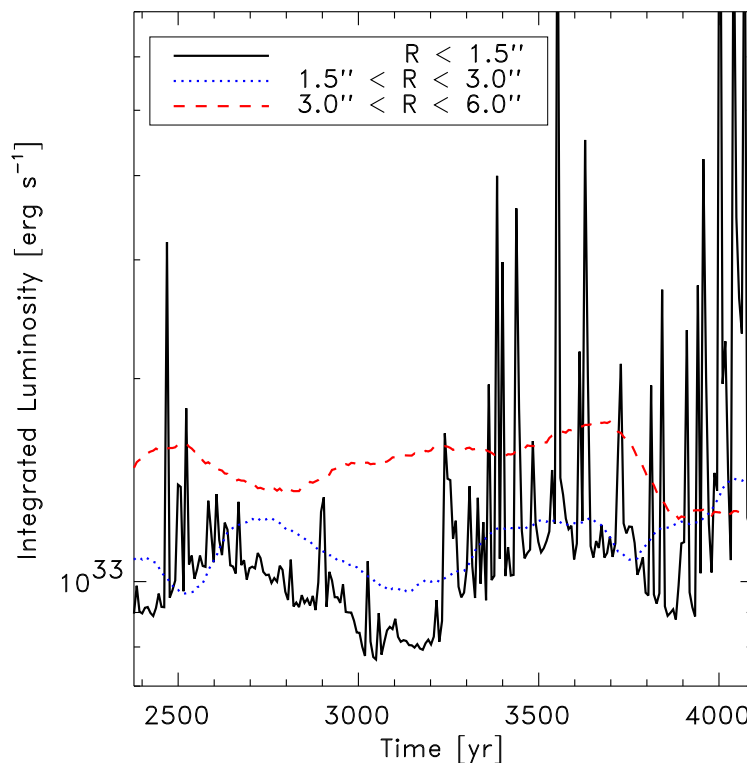


Figure 5.18: The same as for Fig. 5.16 but for the simulation with two rings of stars (see Fig. 5.17). Note that now the central region is brighter and much more variable. The variability in the light received from the central region is mainly caused by cool blobs of gas raining down on to the disc, shock-heating gas to X-ray emitting temperatures.

the X-ray luminosity of the central source is higher and is by far more variable. The steady state X-ray emission is larger simply due to the higher hot gas density in the inner region, whereas the variability is produced by shock-heated blobs impacting the cold disc. During such events the peak in the X-ray intensity can actually shift from Sgr A\* nominal position by  $\sim 0.5''$  or so.

It would be interesting to compute the X-ray spectrum of each pixel, and then compare that to *Chandra* observations of Sgr A\*. This would involve calculation of the local radiation spectrum, radiation transfer along rays and a model for X-ray absorption in the interstellar matter between the GC and us. We leave such a detailed comparison with observations for future work.

## 5.6 Discussion

The theory of accretion flows on to SMBHs is an area of active research (e.g., Narayan, 2002) where observational tests constitute strong drivers in the field. Due to its proximity, Sgr A\* is the only SMBH where it is becoming possible to constrain observationally the accretion flow properties both at small and large radii simultaneously ( $R \sim 10 - 100 R_S$  and  $R \sim 10^5 R_S$ ; see Bower et al., 2003; Baganoff et al., 2003; Nayakshin, 2005a).

The most direct method to measure the accretion rate is through *Chandra* X-ray observations (Baganoff et al., 2003). However, this method has the following drawbacks: (a) gas cooler than  $\sim 10^7$  K cannot be observed due to a very high neutral hydrogen absorbing column to the GC, thus the contribution of cool gas is unknown; (b) bulk motions of the gas can in principle make some of the gas unbound, but these do not directly enhance the X-ray emission, and thus they can be missed; (c) only the instantaneous conditions can be probed, whereas the relevant time scales can be tens and hundreds of years.

The second method to infer the input accretion rate is through observations of stellar winds and models of the outflows and gas accretion on to the SMBH. This method alleviates deficiencies (a-c) discussed above, but of course comes with its own set of problems and uncertainties. In this paper, we have attempted to reduce these in the part of the theoretical (numerical) modelling of the wind hydrodynamical evolution. Conceptually, we built on the previous numerical work in the area (Coker & Melia, 1997; Rockefeller et al., 2004) and on the semi-analytic model of Quataert (2004). However, we have used a Lagrangian SPH/ $N$ -body code, allowing us to follow the problem in its full 3D setting. Compared with previous authors, we have been able to relax assumptions that stellar wind sources are fixed in space and that shocked winds suffer no radiative losses. We have also varied stellar orbital distributions, testing rotating disc-like and isotropic distributions.

### 5.6.1 Reduction of accretion due to anisotropy and net angular momentum

We performed three runs with fast stellar winds ( $v_w = 10^3 \text{ km s}^{-1}$ ) produced by 40 stars. These runs tested the importance of the orbital motions and the source distribution. For a stationary spherical stellar distribution, the accretion rate (see Fig. 5.6) was found to be around  $\sim 10^{-5} M_\odot \text{ year}^{-1}$ , with variability at a level of 10%. These results are consistent with that of Coker & Melia (1997) after correcting for small differences in wind velocities and stellar wind loss rates. Allowing the stars to follow randomly oriented circular Keplerian orbits decreased the accretion rate by a factor of three, and increased the variability up to  $\sim 50 - 70\%$  (blue dotted curve in Fig. 5.6). Placing these same stars into a disc reduced the accretion rate by another factor of three or so, while keeping the variability magnitude at about the same level. The main driver of the differences in these three tests is the net angular momentum of the gas (Fig. 5.4). We find that only the gas with a low enough angular momentum makes

it to the inner boundary and hence is accreted, and the fraction of such gas decreases when the source distribution is rotating with a common direction (a disc).

Another way to view this result is to say that the angular momentum of the gas and ‘random’ gas motions reduce the gas capture radius. Although authors’ definition of the latter differ slightly, most consider the capture radius to be 1–2'' (Baganoff et al., 2003; Rockefeller et al., 2004), whereas we would define  $R_{\text{capt}}$  to be about 0.4'' based on our simulations. Indeed the gas can be called captured only at this region, where accretion (see Fig. 5.11) strongly dominates; at large radii outflow and inflow nearly cancel each other.

### 5.6.2 Cool phase of stellar winds

In a fixed pressure environment, gas cooling time is a very strong function of temperature:  $t_{\text{cool}} \propto T/(\Lambda(T)n) \propto T^2/\Lambda(T)$ , where  $\Lambda(T)$  is the optically thin cooling function, here dominated by metal line cooling. Further, shocked gas temperature is proportional to the initial velocity of the winds squared,  $v_w^2$ . Taking these facts together one finds that gas cooling time scales as  $v_w^{5.4}$  (Cuadra et al., 2005, eq. 2). Therefore, for the Wolf-Rayet winds, with velocities of a thousand  $\text{km s}^{-1}$ , gas cooling time is much longer than the dynamical time and the effect of cooling is negligible. However, for outflow velocity of 300  $\text{km s}^{-1}$ , radiative cooling is faster than the local dynamical time. We therefore find that these winds cool radiatively and form clumps of cold gas.

We find that cold clumps form independently of the geometry of the stellar system, as long as wind velocity is low enough. The morphology of cold gas however strongly depends on the orbital distribution of slow wind sources. In Section 5.4 we tested two extreme cases for the stellar distribution: stars in two discs, and in a spherically symmetric system. An extended cold disk was present in the former configuration, and only a tiny gas ring in the former.

A detailed comparison between the gas morphology in our simulations and in the observations is beyond the scope of this work. However, it is interesting to note that the radio images presented by Wardle & Yusef-Zadeh (1992) show an asymmetry in the gas that these authors attributed to the influence of stellar winds. This anisotropy suggests that the stellar wind sources are not distributed isotropically, whereas the absence of a conspicuous disc points out that the narrow line stars of the inner few arcsec have different orbital planes.

Eckart & Morris have recently reported<sup>5</sup> the presence of extended mid-infrared emission blobs. Their red spectrum is interpreted as dust emission. It is possible that some of these blobs were actually formed from the stellar winds as in our simulations. Since for the slow winds in our simulations cooling is important, and since the gas would probably cool much further than the minimum temperature of  $10^4$  K assumed here, formation of dust would follow. One of the observed blobs is only 0.026'' away from Sgr A\* in projection and is

---

<sup>5</sup>KITP Conference on the GC, talks available online at [http://online.kitp.ucsb.edu/online/galactic\\_c05](http://online.kitp.ucsb.edu/online/galactic_c05).

probably responsible for the offset between the dynamical centre and the Sgr A\* mid-infrared emission detected by Clénet et al. (2004). Monitoring its proper motion will show whether it is physically close to Sgr A\* and therefore if it could be identified with one of the clumps that feed the SMBH in our simulations.

Finally, radio observations (Yusef-Zadeh et al., 1998) have revealed the presence of clumps with proper motions high enough to escape from the GC region. The mass of one of them, ‘the bullet’, is estimated at  $8 \times 10^{-4} M_{\odot}$ . This mass is of same order as the typical mass of cold clumps leaving the inner region in our simulations.

### 5.6.3 Long term evolution of the disc

In Section 5.4.1 we stopped the simulation after  $\sim 4000$  yr. At this point the total mass of cold gas keeps growing in the inner few arc-seconds and there is no obvious tendency for reaching a steady state. However, because of factors not included in the simulation, it is very likely that in a few thousand years the disc would be destroyed. One reason for that is the presence of many massive stars that would explode as a supernova (SN) within a short time-scale. There are currently tens of WR stars in the GC star cluster. This stellar phase is expected to last a few  $\times 10^5$  yr, at the end of which the star explodes as a SN. Therefore a SN explosion is expected every  $\sim 10^4$  yr.

Let  $R_{\text{sn}}$  be the distance between a supernova and Sgr A\*, and  $E = 10^{51} E_{51}$  erg  $\text{s}^{-1}$  be the total energy content of the supernova shell. The disc material will then be accelerated to a velocity  $v_{\text{acc}}$  given by  $\Sigma_{\text{disc}} v_{\text{acc}}^2 \sim E_{\text{sn}} / 4\pi R_{\text{sn}}^2$ . For example, for disc radius  $R_{\text{disc}} = 2''$ , the ratio of this velocity to the local Keplerian velocity is

$$\frac{v_{\text{acc}}^2}{v_{\text{K}}^2} \sim 1 \frac{E_{51}}{M_{10} R_{10}^2}, \quad (5.2)$$

where  $R_{10} = R_{\text{sn}}/10''$  and  $M_{10} = \pi \Sigma_{\text{disc}} R_{\text{disc}}^2$  in units of  $10 M_{\odot}$ . This shows that a supernova occurring within the inner 0.5 pc of the Galaxy would destroy the disc. A fraction of the disc with the lowest angular momentum would likely be captured by the SMBH and would result in a bright flare that would last at least a few hundred years, the dynamical time at a couple of arc-seconds distance from Sgr A\*. Such flares may be responsible for the X-ray/ $\gamma$ -ray echo of Sgr A\* recent activity on nearby giant molecular clouds, most notably Sgr B2 (Sunyaev et al., 1993; Koyama et al., 1996; Revnivtsev et al., 2004), and the observed plumes of hot gas also indicative of former AGN activity (Baganoff et al., 2003).

Another factor that should be taken into account for a realistic simulation on longer time-scales is the presence of the ‘mini-spiral’. This seems to be a collection of infalling gas structures, with masses of dozens of  $M_{\odot}$  (Paumard et al., 2004). Since their orbital time-scales are a few  $\times 10^4$  years, by that time collisions between these structures and the disc are expected, resulting in the destruction or a significant re-arrangement of the latter. Again this would enhance the accretion rate on to Sgr A\*.

#### 5.6.4 Variability

We have shown that adding more realistic ingredients in our simulations introduces substantial variability into the accretion rate on to Sgr A\*. In Section 5.3.2, with 40 identical stars, the variability increased from less than  $\sim 10\%$  to about 50% by just allowing the stars to follow circular orbits (Fig. 5.6). Further, in Section 5.4.1, the inclusion of slow stellar winds led to the formation of cold clumps. The accretion of these clumps proceeds in short bursts, producing a highly variable transfer of mass into the inner  $0.1''$  (Fig. 5.10). The actual rate of accretion on to the SMBH has still to be determined by the accretion flow physics that we cannot resolve here, but it is expected to maintain most of the variability in time-scales longer than  $\sim 100$  yr.

There are additional sources of variability that have not been included in our treatment. Some of the stars with high outflow rates probably have orbits with a non-negligible eccentricity. Then the fraction of winds that can be captured from a given star by the black hole changes with time. In addition, there could be intrinsic variability of the stars themselves. LBVs outside the GC have been observed to vary their mass-loss rates by more than an order of magnitude within a few years (e.g., Leitherer, 1997). In the GC, the line profiles of IRS 16 NE & NW have changed in the last few years. This is usually attributed to orbital acceleration, but it could be partially caused by changes in the winds properties (Najarro, priv. comm.). Variability can also be produced by close X-ray binaries. Recently, Munro et al. (2005) and Porquet et al. (2005) identified a transient source located within 0.1 pc of the GC as a low-mass X-ray binary. Bower et al. (2005) detected its radio counterpart, and argue that it is the signature of a jet interacting with the dense gas of Sgr A West. Such a jet can influence the kinematics of the gas, and in some cases could drive material to the black hole vicinity. Finally, as we noticed in the previous subsection, SNe or the infall of cold gas from larger scales could lead to a strong increase in the accretion rate.

In the extreme sub-Eddington regime of Sgr A\* accretion, the dependence of the luminosity on the accretion rate is very non-linear (see e.g., Yuan et al., 2002). Thus, even small changes in the accretion rate could result in a strongly enhanced X-ray emission. The results from our simulations, the observational evidence for higher luminosity in the recent past (Sunyaev et al., 1993; Koyama et al., 1996; Revnivtsev et al., 2004), and the idea of star formation in an AGN-like accretion disc a few million yr ago (e.g., Levin & Beloborodov, 2003; Nayakshin & Cuadra, 2005), all suggest that on long time-scales Sgr A\* is an important energy source for the inner Galaxy.

#### 5.6.5 Circularisation of the flow

The degree to which accretion flows are rotating is very important for theoretical models of these flows. For example, Melia (1992, 1994) assumes that gas inflows in essentially a quasi-spherical (Bondi, 1952) manner down to a circularisation radius of  $R_c \sim 100R_S$ , whereas, e.g., Narayan (2002) and Yuan et al. (2003)

assume that the flow is strongly rotating already at a sub-arcsecond region. Recent detailed hydro and MHD simulations of Proga & Begelman (2003a,b) confirmed that the nature of the accretion flow strongly depends on the angular momentum of the gas at the outer boundary of the flow.

Here we find that in all of our simulations the accretion flows possess a relatively large angular momentum, and that in the two-phase wind simulations it is larger than in the one phase case. In terms of circularisation radii for the flows, we find  $R_c \sim 0.01'' \sim 10^3 R_S$  for one-phase winds, and  $R_c \sim 0.1'' \sim 10^4 R_S$  for two-phase flows. Physically, one-phase flows are hotter, and any significant rotation unbinds the gas in the inner arcsecond. This works as a surprisingly effective selection criterion for determining which particles do accrete, so in our one-phase simulations the gas in the inner region has roughly the same angular momentum, independent of the stellar motion.

On the other hand, in the two-phase simulations (fast and slow winds), radiative cooling of denser regions reduces the mean temperature of the gas. As a result, less pressure support is available for the gas, and the ‘selection’ criterion does not operate anymore. These flows rotate at almost the local circular Keplerian velocity near the inner boundary of our simulations. Remarkably, this result (for the hot gas) is largely independent of the orbital distribution of the stellar wind sources. Therefore, unless the mass loss rates of the slow (narrow line) wind stars are grossly over-estimated observationally, we conclude that weakly rotating accretion flows are unlikely to form in Sgr A\*.

## 5.7 Conclusions

In this paper we presented a detailed discussion of our new numerical simulations of wind accretion on to Sgr A\*. Compared with previous works, our methodology includes a treatment of stellar orbital motions and of optically thin radiative cooling. While the results are strongly dependent on the assumptions about stellar mass loss rates, orbits, and wind velocities, some relatively robust conclusions can be made.

Unless mass loss rates of narrow line mass losing stars (Paumard et al., 2001) are strongly over-estimated, the gas at  $r \sim 1''$  distances from Sgr A\* has a two-phase structure, with cold filaments immersed into hot X-ray emitting gas. Depending on the geometry and orbital distributions in the mass-losing star cluster, the cold gas may be settling into a coherent structure such as a disc, or be torn apart and heated to X-ray emitting temperatures in collisions. Both the fast and the slow phase of the winds contribute to the accretion flow on to Sgr A\*. The accretion flow is rotating rather than free-falling in sub-arcsecond regions, with a circularisation radius of order  $10^4 R_S$ . The accretion rates we obtain are of the order of  $3 \times 10^{-6} M_\odot \text{ year}^{-1}$ , in accord with the *Chandra* observations (Baganoff et al., 2003). The accretion of cooler gas proceeds separately via clump infall and is highly intermittent, although the average accretion rate is dominated by the quasi-constant inflow of hot gas. As is true for the hot gas, most of the cold gas outflows from the simulated region. However some of this



gas is bound to Sgr A\*, and, had we resolved a larger region, would come back into the inner regions on eccentric orbits.

A generic result of our simulations is the large variability in the accretion rate on to Sgr A\* on time scales of the order of the stellar wind sources orbital times (hundreds to thousands years). Even in the case of one-phase flows the accretion rate shows variability by factors of a few. Simulations including more diverse populations of winds and stellar orbits, the presence of the single, very important mass-losing star cluster IRS13 (Maillard et al., 2004; Schödel et al., 2005), or the observed ionised (e.g.  $T \sim 10^4$  K) gas, can all be expected to further increase the time-dependent effects. This implies that the current very low luminosity state of Sgr A\* may be the result of a relatively unusual quiescent state. It also means that the real time-averaged output of Sgr A\* in terms of radiation and mechanical jet power may be orders of magnitude higher than what is currently observed. The role of Sgr A\* for the energy balance of the inner region of the Galaxy may therefore be far more important than its current meager energy output would suggest. Observations of  $\gamma$ -ray/X-ray echos of past activity of Sgr A\* (e.g., Revnivtsev et al., 2004) seem to confirm these suggestions from our simulations.

Further improvements in the models of wind accretion on to Sgr A\* will benefit most strongly from better observational constraints on the properties of the stellar winds in the central parsec of the Galaxy. Future numerical improvements may be a higher dynamical range between  $R_{\text{in}}$  and  $R_{\text{out}}$ , a larger number of SPH particles, and inclusion of magnetic fields. The latter are now believed to be very important for gas angular momentum transport via generation of the magneto-rotational instability (e.g., Balbus & Hawley, 1991). At the same time, we expect angular momentum transport to be important only inside or close to the circularisation radius, i.e. somewhere near our inner boundary.



## Chapter 6

# Summary and prospects

In this thesis we have studied different aspects of the role that stars play in the accretion onto Sgr A\*. The stars are not only the source of most of the material that is currently accreted by the super-massive black hole: they were most likely formed inside a massive accretion disc in the past, and nowadays their observations constrain the characteristics of the accretion flow.

### 6.1 Observing star–disc interactions

We studied the interaction of bright stars with a cold accretion disc that could exist in the GC (Chapter 2). Star–disc collisions had been proposed as the origin of the recently discovered X-ray flares (Nayakshin et al., 2004). If a disc were indeed present, it would appear on the NIR observations eclipsing and reprocessing stellar light. Despite the exhaustive observational coverage of the GC inner arcsecond, such effects have not been observed. This posed severe constraints on the existence of a cold disc, namely it has to have a large inner radius, or it has to be optically thin in the NIR. These conclusions were drawn from the observations of S2 as of 2002 (Schödel et al., 2002). In the following couple of years, this and other stars have been further monitored without signs of variability detected (Rafelski et al, in prep.). Most likely the constraints would be even stronger when considering these new data.

Genzel et al. (2003a) found later that Sgr A\*'s NIR luminosity does vary, although not in the way expected from the disc reflection idea. Moreover, the origin of the emission was constrained to the inner few milliarcsec (e.g., Ghez et al., 2004), where the stellar density is not enough to explain the observed event rate. Although better statistics are needed, X-ray and NIR flares seem to be correlated and therefore are just different manifestations of the same physical process (Eckart et al., 2006). The absence of flares coming from larger distances from the black hole argues against the existence of a disc around Sgr A\*. Nevertheless, such a disc is expected to exist in other galactic nuclei (Ho, 2003). Future observations could detect its presence via star–disc interactions.

## 6.2 Self-gravitating discs and star formation

Stars severely constrain the current existence of an accretion disc around Sgr A\*. However, a massive accretion disc was likely the birth place for most of the bright He-stars (Chapter 3). AGN discs are expected to be massive enough at their outer parts for self-gravity to be important. Such a disc would then become clumpy and eventually form stars or planets. We showed that, for this process to happen in the GC, the necessary disc mass is  $\sim 10^4 M_\odot$ . Such a mass is consistent with the constraints coming from the stellar dynamics: too massive discs would distort themselves and could not be recognised as discs anymore. We can think of the stars as the fossil of an ancient accretion disc, studying them now we can learn about the feeding of Sgr A\* a few Myr in the past.

More detailed modelling of the stellar discs dynamics has confirmed the constraints on the disc mass, and it has also favoured a stellar initial mass function (IMF) that is considerably top-heavy, i.e., the total mass of the stellar system is dominated by massive stars (Nayakshin, Dehnen, Cuadra, & Genzel, 2006). The top-heavy IMF is also supported by NIR and X-ray observations (Nayakshin & Sunyaev, 2005; Paumard et al., 2006). This result is very interesting considering that everywhere else in the Galaxy the IMF seems to be identical, and dominated by low-mass stars. How massive stars form at all is still an open issue (e.g., Bonnell et al., 2006). Perhaps understanding their formation in extreme environments such as the GC will give the necessary clues to solve this problem.

Further work on this subject includes the numerical modelling of star forming discs (Nayakshin, Cuadra & Springel, in prep.). Unfortunately, star formation simulations – even in a normal environment – are still not able to resolve all the relevant scales. Therefore, recipes have to be introduced to treat processes such as the accretion onto the stars and the feedback of the forming stars on the disc. To make any prediction from these numerical simulations is still quite challenging, since preliminary tests show the strong dependence of the resulting IMF on the implementation of the sub-resolution physics.

Even once star formation in a disc is well understood, remaining issues have to be explained. The first issue is why there are *two* overlapping stellar discs with identical stellar populations. The stellar ages imply that they must have formed at the same time, but two gas discs would coalesce to a single one within a few orbital times. This constrains the time-scale for the gas discs to form stars and disappear to be shorter than the uncertainty on the age of the stellar population,  $\sim 1$  Myr. Alternatively, it would require that all the stars were formed in a single – perhaps warped – disc, with dynamical processes changing their orientation. The second issue is how to form the S-stars. While the disc hypothesis works in principle for stars at  $R \gtrsim 1''$ , inside this region a disc would not be massive enough to form stars. Migration also seems to be too slow to explain their presence in the inner  $1''$ . Most likely, scattering processes are responsible for bringing them from outer regions and putting them in very eccentric orbits, although no satisfactory explanation has been found yet (e.g., Alexander, 2005).

### 6.3 Feeding Sgr A\* with stellar winds

Finally, we studied the dynamics of the gas in the inner parsec of the Galaxy (Chapters 4 and 5). The gas is originated as stellar winds from massive stars, and ends up escaping this inner region, or accreted by the black hole.

The results are not trivial. Stars are distributed in two perpendicular discs and different stars emit winds with different velocities. For the low velocity winds, radiative cooling is fast enough. Then clumps and filaments are formed, creating a two-phase medium with a complicated morphology.

Perhaps more interestingly, the rate at which gas is captured by the black hole strongly changes with time. We estimate that the variability on the actual accretion rate onto the black hole changes by a factor of a few in 10–100 yr. In the very inefficient regime of Sgr A\* accretion, a small change in the accretion rate can produce large changes in the luminosity. Therefore, Sgr A\* may be an important energy source for the inner Galaxy over long time-scales, much more than what it is assumed given its very low current luminosity.

While studying accretion onto Sgr A\* is important for understanding accretion in general, our numerical approach can be easily extended to directly model other galactic nuclei. For instance, Nayakshin & Cuadra (2006) studied the outflow from a nuclear starburst, and showed that the stellar winds cannot account for the torus-like obscuration observed in most of these systems.

Further work on this subject is underway (Cuadra et al, in prep.). While here we used an ensemble of wind sources with roughly the same properties as the observed stars, we are currently using the last available data for individual stars, making the simulations more realistic. We are studying which particular stars are more important for the feeding of Sgr A\*, both in terms of total value and variability. Additionally, we are creating maps of infrared emission from the gas in the inner arcseconds. The emissivity turns out to depend sensitively on the mass loss rate from the slow wind stars. While there is still a large degree of uncertainty on the stellar orbits, so a detailed comparison with the observations cannot be done, it is still possible to constrain some of the stellar wind properties with this approach.

A very interesting direction for future work is the modelling of the region very close to Sgr A\*,  $R \lesssim 10^4 R_S$ , to study the inner accretion flow and understand better Sgr A\*'s dimness. The proper modelling of this region requires the inclusion of more ingredients, such as physical viscosity and magnetic fields, that cannot be treated properly with our current approach. The results presented here, however, should be used as the outer boundary conditions for this further work.



# Bibliography

- Alexander T., 2005, *Phys. Rep.*, 419, 65
- Artymowicz P., 1994, *ApJ*, 423, 581
- Artymowicz P., Lin D. N. C., Wampller E. J., 1993, *ApJ*, 409, 592
- Backer D. C., Sramek R. A., 1999, *ApJ*, 524, 805
- Baganoff F. K., Bautz M. W., Brandt W. N., Chartas G., Feigelson E. D., Garmire G. P., Maeda Y., Morris M., Ricker G. R., Townsley L. K., Walter F., 2001, *Nature*, 413, 45
- Baganoff F. K., Maeda Y., Morris M., Bautz M. W., Brandt W. N., Cui W., Doty J. P., Feigelson E. D., Garmire G. P., Pravdo S. H., Ricker G. R., Townsley L. K., 2003, *ApJ*, 591, 891
- Balbus S. A., Hawley J. F., 1991, *ApJ*, 376, 214
- Balick B., Brown R. L., 1974, *ApJ*, 194, 265
- Bate M. R., Lubow S. H., Ogilvie G. I., Miller K. A., 2003, *MNRAS*, 341, 213
- Bender R., Kormendy J., Bower G., Green R., Thomas J., Danks A. C., Gull T., Hutchings J. B., Joseph C. L., Kaiser M. E., Lauer T. R., Nelson C. H., Richstone D., Weistrop D., Woodgate B., 2005, *ApJ*, 631, 280
- Binney J., Tremaine S., 1987, *Galactic dynamics*. Princeton University Press
- Blandford R. D., Begelman M. C., 1999, *MNRAS*, 303, L1
- Bondi H., 1952, *MNRAS*, 112, 195
- Bonnell I. A., Larson R. B., Zinnecker H., 2006, PPV conference paper (astro-ph/0603447)
- Bower G. C., Roberts D. A., Yusef-Zadeh F., Backer D. C., Cotton W. D., Goss W. M., Lang C. C., Lithwick Y., 2005, *ApJ*, 633, 218
- Bower G. C., Wright M. C. H., Falcke H., Backer D. C., 2003, *ApJ*, 588, 331

- Brown R. L., Johnston K. J., Lo K. Y., 1981, *ApJ*, 250, 155
- Brown R. L., Lo K. Y., 1982, *ApJ*, 253, 108
- Chandrasekhar S., 1943, *ApJ*, 97, 255
- Churazov E., Gilfanov M., Revnivtsev M., 2001, *MNRAS*, 321, 759
- Clénet Y., Rouan D., Gratadour D., Lacombe F., Gendron E., Genzel R., Ott T., Schödel R., Léna P., 2004, *A&A*, 424, L21
- Coker R. F., Melia F., 1997, *ApJL*, 488, L149
- Collin S., Zahn J., 1999, *A&A*, 344, 433
- Cuadra J., Nayakshin S., 2005, in *Growing Black Holes: Accretion in a Cosmological Context*, Merloni A., Nayakshin S., Sunyaev R. A., eds., pp. 248–249
- Cuadra J., Nayakshin S., Springel V., Di Matteo T., 2005, *MNRAS*, 360, L55
- , 2006, *MNRAS*, 366, 358
- Cuadra J., Nayakshin S., Sunyaev R., 2003, *A&A*, 411, 405
- Di Matteo T., Springel V., Hernquist L., 2005, *Nature*, 433, 604
- Draine B. T., Lee H. M., 1984, *ApJ*, 285, 89
- Draine B. T., Salpeter E. E., 1979, *ApJ*, 231, 438
- Eckart A., Baganoff F. K., Schödel R., Morris M., Genzel R., Bower G. C., Marone D., Moran J. M., Viehmann T., Bautz M. W., Brandt W. N., Garmire G. P., Ott T., Trippe S., Ricker G. R., Straubmeier C., Roberts D. A., Yusef-Zadeh F., Zhao J. H., Rao R., 2006, *A&A*, 450, 535
- Eckart A., Genzel R., Ott T., Schödel R., 2002, *MNRAS*, 331, 917
- Eisenhauer F., Genzel R., Alexander T., Abuter R., Paumard T., Ott T., Gilbert A., Gillessen S., Horrobin M., Trippe S., Bonnet H., Dumas C., Hubin N., Kaufer A., Kissler-Patig M., Monnet G., Ströbele S., Szeifert T., Eckart A., Schödel R., Zucker S., 2005, *ApJ*, 628, 246
- Falcke H., Melia F., 1997, *ApJ*, 479, 740
- Ferrarese L., Ford H., 2005, *Space Science Reviews*, 116, 523
- Frank J., King A., Raine D. J., 2002, *Accretion Power in Astrophysics: Third Edition*. Cambridge University Press
- Fryer C. L., Woosley S. E., Heger A., 2001, *ApJ*, 550, 372
- Gammie C. F., 2001, *ApJ*, 553, 174



- Genzel R., Hollenbach D., Townes C. H., 1994, *Reports on Progress in Physics*, 57, 417
- Genzel R., Pichon C., Eckart A., Gerhard O. E., Ott T., 2000, *MNRAS*, 317, 348
- Genzel R., Schödel R., Ott T., Eckart A., Alexander T., Lacombe F., Rouan D., Aschenbach B., 2003a, *Nature*, 425, 934
- Genzel R., Schödel R., Ott T., Eisenhauer F., Hofmann R., Lehnert M., Eckart A., Alexander T., Sternberg A., Lenzen R., Clénet Y., Lacombe F., Rouan D., Renzini A., Tacconi-Garman L. E., 2003b, *ApJ*, 594, 812
- Gerhard O., 2001, *ApJ*, 546, L39
- Gezari S., Ghez A. M., Becklin E. E., Larkin J., McLean I. S., Morris M., 2002, *ApJ*, 576, 790
- Ghez A. M., Becklin E., Duchjné G., Hornstein S., Morris M., Salim S., Tanner A., 2003a, *Astronomische Nachrichten Supplement*, 324, 527
- Ghez A. M., Duchêne G., Matthews K., Hornstein S. D., Tanner A., Larkin J., Morris M., Becklin E. E., Salim S., Kremenek T., Thompson D., Soifer B. T., Neugebauer G., McLean I., 2003b, *ApJ*, 586, L127
- Ghez A. M., Klein B. L., Morris M., Becklin E. E., 1998, *ApJ*, 509, 678
- Ghez A. M., Morris M., Becklin E. E., Tanner A., Kremenek T., 2000, *Nature*, 407, 349
- Ghez A. M., Salim S., Hornstein S. D., Tanner A., Lu J. R., Morris M., Becklin E. E., Duchêne G., 2005, *ApJ*, 620, 744
- Ghez A. M., Wright S. A., Matthews K., Thompson D., Le Mignant D., Tanner A., Hornstein S. D., Morris M., Becklin E. E., Soifer B. T., 2004, *ApJL*, 601, L159
- Goldwurm A., Brion E., Goldoni P., Ferrando P., Daigne F., Decourchelle A., Warwick R. S., Predehl P., 2003, *ApJ*, 584, 751
- Goodman J., 2003, *MNRAS*, 339, 937
- Goodman J., Tan J. C., 2004, *ApJ*, 608, 108
- Hall D. N. B., Kleinmann S. G., Scoville N. Z., 1982, *ApJL*, 260, L53
- Hansen B. M. S., Milosavljević M., 2003, *ApJ*, 593, L77
- Ho L. C., 1999, *ApJ*, 516, 672
- , 2003, in *ASP Conf. Ser. 290: Active Galactic Nuclei: From Central Engine to Host Galaxy*, Collin S., Combes F., Shlosman I., eds., pp. 379–+

- Johnson B. M., Gammie C. F., 2003, *ApJ*, 597, 131
- Kauffmann G., Haehnelt M., 2000, *MNRAS*, 311, 576
- Kim S. S., Figer D. F., Morris M., 2004, *ApJ*, 607, L123
- Kim S. S., Morris M., 2003, *ApJ*, 597, 312
- Kolykhalov P. I., Sunyaev R. A., 1980, *Soviet Astron. Lett.*, 6, 357
- Koyama K., Maeda Y., Sonobe T., Takeshima T., Tanaka Y., Yamauchi S., 1996, *PASJ*, 48, 249
- Krabbe A., Genzel R., Eckart A., Najarro F., Lutz D., Cameron M., Kroker H., Tacconi-Garman L. E., Thatte N., Weitzel L., Drapatz S., Geballe T., Sternberg A., Kudritzki R., 1995, *ApJ*, 447, L95
- Kulsrud R. M., Mark J. W. K., Caruso A., 1971, *Ap&SS*, 14, 52
- Leitherer C., 1997, in *Luminous Blue Variables: Massive Stars in Transition*. Eds: A. Nota & H. Lamers (ASP Conference Series Vol. 120), p. 58
- Levin Y., Beloborodov A. M., 2003, *ApJ*, 590, L33
- Lissauer J. J., 1987, *Icarus*, 69, 249
- Liszt H. S., 2003, *A&A*, 408, 1009
- Loeb A., 2004, *MNRAS*, 350, 725
- Maillard J. P., Paumard T., Stolovy S. R., Rigaut F., 2004, *A&A*, 423, 155
- Maoz E., 1998, *ApJL*, 494, L181+
- McMillan S. L. W., Portegies Zwart S. F., 2003, *ApJ*, 596, 314
- Melia F., 1992, *ApJL*, 387, L25
- , 1994, *ApJ*, 426, 577
- Melia F., Falcke H., 2001, *ARA&A*, 39, 309
- Meyer F., Meyer-Hofmeister E., 1994, *A&A*, 288, 175
- Milosavljević M., Loeb A., 2004, *ApJ*, 604, L45
- Miyoshi M., Moran J., Herrnstein J., Greenhill L., Nakai N., Diamond P., Inoue M., 1995, *Nature*, 373, 127
- Morris M., 1993, *ApJ*, 408, 496
- Morris M., Ghez A. M., Becklin E. E., 1999, *Advances in Space Research*, 23, 959

- Muno M. P., Lu J. R., Baganoff F. K., Brandt W. N., Garmire G. P., Ghez A. M., Hornstein S. D., Morris M. R., 2005, *ApJ*, 633, 228
- Munyanzeza F., Viollier R. D., 2002, *ApJ*, 564, 274
- Najarro F., Krabbe A., Genzel R., Lutz D., Kudritzki R. P., Hillier D. J., 1997, *A&A*, 325, 700
- Narayan R., 2002, in *Lighthouses of the universe: the most luminous celestial objects and their use for cosmology*, Gilfanov M., Sunyaev R., Churazov E., eds., pp. 405–+
- Narayan R., Yi I., 1994, *ApJL*, 428, L13
- Narayan R., Yi I., Mahadevan R., 1995, *Nature*, 374, 623
- Nayakshin S., 2003, *Astronomische Nachrichten Supplement*, 324, 483
- , 2004, *MNRAS*, 352, 1028
- , 2005a, *A&A*, 429, L33
- , 2005b, *MNRAS*, 359, 545
- Nayakshin S., Cuadra J., 2005, *A&A*, 437, 437
- Nayakshin S., Cuadra J., 2006, Submitted to *A&A* (astro-ph/0602366)
- Nayakshin S., Cuadra J., Sunyaev R., 2004, *A&A*, 413, 173
- Nayakshin S., Dehnen W., Cuadra J., Genzel R., 2006, *MNRAS*, 366, 1410
- Nayakshin S., Sunyaev R., 2003, *MNRAS*, 343, L15
- , 2005, *MNRAS*, 364, L23
- Osterbrock D. E., 1989, *Astrophysics of gaseous nebulae and active galactic nuclei*. University Science Books
- Ostriker J. P., 1983, *ApJ*, 273, 99
- Ott T., Schödel R., Genzel R., Eckart A., Lacombe F., Rouan D., Hofmann R., Lehnert M., Alexander T., Sternberg A., Reid M., Brandner W., Lenzen R., Hartung M., Gendron E., Clenet Y., Lena P., Rousset G., Lagrange A.-M., Ageorges N., Hubin N., Lidman C., Moorwood A. F. M., Renzini A., Spyromilio J., Tacconi-Garman L. E., Menten K. M., Mouawad N., 2003, *The Messenger*, 111, 1
- Paczynski B., 1978, *Acta Astron.*, 28, 91
- Paumard T., Genzel R., Martins F., Nayakshin S., Beloborodov A. M., Levin Y., Trippe S., Eisenhauer F., Ott T., Gillessen S., Abuter R., Cuadra J., Alexander T., Sternberg A., 2006, *ApJ*, 643, 1011

- Paumard T., Maillard J.-P., Morris M., 2004, *A&A*, 426, 81
- Paumard T., Maillard J. P., Morris M., Rigaut F., 2001, *A&A*, 366, 466
- Pellegrini S., 2005, *ApJ*, 624, 155
- Porquet D., Grosso N., Bélanger G., Goldwurm A., Yusef-Zadeh F., Warwick R. S., Predehl P., 2005, *A&A*, 443, 571
- Porquet D., Predehl P., Aschenbach B., Grosso N., Goldwurm A., Goldoni P., Warwick R. S., Decourchelle A., 2003, *A&A*, 407, L17
- Portegies Zwart S. F., Baumgardt H., McMillan S. L. W., Makino J., Hut P., Ebisuzaki T., 2006, *ApJ*, 641, 319
- Proga D., Begelman M. C., 2003a, *ApJ*, 582, 69
- , 2003b, *ApJ*, 592, 767
- Quataert E., 2003, *Astronomische Nachrichten Supplement*, 324, 435
- , 2004, *ApJ*, 613, 322
- Quataert E., di Matteo T., Narayan R., Ho L. C., 1999, *ApJ*, 525, L89
- Quataert E., Gruzinov A., 2000, *ApJ*, 539, 809
- Rees M. J., 2002, in *Lighthouses of the universe: the most luminous celestial objects and their use for cosmology*, ed. M. Gilfanov, R. Sunyaev & E. Churazov (Berlin: Springer), p. 345
- Reid M. J., Readhead A. C. S., Vermeulen R. C., Treuhaft R. N., 1999, *ApJ*, 524, 816
- Revnivtsev M. G., Churazov E. M., Sazonov S. Y., Sunyaev R. A., Lutovinov A. A., Gilfanov M. R., Vikhlinin A. A., Shtykovsky P. E., Pavlinsky M. N., 2004, *A&A*, 425, L49
- Rockefeller G., Fryer C. L., Melia F., Warren M. S., 2004, *ApJ*, 604, 662
- Roy A. E., 1982, *Orbital motion*. Bristol : A. Hilger, 1982. 2nd ed.
- Ruffert M., Melia F., 1994, *A&A*, 288, L29
- Sanders R. H., 1998, *MNRAS*, 294, 35
- Schödel R., Eckart A., Iserlohe C., Genzel R., Ott T., 2005, *ApJL*, 625, L111
- Schödel R., Ott T., Genzel R., Hofmann R., Lehnert M., Eckart A., Mouawad N., Alexander T., Reid M. J., Lenzen R., Hartung M., Lacombe F., Rouan D., Gendron E., Rousset G., Lagrange A.-M., Brandner W., Ageorges N., Lidman C., Moorwood A. F. M., Spyromilio J., Hubin N., Menten K. M., 2002, *Nature*, 419, 694

- Schödel R., Ott T., Genzel R., Eckart A., Mouawad N., Alexander T., 2003, *ApJ*, 596, 1015
- Scoville N. Z., Kwan J., 1976, *ApJ*, 206, 718
- Scoville N. Z., Stolovy S. R., Rieke M., Christopher M., Yusef-Zadeh F., 2003, *ApJ*, 594, 294
- Shakura N. I., Sunyaev R. A., 1973, *A&A*, 24, 337
- Shlosman I., Begelman M. C., 1989, *ApJ*, 341, 685
- Shlosman I., Begelman M. C., Frank J., 1990, *Nature*, 345, 679
- Springel V., 2005, *MNRAS*, 364, 1105
- Springel V., Di Matteo T., Hernquist L., 2005, *MNRAS*, 361, 776
- Springel V., Hernquist L., 2002, *MNRAS*, 333, 649
- Springel V., Yoshida N., White S. D. M., 2001, *New Astronomy*, 6, 79
- Sunyaev R. A., Markevitch M., Pavlinsky M., 1993, *ApJ*, 407, 606
- Sutherland R. S., Dopita M. A., 1993, *ApJS*, 88, 253
- Svensson R., Zdziarski A. A., 1994, *ApJ*, 436, 599
- Syer D., Clarke C. J., Rees M. J., 1991, *MNRAS*, 250, 505
- Tanga P., Weidenschilling S. J., Michel P., Richardson D. C., 2004, *A&A*, 427, 1105
- Toomre A., 1964, *ApJ*, 139, 1217
- Torres D. F., Capozziello S., Lambiase G., 2000, *Phys. Rev. D*, 62, 104012
- Voshchinnikov N. V., 2002, in *Optics of Cosmic Dust*, p. 1
- Wardle M., Yusef-Zadeh F., 1992, *Nature*, 357, 308
- Yu Q., Tremaine S., 2002, *MNRAS*, 335, 965
- Yuan F., Markoff S., Falcke H., 2002, *A&A*, 383, 854
- Yuan F., Quataert E., Narayan R., 2003, *ApJ*, 598, 301
- Yusef-Zadeh F., Roberts D. A., Biretta J., 1998, *ApJL*, 499, L159
- Zang Z., Meurs E. J. A., 2001, *ApJ*, 556, 24



# Curriculum Vitae

## Jorge Cuadra

Date and place of birth:	October 18, 1977; Santiago, Chile
Citizenship:	Chilean and Croatian
Current Affiliation:	Max-Planck-Institut für Astrophysik D-85741 Garching, Germany
E-mail:	jcuadra@mpa-garching.mpg.de
Homepage:	www.mpa-garching.mpg.de/~jcuadra

## Education

**2002–2006** Ph.D. at the Ludwig-Maximilians-Universität München. Thesis work supervised by Dr. S. Nayakshin and Prof. R. Sunyaev at the Max-Planck-Institut für Astrophysik (MPA).

**1998–2001** Degree in Astronomy (*Licenciado*), P. Univ. Católica (PUC), Santiago, Chile. Four years of courses in Astrophysics, Physics, and Mathematics, plus one semester of practical research.

**1996–2000** Engineering and Computer Science studies, PUC.

### Astrophysics Schools

- Cerro Tololo Inter-American Observatory (CTIO) ‘Research Experience for Undergraduates’ Programme; La Serena, Chile, Jan.–Mar. 2001
- Vatican Observatory Summer School on ‘Stellar Remnants’; Castel Gandolfo, Italy, June–July 2001
- Sigra Graduate School on ‘Black Holes and Galaxies’; Como, Italy, May 2003
- ‘Modest’ School on ‘Numerical  $N$ -body Dynamics’; Strasbourg, France, March 2004

## Publications in refereed journals

- Cuadra, Nayakshin, Springel, Di Matteo: ‘*Galactic Centre stellar winds and Sgr A\* accretion.*’ MNRAS 366, 358 (2006)

- **Cuadra**, Nayakshin, Springel, Di Matteo: ‘*Accretion of cool stellar winds on to Sgr A\*: another puzzle of the Galactic Centre?*’ MNRAS 360, L55 (2005)
- **Cuadra**, Nayakshin, Sunyaev: ‘*Bright stars and an optically thick inactive disk in Sgr A\* and other dormant galaxy centers.*’ A&A 411, 405 (2003)
- Nayakshin & **Cuadra**: ‘*A self-gravitating accretion disk in Sgr A\* a few million years ago: Is Sgr A\* a failed quasar?*’ A&A 437, 437 (2005)
- Nayakshin, **Cuadra**, Sunyaev: ‘*X-ray flares from Sgr A\*: Star-disk interactions?*’ A&A 413, 173 (2004)
- Nayakshin, Dehnen, **Cuadra**, Genzel: ‘*Weighing the young stellar discs around Sgr A\*.*’ MNRAS, 366, 1410 (2006)
- Paumard et al. (including **Cuadra**): ‘*The Two Young Star Disks in the Central Parsec of the Galaxy: Properties, Dynamics and Formation.*’ ApJ 643, 1011 (2006)
- Candia et al. (including **Cuadra**): ‘*Optical and Infrared Photometry of the Unusual Type Ia Supernova 2000cx.*’ PASP 115, 277 (2003)
- Day et al. (including **Cuadra**): ‘*Light and Color Curves of Six Field RR Lyrae Variable Stars.*’ PASP 114, 645 (2002)

## Selected talks

- Black Holes – From Stars to Galaxies (XXVIth IAU General Assembly); Prague, Czech Rep., Aug. 2006
- Lunch Talk; Sterrewacht Leiden, Netherlands, June 2006
- Galactic Center Workshop: From the Center of the Milky Way to Nearby Low-Luminosity Galactic Nuclei; Bad Honnef, Germany, April 2006
- Star Formation Seminar; Astrophysikalisches Institut Potsdam, Germany, Feb. 2006
- 11th Latin-American Regional IAU Meeting; Pucón, Chile, Dec. 2005
- Relativistic Astrophysics and Cosmology – Einstein’s Legacy; Munich, Germany, Nov. 2005
- Workshop on Simulations with Gadget; Garching, Germany, Oct. 2005
- High Energy Phenomena in the Galactic Center; Paris, France, June 2005
- Institute Seminar; MPA Garching, Germany, March 2005
- Modelling Dense Stellar Systems (Modest-5a); Edinburgh, UK, Dec. 2004



# Acknowledgements

Even though this is my thesis, almost all of the ideas belong to Sergei Nayakshin. I thank him first for his generosity in sharing them with me, and then for actually doing a lot of the work himself. I also thank him for constantly motivating me and for being at the same time a friend, a colleague and a supervisor. If I have been a successful PhD student is more his merit than mine.

Rashid Sunyaev was, especially at the beginning, very important in ensuring that in our work everything was checked thoroughly and that every effect was taken into account. I also thank him for always pushing me to work harder and for his advice on dealing with the university, MPA administration and job applications.

I thank Volker Springel and Tiziana Di Matteo for sharing their accretion code with us. Volker was also always very helpful when we wanted to try our new ideas in his code. I also thank Debora Sijacki and Cecilia Scannapieco for helping me during my first attempts to use Gadget.

All through my stay in Garching, I've benefited from discussions with the members of the Galactic centre group at MPE, especially Reinhard Genzel, Fabrice Martins, Thibaut Paumard and Rainer Schödel. I thank them for that and for sharing their data with us.

Kees Dullemond helped us to estimate disc opacities and emission for Chapter 2. Eliot Quataert sent us output from his calculations for Chapter 5. Discussions with Fred Baganoff, Mark Morris, Paco Najarro and Farhad Yusef-Zadeh, besides those mentioned above, were very useful for the papers comprising this thesis. I also thank the papers' referees.

Thanks to Sascha Trippe for writing the German version of the abstract and Jens Chluba for checking it.

My four years in Garching were very nice. I thank all my friends for the time we spent together and I hope we meet again. I will not however list them, because I'm sure I would forget a few.

Thanks to the Astro-WGers for giving me shelter after I left my apartment. Also thanks to my friends in Mediterranean countries, Pere, Dimitris, Paola and Aybüke, for hosting me during holidays.

I thank my family for bringing me up in a stimulating environment, that probably made me become a scientist, and for their support when I decided to change to astronomy and move out of Chile.

Finally I thank Patricia for everything we share.